

**Molecular imaging of cancer stem cells (CSCs)
during development of chemo resistance in
ovarian carcinoma**

By

RAM KUMAR SINGH

[LIFE09201004017]

TATA MEMORIAL CENTRE

MUMBAI

A thesis submitted to the

Board of Studies in Life Sciences

in partial fulfilment of the requirements

for the Degree of

DOCTOR OF PHILOSOPHY

of

HOMI BHABHA NATIONAL INSTITUTE



April, 2016

Homi Bhabha National Institute

Recommendations of the Viva Voce Committee

We members of the Viva Voce Committee, we certify that we have read the dissertation prepared by Mr. Ram Kumar Singh entitled "Molecular Imaging of cancer stem cells (CSCs) during development of chemoresistance in ovarian carcinoma" and recommend that it may be accepted as fulfilling the thesis requirement for the award of Degree of Doctor of Philosophy.

S.V. Chiplunkar
Chairman - Dr. S.V. Chiplunkar Signature Date: 4/1/2016

Pritha Ray
Guide / Convener - Dr. Pritha Ray Signature Date: 4.4.2016

S. N. Dalal
Member 1 - Dr. Sorab N Dalal Signature Date: 4/4/16

Shilpee Dutt
Member 2 - Dr. Shilpee Dutt Signature Date: 4/4/2016

Supriya Chopra
Member 3 - Dr. Supriya Chopra Signature Date: 19/4/16

Tanya Das
External Examiner - Dr. Tanya Das Signature Date: 04/04/2016

Final approval and acceptance of this thesis is contingent upon the candidate's submission of the final copies of the thesis to HBNI.

I/We hereby certify that I/we have read this thesis prepared under my/our direction and recommend that it may be accepted as fulfilling the thesis requirement.

4-4-16
Mumbai

Pritha Ray
Signature
Guide

Statement by author

This dissertation has been submitted in partial fulfilment of requirements for an advanced degree at Homi Bhabha National Institute (HBNI) and is deposited in the Library to be made available to borrowers under rules of the HBNI.

Brief quotations from this dissertation are allowable without special permission, provided that accurate acknowledgement of source is made. Requests for permission for extended quotation from or reproduction of this manuscript in whole or in part may be granted by the Competent Authority of HBNI when in his or her judgment the proposed use of the material is in the interests of scholarship. In all other instances, however, permission must be obtained from the author.



Ram Kumar Singh

Navi Mumbai,

April, 2016

Declaration

I, hereby declare that the thesis entitled “Molecular imaging of cancer stem cells (CSCs) during development of chemoresistance in ovarian carcinoma” is a record of the work carried out by me under the supervision of Dr. Pritha Ray. This work is original and it has not been submitted earlier as a whole or in part for a degree, diploma, associateship or fellowship at this or any other institute or university.



Ram Kumar Singh

New Mumbai,

April, 2016



Homi Bhabha National Institute

Ph. D. PROGRAMME

1. Name of the Student:	Ram Kumar Singh
2. Name of the Constituent Institution:	Tata Memorial Centre, Advanced Centre for Treatment Research and Education in Cancer
3. Enrolment No. :	LIFE09201004017
4. Title of the Thesis:	Molecular imaging of cancer stem cells (CSCs) during development of chemoresistance in ovarian carcinoma.
5. Board of study:	Life Science

1. Introduction

Ovarian cancer is the seventh most common cancer amongst women and ranks 4th in cancer related deaths across the globe. In Indian scenario, it is the 4th most common cancer amongst women. Approximately 26,834 new cases are reported every year with 4.9% of 5 year prevalence rate[1] [2]. Ovarian cancer, often does not have any symptoms at early stage of tumor development, hence it remains unnoticed for long. In majority of the cases the disease is diagnosed at Stage III and IV and only < 25% of the patients with advanced stage survive beyond 5years [3]. A major challenge in successful treatment of late stage ovarian cancer is the generation of resistance against chemotherapeutic drugs resulting in tumor recurrence and molecular alteration in drug transporters, detoxifying enzymes, apoptotic machinery, DNA repair pathway and cell survival signalings are known to attribute to chemoresistance [3, 4]. In recent times, a small subset of cells present in the heterogeneous tumor bulk and termed as cancer stem cells (CSC) or cancer initiating cells is hypothesized to be the prime cause for tumor relapse and chemo resistance. These CSCs are quiescent in nature having extensive self-renewal property, high DNA repair efficiency, increased ALDH activity and ability to differentiate[5, 6]. After the discovery of cancer stem cells by John Dick and his colleagues in 1994 in haematological malignancies [7, 8], CSCs have been identified in breast cancer (solid tumor) based on surface biomarkers i.e. CD44⁺/CD24⁻ cells and many other malignancies like pancreatic, colorectal, lung and brain cancer [9-12]. Bapat and colleagues were the first to present direct evidence for existence of ovarian cancer stem cells[13]. CSCs are innately resistant towards treatment, so bulk of the tumour that initially appears to be eliminated again rebuilt (recurrence) from this population. Such findings have stimulated interest amongst scientists to develop various approaches to target CSCs. Currently four different methodologies exist for the correct identification of cancer stem cells. The first method relies on expression of specific biomarkers, second is spheroid formation capability, third is side population assay and

the fourth one is based on high aldehyde dehydrogenase activity. CD44, CD24, CD133, CD117 and Myd88 are the well-known ovarian cancer stem cell markers. Recently EpCAM and CXCR4 have emerged as a new biomarkers for ovarian CSCs [5, 14]. In order to target the CSCs understanding the basic mechanism of their regulation is very important. It is also equally important to follow the therapeutic efficacy against these CSCs noninvasively in *in-vivo* situation. Liu et al., in 2010 showed that cancer stem cells from human breast tumors were involved in spontaneous metastases in orthotopic mouse models through bioluminescence imaging (BLI)[15]. Thus real time monitoring of CSCs would help in revealing the kinetics of tumor development and therapy efficacy. Among several deregulated signaling pathways, receptor tyrosine kinases (RTKs) have been the subject of intense investigation due to their widespread deregulation in cancer. System-wide analyses of tumors have recently identified receptor tyrosine kinase (EGFR, IR, IGF-1R, VEGFR 1-3, and PDGF etc) activation and co-activation as important mechanisms to achieve both CSC phenotype and chemoresistance [16] *In vitro* studies and approaches using mouse knockout models for Insulin growth factor (IGF) family members have revealed that IGFs are key regulators of follicular growth, cellular differentiation, oocyte maturation, and cumulus expansion. This study suggested that all necessary components for an IGF-I mediated autocrine loop are present in ovarian cancer cells [17]. Ouban et al., confirmed the presence of the IGF-IR expression by immunohistochemistry (IHC) in 100% of the ovarian carcinomas samples (n=9) suggesting the association between IGF-1R and ovarian cancer[18]. However nothing was known about the role of IGF-1R in the acquirement of chemoresistance until Eckstein et. al., in 2009 showed that hyper activation of the IGF-1R pathway is an essential event for cisplatin resistance in ovarian cancer cells [19]. Role IGF-1R has also been implicated in the regulation of breast cancer stem cells where sorted IGF-1R expressing cells displayed features of cancer stem cells [20]. However role of IGF-1R

in generation of chemoresistance and maintenance of CSC like phenotype and their mutual dependency in ovarian cancer is not fully investigated.

2. Rationale

Generation of chemoresistance and recurrence of the tumor are the two major hurdles in the path of successful treatment of ovarian cancer. This confers an imperative need for the identification of right target which could battle against generation of chemoresistance and relapse. As mentioned in the introduction, cancer stem cells are the key components in the entire tumor mass which can resist the effect of conventional chemotherapeutic drugs and has the ability to recapitulate the primary tumor. IGF-1R signaling plays an important role in cellular proliferation and cell survival. It also plays a vital role in transforming events during carcinogenesis. Recently Chang et al (2013) have shown that IGF-1R could serve as a novel biomarker for breast cancer stem cells, where they documented that IGF-1R^{high} population has enriched CD44⁺/CD24⁻ subpopulation, increased ALDH activity and more tumorigenicity. Blockade of IGF-1R signaling also showed abolishment of CSC features *in vitro* and *in vivo*. However, the role of IGF-1R in the maintenance of chemoresistance and ovarian cancer stem cells is still unclear, which needs further investigation. This study therefore is based on the key questions as mentioned below.

3. Key Questions:

- I. How is the association of CSCs with the acquirement of chemo resistance (independent of drug regime) in ovarian cancer cells?
- II. Does IGF-1R signaling play any role in regulation and maintenance of CSC population and chemoresistant phenotype?

4. Objectives: To address these key questions following objectives were designed.

Objective 1: Isolation and characterization of cancer stem cells (CSC) from chemo sensitive & chemo resistant ovarian carcinoma cell lines.

In order to understand the association of CSCs with acquirement of chemoresistance, three resistant models were developed against cisplatin, paclitaxel and combination of cisplatin and paclitaxel in A2780 ovarian cancer cells. Based on the viability, these resistant models were categorized into early (Cis^{ER}, Pac^{ER} and Cis-Pac^{ER}) and late resistant stages (Cis^{LR}, Pac^{LR} and Cis-Pac^{LR}). The early resistant cells exhibited 60–65% viability and the late resistant cells showed 90–95% viability at IC₅₀ concentration of respective drug regime of the sensitive cells. Among the four established techniques for isolation and characterization of ovarian cancer stem cells (OCSCs), Biomarker, side population assay and spheroid formation assay were adopted in the present investigation.

- Significant enrichment in Side Population fraction was observed in all the three resistant models compared to the A2780 sensitive cells as mentioned in the table below.

S.No.	Cells	SP Fraction
1	A2780 sensitive	1.5% ± 0.05
2	Cis ^{ER}	2.4% ± 0.08
3	Cis ^{LR}	5.73% ± 0.42
4	Pac ^{ER}	4.06% ± 0.38
5	Pac ^{LR}	6.8% ± 0.10
6	Combi ^{ER}	5.05% ± 0.65
7	Combi ^{LR}	17.6% ± 0.74

This suggested that with acquirement of resistance there was a gradual enrichment of SP fraction which was independent of the drug regime.

- Self-renewal property is an important feature for CSC population. It was observed that spheroid forming abilities of the resistant cells were significantly higher than the sensitive cells. In addition, SP cells sorted from sensitive, ER and LR stage had higher self-renewal ability than NSP cells. While monitoring the spheroid forming ability at multiple passage, NSP could not form spheroids beyond 2-3 passages. However SP cells were able to form

spheroids till 7-8 passages. Self-renewal ability is partly attributed by the core pluripotent transcription factors (oct4, sox2 and nanog). Transcript levels of these pluripotent genes were monitored through real time PCR where mRNA levels of oct4, sox2 and nanog showed marked increase at early resistance stages compared to the sensitive cells which remained unaltered at late resistant stages in all the three models. Using a shRNA mediated approach, oct4 knockdown clones were generated in all the three resistant models and validated by real time PCR and western blots. Reduced level of oct4 was found to be associated with decreased sphere forming ability in both sensitive and resistant cells.

- Expression levels of CD44, CXCR4 and CD133 ovarian CSC marker were monitored in sensitive and resistant cells by FACS. In Cis^{LR} cells increased CD44, CD133 and CXCR4 population compared to sensitive cells was observed. A gradual increase in CD133 level with increasing resistance was found in all three resistant models. Since cancer stem cells are hypothesized to be the prime cause for tumor relapse, it is important to understand the kinetics of tumor forming ability of CSCs isolated from these resistant cells.

Objective 2: Longitudinal monitoring CSCs labelled with bi-fusion (CMV-Fl2tdt) reporter in living subjects by non-invasive molecular imaging.

The ultimate proof of designating a cell as a Cancer Stem Cell lies in its ability to form tumor from a very low number (theoretically one single cell) in immune-compromised mouse. After isolating the putative CSCs by virtue of one or two of the CSC properties as described above, researchers have shown that even as low as 100 cells can form tumors with due course of time[9] However, depending on the tumor type, method of isolation, strain of mice and their tumor intake ability, implantation of a broad range (1×10^2 - 5×10^5) of cells have been reported in literature[21]. While monitoring the CSC phenotype we observed that SP fraction was enriched with acquirement of resistance. Hence we performed tumor xenograft experiments using SP cells which are enriched with CSC like cells. This was performed by implanting

50,000 SP and NSP cells in NOD/SCID mice (n=5) subcutaneously. A higher number of cells were chosen primarily to understand the ability of the NSP cells for tumor initiation in comparison to their SP counterparts. Real time bioluminescence imaging was performed to not only monitor the tumor formation from SP cells but also to monitor the dynamics of tumor initiation from the early and late resistant cells.

- Tumor initiation from SP cells of Pac^{ER} stage started from day 15 (tumor volume = 0.04cm³) and formed a palpable tumor at the end of day 40 (tumor volume = 0.98cm³). With increase in tumor volume bioluminescence signal increased from $3.43 \times 10^7 \pm 2.8 \times 10^7$ p/sec/cm²/sr to $1.8 \times 10^{10} \pm 1.2 \times 10^{10}$ p/sec/cm²/sr from day 15 to day 40. Of the 5 mice, 3 showed palpable tumor after 40 days of tumor implantation. However NSP cells of Pac^{ER} stage did not show any tumor formation till day 40.
- Tumor xenograft experiment was performed from Pac^{LR} SP/NSP cells. In a cohort of three mice (NOD/SCID), 50000 SP and NSP cells were implanted subcutaneously and imaged (day 0). Bioluminescence imaging of tumor formation from SP and NSP cells are in progress and the data obtained so far given below. NSP cells did not show any signal after day 0 during follow-up imaging.

	Day 0	Day 25	Day 40	Day 60
Mouse1	1.71 X 10 ⁶	7.71 X 10 ⁵	2.6 X 10 ⁵	3.15 X 10 ⁵
Mouse 2	2.29 X 10 ⁶	4.72 X 10 ⁵	1.02 X 10 ⁵	1.66 X 10 ⁵
Mouse 3	1.62 X 10 ⁵	1.79 X 10 ⁵	7.8 X 10 ⁴	Died

- In parallel, 50,000 Cis^{LR} SP & NSP cells were implanted subcutaneously in a cohort of 5 NOD/SCID mice. Interestingly, Cis^{LR} SP cells initiated tumor formation from day 80 (tumor volume = 0.008 cm³), and at day 110 palpable tumors (tumor volume = 1.7cm³) were found. Bioluminescence signal increased from $2.49 \times 10^5 \pm 5.57 \times 10^4$ p/sec/cm²/sr (day 0) to $4.03 \times 10^6 \pm 1.8 \times 10^6$ p/sec/cm²/sr (day 80) and on 110th day the bioluminescent signal reached to $1.96 \times 10^{10} \pm 2.33 \times 10^9$ p/sec/cm²/sr. At day 110, three mice out of five showed tumor

formation from Cis^{LR} SP cells. Similar to Pac^{ER} NSP fraction, Cis^{LR} NSP cells were not able to initiate the tumor formation even after 110 days and the bioluminescence signal decreased from $1.27 \times 10^5 \pm 1.64 \times 10^4$ p/sec/cm²/sr to $9.7 \times 10^4 \pm 1.4 \times 10^4$ p/sec/cm²/sr from day 0 to day 90. All these results suggest that the SP fractions are enriched with CSC like cells and possess higher tumorigenic property in comparison to the corresponding NSP fractions.

Unfortunately due to certain technical limitation in SP cell sorting, experiments to understand the dynamics of tumor formation from Cis^{ER}, Cis-Pac^{ER} and Cis-Pac^{LR} cells could not be performed. However, experiment to monitor the tumor dynamics of early and late resistant cells from spheroid culture (from at least one cellular resistant model) is in progress. Since the data from *in vivo* bioluminescence imaging showed that SP cells from Pac^{ER} stage initiated the tumor formation much earlier than SP cells from Pac^{LR} and Cis^{LR} stages, we further proceeded to identify the signalling pathway/s exhibiting differential regulation during early and late resistant stages.

Objective 3: *To study the role of IGF-1R in maintenance of OCSC biology and epithelial mesenchymal transition.*

As mentioned in the introduction, IGF-1R signaling plays a crucial role in chemoresistance as well as CSC phenotype. We monitored the expression of IGF-1R across all the three resistant models.

- Significantly higher IGF-1R transcripts were observed in Cis^{ER}, Pac^{ER} and Cis-Pac^{ER} cells (4.9, 8.1 and 13.1 fold respectively) that considerably decreased at Cis^{LR}, Pac^{LR} and Cis-Pac^{LR} stages in comparison to sensitive cells. Similar oscillatory pattern was observed in IGF-1R protein level as well. However it was observed that during late resistant stage pAKT levels were very high. Transcriptional regulators of IGF-1R (SP1, FOXO3 and WT1) were also monitored through real time PCR. Only FOXO3 expression was found to

correlate with IGF-1R expression profile in cisplatin and paclitaxel model. In dual resistant model none of these transcriptional regulators showed any change.

- Since IGF-1R expressions were found to be significantly high at early resistant stages, we sought to monitor reversal of chemoresistance by combinatorial approach by inhibiting IGF-1R followed by drug treatment. We chose a specific inhibitor, picropodophyllin (PPP) which inhibits auto phosphorylation and thereby inhibiting its activation. Among all the combinations of drug and inhibitor (IC_{10} and IC_{20}), IC_{20} of both PPP and respective drug exhibited maximum reversal of resistance which was found to be even more pronounced in clonogenic assay.
- While examining EMT phenomenon across the resistant models, it was observed that A2780 cells were enriched in vimentin expression but devoid of E-cadherin expression. We investigated the expression status of four (snail, slug, Zeb1 and twist) potential regulators of EMT at transcript level. Expression levels of snail and slug did not change with increasing resistance in all the three models. However Zeb1 and twist showed a significant increase at the transcript level in late resistant cells (Cis^{LR}, Pac^{LR} and Cis-Pac^{LR}).
- In order to monitor the role of IGF-1R signaling in maintenance of OCSCs, we examined the spheroid forming abilities of cellular resistant cells after inhibiting IGF-1R signaling. It was observed that after PPP treatment there was a significant decrease in spheroid formation and stemness gene expression across the models. We also performed oct4 knockdown studies across the resistant models where knockdown cells were compromised for their spheroid forming abilities but did not show any change in IGF-1R levels.
- One interesting fact observed in all the three chemoresistant models is that the late resistant cells contain higher levels of phosphorylated AKT. Since Akt is an important downstream effector of IGF-1R signaling, we investigated for possible feedback loop between IGF-1R and AKT. We treated late resistant cells with AKT inhibitor at different concentrations

(10nM, 50nM, 100nM and 150nM) for 12 hours showing a dose dependent decrease in pAKT and t-AKT levels. Interestingly with decreasing pAKT levels there was marked increase in the level of IGF-1R, suggesting a cross talk between IGF-1R and AKT. However, no significant change in oct4 expression at mRNA levels was observed after AKT inhibition.

5. Conclusions and Future Prospects:

We found an enrichment of SP fraction with increased self-renewal and stemness phenotype during acquirement of resistance against cisplatin, paclitaxel and combination treatment in ovarian cancer cells. Real time monitoring of tumor formation with bioluminescence imaging, showed that SP cells from Pac^{ER} stage initiated the tumor formation much earlier than SP cells from Cis^{LR} stage. We also reported a preferential regulation of IGF-1R and AKT signaling at early and late resistant stages respectively. While IGF-1R levels were found to be up regulated only at early stages (Cis^{ER}, Pac^{ER} and Cis-Pac^{ER}), higher levels of activated Akt was associated with late resistance. Inhibition of IGF-1R expression resulted in down regulation of stemness like phenotype and stemness gene expression. Thus it is probable that higher IGF-1R expression is required for initiation of resistance development along with maintenance the CSC like phenotype. Using small molecule inhibitor against IGF-1R auto phosphorylation, we showed increased potentiating cytotoxic effects of chemotherapeutic agents at early stage of resistance. As IGF-1R levels go down in late resistant cells (Cis^{LR}, Pac^{LR} and Cis-Pac^{LR}), it is possible that high level of pAKT maintain the chemoresistance and CSC like phenotype. We also found a feedback loop between IGF-1R and pAKT, where inhibition pAKT relieved the suppression and resulted in up regulation of IGF-1R. It would be interesting to identify the transcriptional regulators of IGF-1R and AKT signaling and understand the relation between stemness genes and IGF-1R/Akt at early and late resistant stages in future.

6. References

1. Torre, L.A., et al., *Global cancer statistics, 2012*. CA Cancer J Clin, 2015. **65**(2): p. 87-108.
2. Chen, V.W., et al., *Pathology and classification of ovarian tumors*. Cancer, 2003. **97**(10 Suppl): p. 2631-42.
3. Agarwal, R. and S.B. Kaye, *Ovarian cancer: strategies for overcoming resistance to chemotherapy*. Nat Rev Cancer, 2003. **3**(7): p. 502-16.
4. Pliarchopoulou, K. and D. Pectasides, *Epithelial ovarian cancer: focus on targeted therapy*. Crit Rev Oncol Hematol, 2011. **79**(1): p. 17-23.
5. Heryanto, Y.D., et al., *In vivo molecular imaging of cancer stem cells*. Am J Nucl Med Mol Imaging, 2015. **5**(1): p. 14-26.
6. Deng, S., et al., *Distinct expression levels and patterns of stem cell marker, aldehyde dehydrogenase isoform 1 (ALDH1), in human epithelial cancers*. PLoS One, 2010. **5**(4): p. e10277.
7. Bonnet, D. and J.E. Dick, *Human acute myeloid leukemia is organized as a hierarchy that originates from a primitive hematopoietic cell*. Nat Med, 1997. **3**(7): p. 730-7.
8. Lapidot, T., et al., *A cell initiating human acute myeloid leukaemia after transplantation into SCID mice*. Nature, 1994. **367**(6464): p. 645-8.
9. Al-Hajj, M., et al., *Prospective identification of tumorigenic breast cancer cells*. Proc Natl Acad Sci U S A, 2003. **100**(7): p. 3983-8.
10. Dalerba, P., R.W. Cho, and M.F. Clarke, *Cancer stem cells: models and concepts*. Annu. Rev. Med., 2007. **58**: p. 267-284.
11. Singh, S.K., et al., *Identification of human brain tumour initiating cells*. nature, 2004. **432**(7015): p. 396-401.
12. Li, C., et al., *Identification of pancreatic cancer stem cells*. Cancer research, 2007. **67**(3): p. 1030-1037.
13. Bapat, S.A., et al., *Stem and progenitor-like cells contribute to the aggressive behavior of human epithelial ovarian cancer*. Cancer Res, 2005. **65**(8): p. 3025-9.
14. Charafe-Jauffret, E., et al., *Breast cancer cell lines contain functional cancer stem cells with metastatic capacity and a distinct molecular signature*. Cancer Res, 2009. **69**(4): p. 1302-13.
15. Liu, H., et al., *Cancer stem cells from human breast tumors are involved in spontaneous metastases in orthotopic mouse models*. Proc Natl Acad Sci U S A, 2010. **107**(42): p. 18115-20.
16. Eckstein, N., *Platinum resistance in breast and ovarian cancer cell lines*. J Exp Clin Cancer Res, 2011. **30**: p. 91.
17. Spentzos, D., et al., *IGF axis gene expression patterns are prognostic of survival in epithelial ovarian cancer*. Endocr Relat Cancer, 2007. **14**(3): p. 781-90.
18. Ouban, A., et al., *Expression and distribution of insulin-like growth factor-1 receptor in human carcinomas*. Human Pathology, 2003. **34**(8): p. 803-808.
19. Eckstein, N., et al., *Hyperactivation of the insulin-like growth factor receptor 1 signaling pathway is an essential event for cisplatin resistance of ovarian cancer cells*. Cancer Res, 2009. **69**(7): p. 2996-3003.
20. Chang, W.W., et al., *The expression and significance of insulin-like growth factor-1 receptor and its pathway on breast cancer stem/progenitors*. Breast Cancer Res, 2013. **15**(3): p. R39.
21. Vlashi, E., et al., *In vivo imaging, tracking, and targeting of cancer stem cells*. J Natl Cancer Inst, 2009. **101**(5): p. 350-9.

Publications in referred journals:

Published Articles.

- **Ram K. Singh**, Snehal M. Gaikwad , Ankit Jinager , Smrita Chaudhury , Amita Maheshwari , Pritha Ray (2014). "IGF-1R inhibition potentiates cytotoxic effects of chemotherapeutic agents in early stages of chemoresistant ovarian cancer cells." *Cancer Lett* 354(2): 254-262.
- Snehal M. Gaikwad¹, Bhushan Thakur, Asmita Sakpal, **Ram K. Singh**, Pritha Ray (2015). "Differential activation of NF-kappaB signaling is associated with platinum and taxane resistance in MyD88 deficient epithelial ovarian cancer cells." *Int J Biochem Cell Biol* 61: 90-102
- Mrinal Srivastava, Mridula Nambiar, Sheetal Sharma, Subhas S. Karki, G. Goldsmith, Mahesh Hegde, Sujeet Kumar, Monica Pandey, **Ram K. Singh**, Pritha Ray, Renuka Natarajan, Madhura Kelkar, Abhijit De, Bibha Choudhary, and Sathees C. Raghavan. 2012. "An inhibitor of nonhomologous end-joining abrogates double-strand break repair and impedes cancer progression." *Cell* 151(7): 1474-1487
- **Accepted Articles.** Not applicable
- **Communicated Articles.** Not applicable

Other publications.

Book Chapter:

- **Ram K Singh**, Snehal M Gaikwad, Subhoshree Chatterjee and Pritha Ray (2014). 'Stem cell: The Holy Grail of Regenerative Medicine', 19- 70, Engineering in Translational Medicine ISBN 978-1-4471-4371-0 ISBN 978-1-4471-4372-7 (eBook) DOI 10.1007/978-1-4471-4372-7 Springer London Heidelberg New York Dordrecht Springer Publications, London.

Conference abstracts

- **Ram K Singh**, Ankit Jinager, A. De and Pritha Ray, IGF-1R: A key linker between chemoresistance and cancer stem cells in epithelial ovarian cancer cells, **platform presentation** at "5th Asia Pacific Summit on Cancer Therapy under young researcher's forum: 20-22 July, 2015, Brisbane, Australia.
- **Ram K Singh**, Ankit Jinager, Snehal M. Gaikwad and Pritha Ray "Association of cancer stem/initiating cells with chemoresistance and epithelial-mesenchymal transition in ovarian carcinoma" Poster presentation at XXXVIII All India Cell Biology Conference, 2014 Central Drug Research Institute, Lucknow, India.
- **Ram K Singh**, Snehal M Gaikwad, Pritha Ray "The IGF-1R signaling oscillates during acquirement of resistance to cisplatin and paclitaxel in ovarian cancer cells" Poster presentation at XXXVII All India Cell Biology Conference, 2013 in Stem, JN Tata Auditorium, IISC, Bangalore, India.

- **Ram K Singh**, Ankit Jinager, Snehal M. Gaikwad and Pritha Ray “Association of cancer stem/initiating cells with chemoresistance and epithelial-mesenchymal transition in ovarian carcinoma” Poster presentation at XXXVIII All India Cell Biology Conference, **2014** Central Drug Research Institute, Lucknow, India.
- **Ram K Singh**, Snehal M Gaikwad, Pritha Ray “The IGF-1R signaling oscillates during acquirement of resistance to cisplatin and paclitaxel in ovarian cancer cells” Poster presentation at XXXVII All India Cell Biology Conference, **2013** in Stem, JN Tata Auditorium, IISC, Bangalore, India.
- **Ram Kumar Singh**, Ankit Jinager, Snehal M Gaikwad and Pritha Ray, “Role for Oct4 and Sox2 in Chemoresistant Epithelial Ovarian Cancer” **platform presentation** at “4th International Conference on Stem Cells and Cancer (ICSCC-2013): Proliferation, Differentiation, and Apoptosis. , 19 - 22 October, **2013**, Haffkine institute, Mumbai, India.
- **Ram K Singh** and Pritha Ray, “Ovarian Cancer Stem Cells (OCSC) in Acquired Chemoresistance” poster presentation during Asia Oceania research organisation on Genital Infections and Neoplasia- India (AOGIN-India), **2012**, Mumbai, India.

Signature of Student: *Ram K Singh*

Date: *3/7/15*

Doctoral Committee:

S. No.	Name	Designation	Signature	Date
1.	Dr. S.V. Chiplunkar	Chairperson	<i>S.V. Chiplunkar</i>	<i>9/7/15</i>
2.	Dr. Pritha Ray	Guide & Convener	<i>Pritha Ray</i>	<i>3/7/15</i>
3.	Dr. Sorab N Dalal	Member	<i>S. N Dalal</i>	<i>3/7/15</i>
4.	Dr. Shilpee Dutt	Member	<i>Shilpee Dutt</i>	<i>3/7/15</i>
5.	Dr. Supriya Chopra	Member	<i>Supriya Chopra</i>	<i>3/7/15</i>

S.V. Chiplunkar

Dr. S.V. Chiplunkar
Director, Chairperson
Academics Training Program,
ACTREC-TMC

Dr. S. V. Chiplunkar
Director
Advanced Centre for Treatment, Research &
Education in Cancer (ACTREC)
Tata Memorial Centre
Kharghar, Navi Mumbai 410210.

2

K. Sharma

Prof. K. Sharma
Director, Academics
Tata Memorial Centre
PROF. K. S. SHARMA
DIRECTOR (ACADEMICS)
TATA MEMORIAL CENTRE,
PAREL, MUMBAI

Chapter 1
Introduction and Review of Literature

Hypothesis:

Since acquisitions of resistance towards drugs exert dynamic and gradual changes in molecular and cellular pathways in cancer cells, it is possible that differential regulation of critical signalling pathways are associated with resistance development. These differentially regulated cascades would not only influence the kinetics and stages of resistance but also the properties of Cancer Stem Cells which are indispensable entities of drug resistant tumors.

Chemoresistance:

Majority of the cancers are curable if diagnosed at early stages. Once diagnosed the primary treatment modalities involve surgery, chemotherapy and radiotherapy. Despite of having significant advancements in disease management in recent years, only a handful of them are cured for life time[1, 2]. Ovarian cancer is the one of the malignancies where diagnosis is done very late because of the asymptomatic nature of the early phases of the disease. Surgery followed by chemotherapy or neo-adjuvant chemotherapy followed by surgery are the main lines of treatments, however generation of chemoresistance delimits the therapeutic efficacy [3, 4]. Chemoresistance is a multifactorial event that involves defects in cell cycle regulatory proteins, DNA repair enzymes, membrane transporters, detoxification enzymes, increased cell survival pathways and alterations in receptor tyrosine kinases (RTKs)[5, 6]. Plethora of drugs targeting RTKs are now in clinical trials for various malignancies [7-9]. However, very few targeted therapies (such as VEGFR targeting) have shown promising result for ovarian cancer patients [10-13]. During ovarian development Insulin like Growth Factor 1 Receptor (IGF-1R) is found to be indispensable for its normal growth and functioning[14]. In the diseased stage, IGF-1R signaling gets altered giving rise to transformed phenotype[15]. This altered signalling may also impart drug resistance to the cancer cells [5, 16, 17]. Generation of resistance towards chemotherapeutic drugs could be innate or adaptive. Intrinsic or innate resistance originates

from cells which have higher capacity of sustenance and survival under the pressure of chemotherapeutic drugs (Figure1A) [18]. This resistance could be attributed through limited drugs uptake, enhanced efflux, or activating detoxification of drugs, enhanced DNA repair machinery and up-regulated anti apoptotic proteins[19-23]. Such innate resistance could arise due to presence of tumor cells bearing specific mutations responsible for developing resistant characters [24] or from the existence of special type of cancer cells, often termed as cancer stem cells which are inherently resistant towards various chemotherapeutic regimen and are highly tumorigenic in nature (Figure 1B) [25-27]. On the other hand adaptive resistance or acquired resistance is a result of multiple insults occurring on the tumor cells during therapy resulting in several mutations and alterations in key signaling pathways. Furthermore, in the process of acquiring resistance, the tumour may become cross-resistant to a range of chemotherapies and result in resistance [23], which ultimately leads to treatment failure in over 90% of patients. Enrichment of cancer stem cells during the course of therapy is seen as another plausible cause for acquired resistance [28].

Cisplatin/carboplatin and paclitaxel form the main line of chemotherapeutic regimen in ovarian cancer. However the emergence of platinum and taxol resistance is a major obstacle for clinical management of this deadly disease. Even though 1st line of chemotherapy has shown good response, majority of the patients face relapse of the disease and succumb to death [29, 30]. The intimate association of cancer stem cells with both innate and acquired resistance demands extensive research to understand their biology for future targeted therapy, the ultimate solution to embark upon advanced stage ovarian cancers.

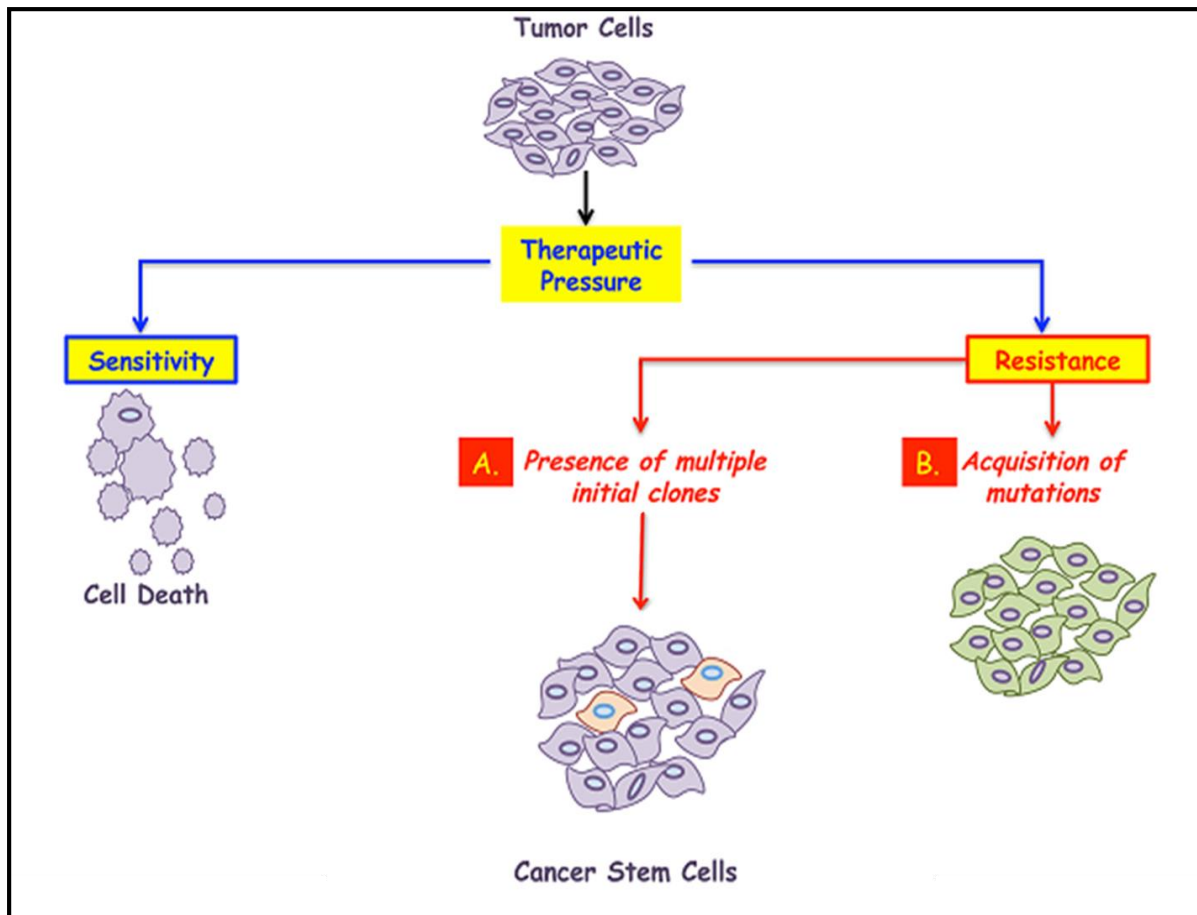


Figure 1: Generation of resistance to therapeutic pressure: (A) Presence of multiple initial clones within the heterogeneous tumor which upon exposure to drugs emerges as a dominant population (cancer stem cells). (B) Acquisition of deleterious mutations within the cancerous cell upon exposure to various chemotherapeutic drugs leads towards generation of chemoresistance.

Ovarian Cancer

The Epidemiology of Ovarian Cancer:

Ovarian cancer is a foremost cause of morbidity and mortality, especially in middle-aged women suffering from gynaecologic malignancies. As per Globocan report, approximately 239,000 new cases are reported worldwide annually and around 152,000 women annually succumb to this fatal disease [31]. Across the globe, ovarian cancer ranks 7th on its prevalence rate as compared to other cancer types. However in India, the situation is alarming

as it is the fourth most common cancer amongst women with an annual occurrence of 26,834 new cases [31, 32].

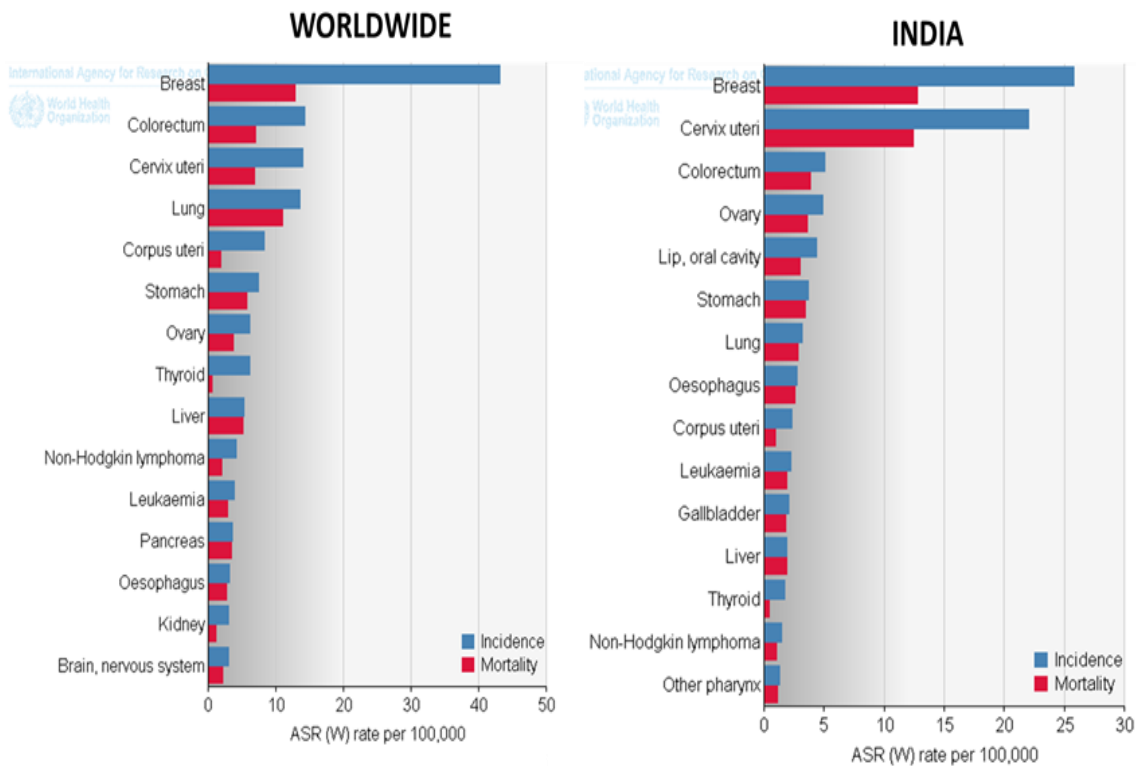


Figure 2: Prevalence rate of various malignancy amongst women in India and world: Prevalence of ovarian cancer across the globe ranks 7th however in India it is 4th leading cause for cancer related death amongst women.

Incidence and Mortality of Ovarian cancer across India and worldwide:

According to the Globocan report 2012, worldwide incidence and mortality rate for ovarian cancer are estimated to be 3.6 and 4.3 percent respectively. However, in India the scenario of incidence and mortality is much higher with 5.0% incidence and 6.0% mortality rate as shown in the figure 3[31, 32]. This draws more attention for an imperative need of active research in the field of ovarian cancer. There could be various reasons for the higher rate of mortality in

case of ovarian cancer. The major causes are late diagnosis of the disease and generation of chemoresistance.

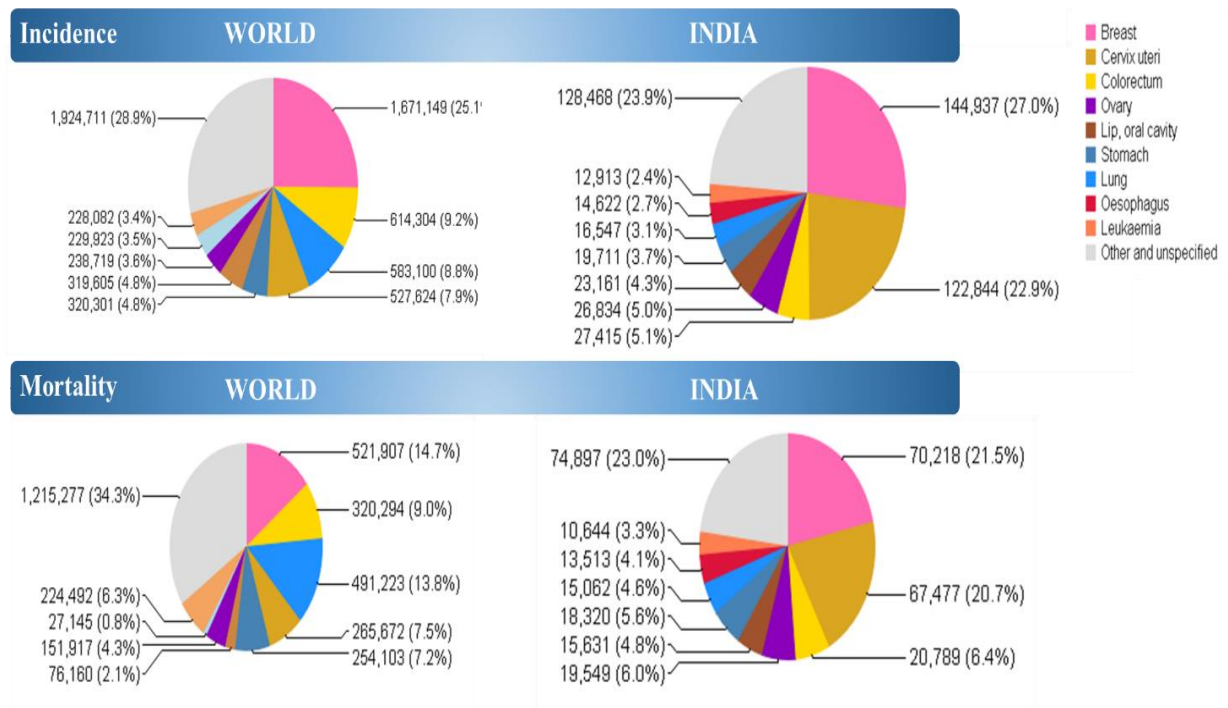


Figure 3: Incidence and mortality rate of various malignancy amongst women in India and worldwide: Incidence of ovarian cancer across the world is 3.6% with mortality rate 4.3%. In India rate of incidence and mortality is 5.0% and 6.0% respectively.

Heterogeneity of the disease:

Ovarian cancer is a highly heterogeneous disease which involves different cell types present in the normal ovary[33]. Based upon the histology of tumor specimen, and cell of origin World Health Organization (WHO) has broadly classified the ovarian tumors into three major groups. (1) Epithelial Ovarian Carcinoma (EOC); (2) Ovarian Germ cell Carcinoma; (3) stromal Cell Carcinoma [33, 34].

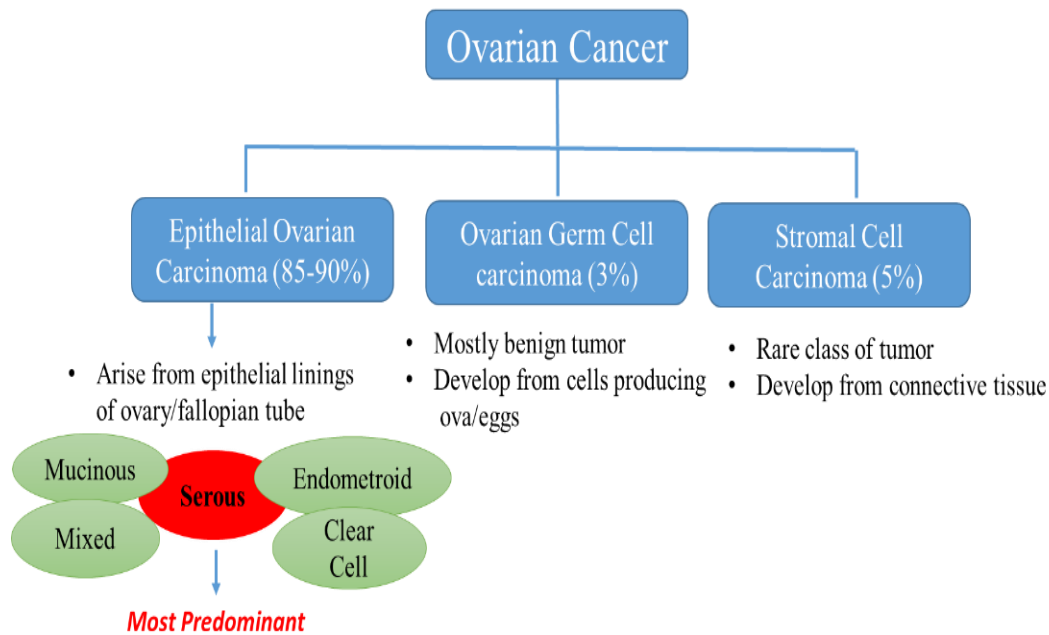


Figure 4: Heterogeneity in ovarian cancer: Ovarian cancer can be classified into three broad categories depending upon the cell of origin. (1) Epithelial ovarian cancer which constitutes 85-90% of cases. (2) Ovarian germ cell tumor that constitutes only 3% of diseased population. (3) Stromal cell carcinoma which constitutes 5% of the total diseased population.

1. **Epithelial Ovarian Carcinomas (EOCs):** The majority of the ovarian cancers (85-90%) arise from the thin layer of cuboidal cells known as germinal epithelium that sheaths the ovaries. EOCs are mostly found in women aged 45-70 years who have been through their menopause. Epithelial tumors are again classified into five broad histological subtypes: Serous (70%), Mucinous (10%), Endometrioid (5%) and Clear cell (5%), mixed or carcinosarcomatous müllerian tumours (less than 5%) (Percentage denoting the prevalence of occurrence).
2. **Ovarian Germ Cell Tumors:** Ovarian germ cell tumors develop from the cells that produce ova or eggs. Most germ cell tumors are benign (non-cancerous) in nature and accounts for 3% of all ovarian cancers. They are frequently found in teen age girls or women in their twenties.
3. **Stromal Cell Tumors:** Ovarian stromal tumors are a rare class of tumors that develop from the connective tissue cells that hold the ovary together and those that produce the

female hormones like oestrogen and progesterone. It accounts for 5% of ovarian cancer and occur in women aged 40-60 years.

1.2.2. Diagnosis and staging of ovarian cancer:

Any cancer if detected early significantly improves the survival rate, however ovarian cancer is still one of the deadliest cancer because it is difficult to be diagnosed at early stages. At early stages, ovarian cancer is highly asymptomatic in nature. Altered bowel and bladder habits, abdominal pain and swelling, dyspepsia, nausea, vomiting, unusual fatigue and weight changes that are often not recognised as indication of ovarian cancer, are the typical problems [35, 36]. In majority of the cases, disease is detected once the patient shows persistent bloating, distension along with accumulation of ascetic fluid in the peritoneum cavity. Till the time of such observations, the disease already reaches to stage III or IV with substantial metastasis which creates a major hurdle in the disease management. The cancer antigen 125 (CA125), a serum based biomarker is still the only diagnostic marker used in the clinics[37]. However CA-125 is not absolutely specific to diseased state of the ovary. CA-125 levels may also increase in many other clinical manifestations like, endometriosis, tuberculosis, fibroids and pelvic inflammatory disease. Another candidate molecule that might serve the purpose of tumor marker is a secreted glycoprotein, human epididymis protein 4 (HE4) which is highly expressed by serous and endometrioid epithelial ovarian cancer cells (Drapkin et al 2005, cancer research). In pre-menopausal women, HE4 is the most sensitive and specific marker for ovarian malignancy. Various combinations of tumor markers (CEA, CA72-4, hCG; inhibin B and Anti-Mullerian Hormone) along with CA125 are under investigations for their potential in determining the disease. However, HE4 along with CA125 appears to be the most potent candidate as a tumor marker for initial diagnosis of the disease[38]. Along with this CA-125 based ELISA, transvaginal sonography, magnetic resonance imaging (MRI), and computed tomography scan (CT) are used for diagnosis with higher precision[39]. One of the elegant

studies performed by CB Bankhead in 2008 says that ovarian cancer is not a silent killer rather clinicians should distinguish between persistent and fluctuating distension. Recognition of the significance of symptoms described by women could lead to earlier and more appropriate referral and thus early detection of the disease [35, 36]. In this study author has tried to mark the symptoms (Abdominal distension and bloating) in women with and without cancer in order to identify the diagnostic factors. However the accurate diagnosis of early stage disease is still elusive.

According to the classification made by the International Federation of Gynaecology and Obstetrics (FIGO), ovarian cancer is been grouped into four different stages (Stage I to IV) as described in table 1. However from January 2014, FIGO classification has brought certain refinements which are mentioned in table 1. [40].

STAGE I: Tumor confined to ovaries			
OLD		NEW	
IA	Tumor limited to 1 ovary, capsule intact, no tumor on surface, negative washings/ascites.	IA	Tumor limited to 1 ovary, capsule intact, no tumor on surface, negative washings.
IB	Tumor involves both ovaries otherwise like IA.	IB	Tumor involves both ovaries otherwise like IA.
IC	Tumor involves 1 or both ovaries with any of the following: capsule rupture, tumor on surface, positive washings/ascites.	<i>IC Tumor limited to 1 or both ovaries</i>	
		IC1	<i>Surgical spill</i>
		IC2	<i>Capsule rupture before surgery or tumor on ovarian surface.</i>
		IC3	<i>Malignant cells in the ascites or peritoneal washings.</i>

STAGE II: Tumor involves 1 or both ovaries with pelvic extension (below the pelvic brim) or primary peritoneal cancer			
OLD		NEW	
IIA	Extension and/or implant on uterus and/or Fallopian tubes	IIA	Extension and/or implant on uterus and/or Fallopian tubes
IIB	Extension to other pelvic intraperitoneal tissues	IIB	Extension to other pelvic intraperitoneal tissues
IIC	IIA or IIB with positive washings/ascites.		

****Old stage IIC has been eliminated****

STAGE III: Tumor involves 1 or both ovaries with cytologically or histologically confirmed spread to the peritoneum outside the pelvis and/or metastasis to the retroperitoneal lymph nodes			
OLD		NEW	
IIIA	Microscopic metastasis beyond the pelvis.	<i>IIIA (Positive retroperitoneal lymph nodes and /or microscopic metastasis beyond the pelvis)</i>	
		<i>IIIA1 Positive retroperitoneal lymph nodes only</i>	
		<i>IIIA1(i)</i>	<i>Metastasis ≤ 10 mm</i>
		<i>IIIA1(ii)</i>	<i>Metastasis > 10 mm</i>
		<i>IIIA2 Microscopic, extrapelvic (above the brim) peritoneal involvement ± positive retroperitoneal lymph nodes</i>	
IIIB	Macroscopic, extrapelvic, peritoneal metastasis ≤ 2 cm in greatest dimension.	IIIB	<i>Macroscopic, extrapelvic, peritoneal metastasis ≤ 2 cm ± positive retroperitoneal lymph nodes. Includes extension to capsule of liver/spleen.</i>
IIIC	Macroscopic, extrapelvic, peritoneal metastasis > 2 cm in greatest dimension and/or regional lymph node metastasis.	IIIC	<i>Macroscopic, extrapelvic, peritoneal metastasis > 2 cm ± positive retroperitoneal lymph nodes. Includes extension to capsule of liver/spleen.</i>

STAGE IV: Distant metastasis excluding peritoneal metastasis			
OLD		NEW	
IV	Distant metastasis excluding peritoneal metastasis. Includes hepatic parenchymal metastasis.	IVA	<i>Pleural effusion with positive cytology</i>
		IVB	<i>Hepatic and/or splenic parenchymal metastasis, metastasis to extra-abdominal organs (including inguinal lymph nodes and lymph nodes outside of the abdominal cavity)</i>

Table: 1 FIGO classification of ovarian cancer: Table showing the comparison made between old and new classification of ovarian cancer from

Apart from FIGO staging of ovarian cancer, its classification has also been made on the basis of frequent mutations identified in several genes like *KRAS*, *BRAF*, *ERBB2*, *P53*, *CTNNB1*, *PIK3CA* and *PTEN* which has been briefly described under the dualistic model of ovarian carcinoma [41, 42].

Dualistic Model of ovarian carcinoma:

Several genetic and epigenetic changes have been discovered in ovarian cancer patients and approximately 30 genetic abnormalities either in oncogenes or tumor suppressor genes have been described by J Mendelsohn [43]. Based on morphology and genetic mutations, ovarian cancer arising from surface epithelium of diseased ovary/fallopian tube can be grouped under two different types. This “dualistic model”, was proposed by Kurman et al., (2010), where EOC can be broadly classified into two broad categories, type I and type II [42].

Type I: These are low grade serous, low-grade endometrioid, clear cell and mucinous carcinomas having slow proliferation rate. Common mutations observed under this category involve *KRAS*, *BRAF*, and *ERBB2* mutations which occur in approximately two thirds of low-grade serous carcinomas whereas *TP53* mutations are very rare in these tumors. Low-grade endometrioid carcinomas also have aberrations in the Wnt signaling pathways involving somatic mutations of *CTNNB1* (encoding β -catenin), *PTEN* and *PIK3CA*.

Type II: Type II tumors comprise of high-grade serous carcinoma, high-grade endometrioid carcinoma, malignant mixed mesodermal tumors (carcinosarcomas), and undifferentiated carcinomas. They are usually present in advanced stage (stages II-IV) in more than 75% of cases. The high grade ovarian carcinoma is often accompanied with higher proliferation rate of the tumor cells. This type of tumor harbours TP53 mutations in more than 95% cases.

However, till today drugs used to treat ovarian cancer do not account for these heterogeneity and produce toxic effects in general. Apart from platinum-taxol based therapy, few targeted therapies like poly(ADP-ribose) polymerase inhibitor olaparib for the patients with BRCA1 or

BRCA2 mutations and recurrent ovarian cancer are used in clinic[44]. PARP inhibitors in BRCA mutation posed synthetic lethality via combination of base excision repair inhibition with a defective homologous DNA repair pathway which results in accumulation of double-strand breaks, collapsed replication forks, and eventual cell death [44, 45]. Trastuzumab or Herceptin, are monoclonal antibody which are directed against ERBB2 and has been studied in a phase II trial in patients with recurrent or refractory ovarian or primary peritoneal carcinoma with overexpression of HER2. Similarly a phase II trial of single agent sorafenib which is a multikinase inhibitor targeting both MAPK and VEGFR 1, 2 and 3 and platelet-derived growth factor receptor (PDGFR) in persistent or recurrent EOC or primary peritoneal cancer was also performed [45]. There were 2 partial responders and 20 patients with stable disease out of total 59 patients. Despite of this there is generation of resistance against targeted therapy also.

Site of Origin:

Each of the subtypes of epithelial ovarian cancers is recognized by a set of unique clinical, morphological and molecular features owing to which the understanding of the origin of these subtypes becomes necessary. However, the site of origin of these subtypes is a matter of debate. Earlier it was believed that the ovarian tumors originate in the mesothelium, invaginates into the stroma to form inclusion cysts that ultimately undergo malignant transformation. Recent studies have shown that most of the epithelial ovarian tumors have an extra ovarian origin. Like, the high grade serous is believed to originate as a metastatic event of serous tubal intraepithelial carcinomas and occult high grade serous carcinoma of the fallopian tube [41]. Whereas the origin of low grade serous is considered to be a result of the event of mullerian metaplasia. Similarly, endometriosis is considered to be the source of endometrioid and clear cell carcinoma although the proper site of origin for clear cell carcinoma is still unclear. Another subtype of ovarian cancer that is transitional in nature arises from transitional

epithelium of urinary bladder. Mucinous is thought to originate from the translational epithelium of the extra peritoneal cavity[41, 42].

Mode of action of cisplatin:

Cisplatin, also called cis-diamminedichloroplatinum (II), is a metallic (platinum) coordination compound with a square planar geometry which is a white or deep yellow to yellow–orange crystalline powder at room temperature synthesized from potassium tetrachloroplatinate [45]. It is slightly soluble in water and soluble in dimethylprimanide and N, N-dimethylformamide (DMSO) but Sigma recommends 0.9% saline. Cisplatin is a well-known chemotherapeutic drug which has been used for treatment of numerous human cancers including bladder, head and neck, lung, ovarian, and testicular cancers. Its mode of action has been linked to its ability to crosslink with the purine bases on the DNA and thus interfering with DNA repair mechanisms, causing DNA damage, and subsequently inducing apoptosis in the cancer cells via different molecular players [46] (Figure 5).

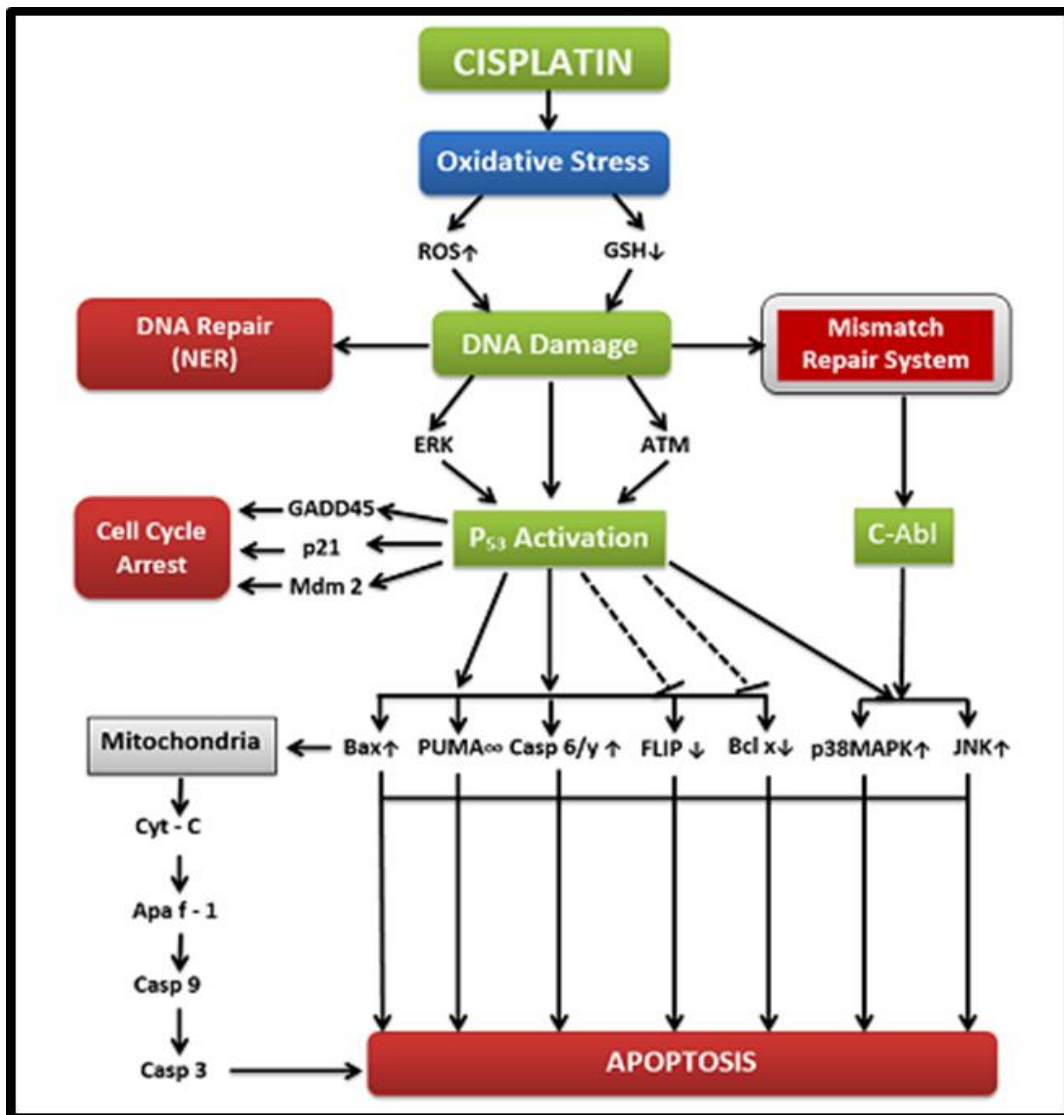


Figure 5: Mode of action of cisplatin: Cisplatin intercalates the DNA and induces generation of reactive oxygen species ROS. Damaged DNA activates P53 via ERK and ATM proteins. This results in either cell cycle arrest or apoptosis via various molecular players.

Apart from cisplatin there are two other platinum based drugs, oxaloplatin and carboplatin that are currently being used in the clinics as a major line of chemotherapeutic regimen[47, 48]. Other class of drug that entered into the clinics after cisplatin for the treatment of ovarian cancer was paclitaxel [49, 50].

Mode of action of paclitaxel:

Paclitaxel, another antitumor drug isolated from bark of the Pacific yew, *Taxus brevifolia* demonstrated encouraging activity in human malignancies currently plays a major role in cancer chemotherapy[51]. Paclitaxel is a complex diterpene having a taxane ring with a four-membered oxetane ring and an ester side chain at position C-13. Paclitaxel binds to tubulin towards negative end and protects microtubule against disassembly and thus hinders cell division and also chromosome segregation leading to cell death [52].

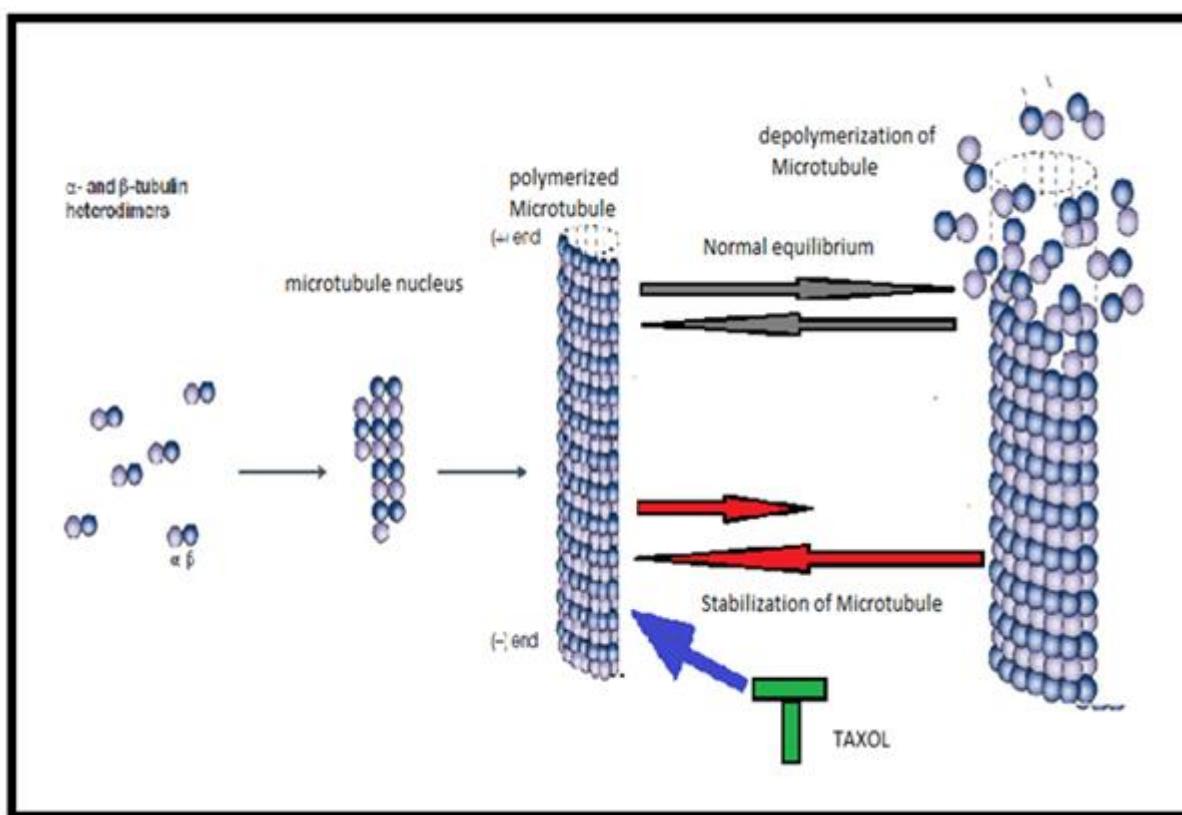


Figure 6: Mode of action of paclitaxel: Paclitaxel binds to the negative terminal end of tubulin and brings stabilization and protects against disassembly. This alters the normal equilibrium of polymerization and depolymerisation resulting in defective chromosome segregation during cell cycle.

In 1992, FDA approved Taxol for the first time to treat ovarian cancer patients, since then it has been in clinical practice as a combinatorial agent with cisplatin[52]. Although treatment with Taxol has led to improvement in the duration and quality of life for some cancer patients, the majority eventually develop progressive disease even after initial response to taxol treatment. Other than paclitaxel, docetaxel is another chemotherapeutic drug used in the clinics[53, 54]. For the last two decades, platinum (cisplatin & carboplatin) and taxol (paclitaxel and docetaxel) based drugs are the main line of chemotherapeutic treatment for ovarian cancer. Therefore it is important to understand the basic mechanism of generation of chemoresistance against these two drugs.

Disease Management and treatment modality:

Ovarian carcinoma at stage I & II can be cured with higher efficacy through surgical removal of the diseased organs/s such as the uterus, both fallopian tubes, and both ovaries (a hysterectomy with bilateral salpingo-oophorectomy). However the biggest challenge lies in identifying the disease at these early stages. Currently there are no early diagnostic markers for the correct identification of this deadly disease and hence the majority of the cases belong to advanced-stage ovarian carcinoma (Stage III and Stage IV) which means that the disease has extended to pelvic/ aortic lymph nodes, peritoneum, intra-abdominal organs or disease outside the abdominal cavity[40]. In such cases there are two possible treatment modalities as mentioned in figure 7. First, the cancer is surgically removed followed by the removal of the uterus, both fallopian tubes, both ovaries, and omentum (fatty tissue from the upper abdomen near the stomach and intestines). Sometimes tumor deposits are also seen growing on the intestines, in such cases, part of the intestine need to be removed[55, 56]. Once the tumor has been optimally debulked, combination chemotherapy is given for 6 cycles. The combination used most often is carboplatin (or cisplatin) and a taxane, such as paclitaxel.

Another option for the treatment starts with neoadjuvant chemotherapy followed by surgery. Neoadjuvant refers to the administration of anti-cancer chemotherapeutic drug prior to surgery [57-59]. When surgery is performed after chemotherapy treatment, it is referred to as interval cytoreduction. Since neoadjuvant chemotherapy can reduce the size of the cancer, it allows the surgeons to remove the tumor more efficiently and thus more effective results are obtained from subsequent chemotherapy. Currently at Tata Memorial Centre, Mumbai, the treatment of stage III and stage IV involves 3-4 cycles of neoadjuvant chemotherapy followed by surgery and again 2-3 cycles of chemotherapy.



Figure 7: Different treatment strategy for ovarian cancer: There are two different treatment strategy for ovarian cancer. Option 1 where surgery is followed by six cycles of chemotherapy and option 2 where three cycles of adjuvant chemotherapy is given followed by surgery and again three cycles of chemotherapy.

Recently Kehoe et al (2015) have shown that in women with stage III or IV ovarian cancer, survival with primary chemotherapy before surgery to be an acceptable standard of care for women with advanced ovarian cancer[60]. In this study they have randomly divided 552 ovarian cancer patients for the treatment with either option # 1 or option # 2 as described above. Hence 276 patients were assigned to primary surgery and 274 to primary chemotherapy. Till May 31, 2014, out of 552 patients, 451 deaths had occurred: 231 in the primary-surgery group versus 220 in the primary-chemotherapy group with median overall survival of 22.6 months in

the primary-surgery group versus 24.1 months in primary chemotherapy. This study shows that primary chemotherapy before surgery is an alternative clinical management strategy to primary surgery, which could reduce morbidity in many women with advanced ovarian cancer. An extensive study designed under moon shot programme for ovarian cancer at M D Anderson centre has proven to be of great benefit for increased survival. Here they developed a unique surgical management algorithm which has already being used to treat more than 155 ovarian cancer patients. With this algorithm-based approach, all women with suspected advanced ovarian cancer undergo laparoscopic assessment of the tumor burden. This algorithm based approach allowed distribution of patients to the right treatment arm by determining who should immediately undergo aggressive surgery and who should first receive adjuvant chemotherapy followed by surgery [61].

Even though patient responds to initial treatments of chemotherapy in majority of cases, still the relapse rate is still very high and thus overall survival rate for EOC is only 45%. Depending upon the time of relapse resistance has been classified into four groups as shown in the figure below.

1. Chemo refractory (no response to initial treatment),
2. Chemoresistant (relapse within six months)
3. Partially resistant (relapse within 12 months)
4. Chemosensitive (relapse after a year).

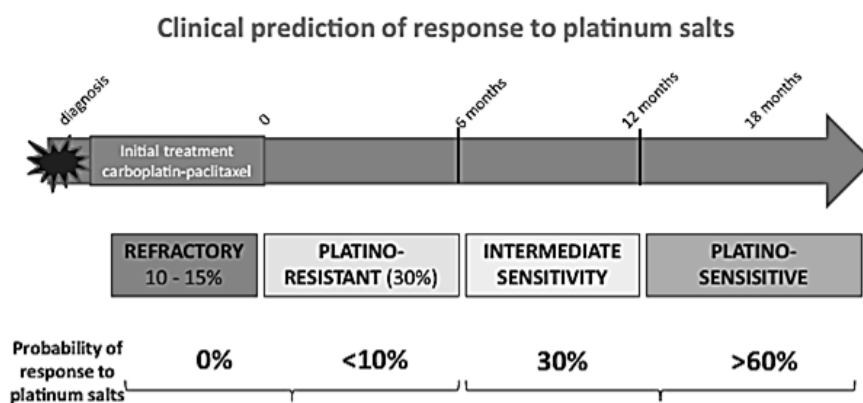


Figure 8: Classification of resistance: Depending up on the response and recurrence of the disease post chemotherapy resistance has been categorized into refractory (no response), platinum resistant (relapse within six months), intermediate sensitivity (relapse within 12 months) and sensitive (relapse after one year).

Chemo resistance can be of two types: Acquired/adaptive resistance and Innate resistance. Acquired resistance develops when the deregulated cancer cells further modify themselves insensitive to drugs by altering more pathways or membrane drug transporters or mutating the protein against which the therapy is developed [62-64]. The classical example is generation of resistance against PARP inhibitors by correcting reversion mutation in *BRCA1* and *BRCA2*. Another way of developing resistance involves activation of alternative pathway when one pathway is blocked. Isoyama et al (2012) showed that resistance was acquired against ZSTK474 (PI3K inhibitor) upon simultaneous upregulation of insulin-like growth factor 1 receptor (IGF1R) pathway [65]. They also extended their study showing that inhibition IGF-1R pathway with selective inhibitors (OSI906 and NVP-AEW541) reverses the acquired PI3K inhibition resistance in glioblastoma cell line SF295.

Innate resistance corresponds to cancer cells harbouring mutations in DNA repair genes and apoptotic genes like P53 along with enhanced drug efflux caused by increased expression of ATP binding cassette (ABC) membrane transporters [66]. These factors make them naturally

resistant towards certain drugs. Innate resistance can also be developed by a small population of cells known as cancer stem cells which has high DNA repair efficiency, increased expression of efflux transporters, increased drug detoxification mechanism, self-renewal property [29, 66-70].

Cancer Stem Cells:

First evidence supporting existence of CSC was obtained from the investigation on acute myeloid leukaemia (AML) when a leukaemia tumor-initiating subpopulation of cells was identified and purified from multiple patients bone marrows with specific set of cell surface phenotype (CD34⁺CD38⁻) which was similar to normal hematopoietic progenitors [71, 72]. Later to this study Al Hajj et al (2003) assayed the tumorigenic property of human breast cancer cells in a xenograft model (NOD/SCID mice). In this model, they showed that only a subset of the breast cancer cells known as breast cancer stem cells (BCSC) with CD44⁺/CD24⁻ phenotype had the ability to initiate and recapitulate the primary tumor [73]. Further many groups came up with reports for the existence of CSCs in different solid tumors of prostate, lung, colon and liver [73-75]. All these CSCs satisfies the basic hall marks to become a Cancer Stem Cell. Efforts are now underway to elucidate the mechanism that regulates CSC function, towards development of chemoresistance and relapse. CSCs have innate ability of drug resistance because of over expression of multiple drug transporters, enhanced DNA repair mechanism, increased self-renewal ability and tumor initiating property [27, 76]. As stated above, several studies focused on the identification of tumor initiating subpopulations in different types of cancer. Bapat et al (2005) for the first time isolated ovarian cancer stem cells from the patients ascitic fluid [77] and developed two immortalized clones, A2 and A4-T that showed CSC like phenotypes expressing CD44, OCT4, NANOG and NESTIN. These immortal clones were able to generate *in vitro* non-adherent, self-renewing spheroids formed tumor xenografts over several generations in mice. Later other groups identified ovarian cancer stem cells based on

different surface markers and different assays as shown in the figure below. After first identification of ovarian cancer stem cells from the patient's ascites, Zhang et al (2008) isolated OCSCs on the basis of presence of cell surface receptor, CD44⁺/CD117⁺ from human primary tumor samples [78]. In the same year Szotech et. al. isolated OCSCs using a functional assay based on the efflux mechanism of a cell called side population (SP) cells, which showed the properties of OCSCs [79, 80]. In later years different cell surface markers (CD133, CD24 and ALDH,) were used by different investigators either alone or in combination for the isolation of ovarian cancer stem cells [81-83].

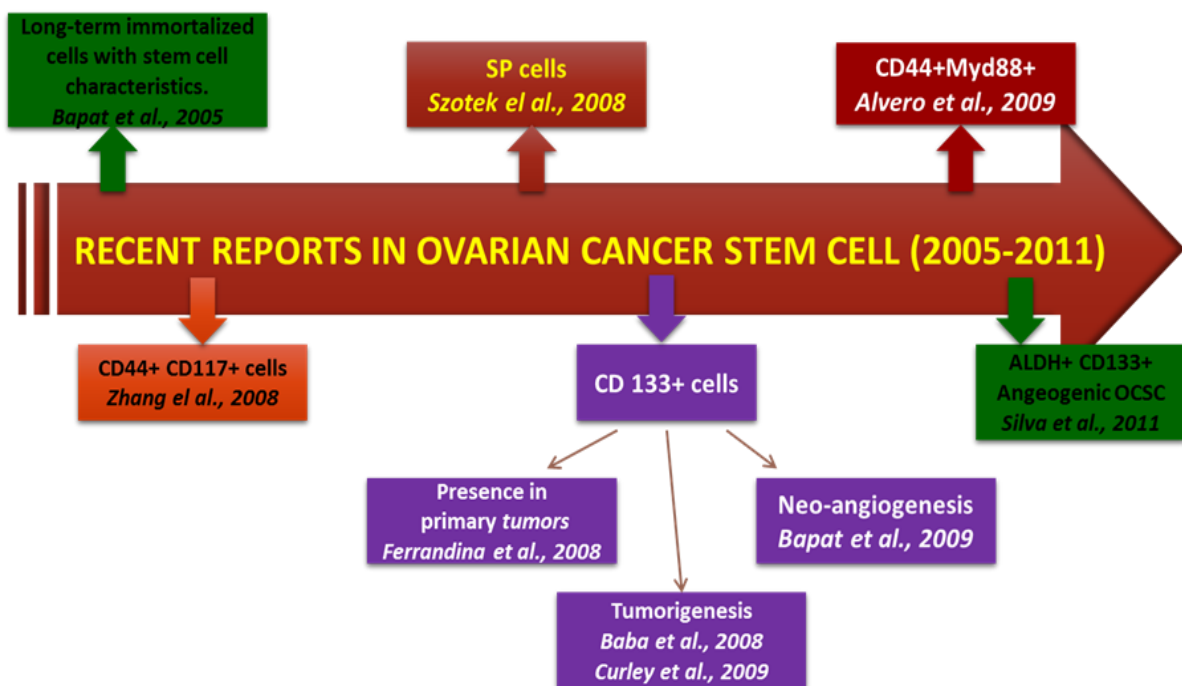


Figure 9: Time line for the identification of different biomarkers in ovarian cancer stem cells (OCSCs): Use of different biomarkers for the isolation of OCSCs which was pioneered by Bapat and group and other functional assays like SP and ALDH assay to isolate OCSCs.

Isolation of cancer stem cells:

To understand the complex behaviour of cancer stem cells, isolation and characterization need to be done with utmost precision. Currently there are four standard methodologies for CSC isolation.

- I. Expression of bio markers:** Majority of the cancer stem cells expresses specific cell surface proteins or receptors through which they can be identified.
- II. Spheroid formation capability:** Spheroids are the multicellular, three dimensional structures that possess stem cell like property by virtue of its increased self-renewal ability.
- III. Side population phenotype:** By virtue of their intrinsic drug resistant character, CSCs can be isolated as 'side population' using fluorescent dye efflux through FACS.
- IV. Aldehyde dehydrogenase (ALDH) activity:** Aldehyde dehydrogenases are group of enzymes that catalyze dehydrogenation (oxidation) of aldehydes to carboxylic acids. This enzymatic activity is found to be over expressed in different types of malignancies as well as in CSCs.
- V. Expression of bio markers:** Isolation of cancer stem cells has been reported by the use of specific set of cell surface markers which majorly comprised of CD (Cluster of differentiation) belonging to the immune cells. Ovarian CSCs were identified and prospectively isolated by several cell surface markers, including CD44⁺, CD117⁺, CD133⁺ and CD24⁺. Apart from these cell surface markers, ALDH1 and ROR1 expression were also associated with cancer stem cells [84]. Di et al (2011) showed that considerable degree of heterogeneity in cell surface markers is present in primary ovarian carcinoma patients [85]. They found that 2/11 patients expressed CD133, of which one patient had 73.3% CD133⁺ and the other possessed only 3.7%. The CD24 status in 13 patients varied from 3.2% - 86.7%. Similar results were observed for CD44⁺

with wide range of expression from 2.2% - 88.2%. In contrast to CD24 and CD44, CD117⁺ was found in 7/11 patients but the expression level varied from 2.9% to 11.2%. ABCG2 expression (a marker for resistance development) was also not observed in all patients. Thus biomarker alone cannot be a good criterion to isolate OCSC.

Spheroid formation capability: This method assess the ability of CSCs to form multi-cellular spheroids in serum free media supplemented with growth factors like EGF, insulin, LIF and bFGF. Not every cancer cell is capable of forming spheres in serum free media. Such unique features of CSCs were exploited by various researchers to isolate CSCs from cancer cell lines and tissues [86]. This technique of CSC isolation was used for neuronal stem cell culture where it was found that only small subsets of cells from the single suspension were capable of growing spheroids in serum deprived media [87]. Recently Vermeulen group (2008) have shown that spheroid cultures of freshly isolated tumor cells from multiple colon carcinomas have the capacity to propagate as a tumor with all differentiated progeny and they can self-renew with the capability of multilineage differentiation [88]. Similarly when ovarian cancer cells are grown in serum free media, only cells with stem cell properties started forming spheroid bodies. These spheroids were found to express stem cell specific biomarkers like Oct4, Nanog and Bmi that allow spheroid to maintain their undifferentiated status [89]. When these spheroids were allowed to grow in serum containing media they failed to differentiate into the primary tumor phenotype. Currently many groups use this property of spheroid formation to enrich the CSC population from established cancer cell lines and primary tissues. Importantly, these enriched CSCs possess both the characteristics of stem cells and malignant tumors cells. Expressions of various other stemness markers (Nanog/Oct-4/CD133/Nestin/Nanog/OCT-4, and ABCG2) were also found in spheroid population [78, 90]. Toru Kondo (2007) in their study have shown

that hoechst 33342 dye based sorted SP cells were able to form spheroids in serum free predefined media whereas NSP cells failed to form spheres [91].

Side population phenotype:

Side population (SP) cells are special group of cells with high expression of membrane transporters. These cells are isolated through flow cytometry using their inherent dye efflux properties of ATP-binding cassette (ABC) transporter proteins [92] (Figure 10). Hoechst 33342/Dye Cycle Violet dye used in this assay binds to the AT rich regions of the minor groove of the DNA. All Non side population (NSP) cells take up the dye and gets stained with Hoechst. On the other hand SP cells because of over expressed ATP transporter proteins do not retain this dye and effluxes it out of the cell. This gives SP cells very low intensity signal when excited under UV laser [93]. Now it becomes easy to differentiate SP vs. NSP cells on the scatter plot during FACS analysis. Such type of population was first identified in mouse bone marrow cells. SP cells are gated using verapamil (drug transport inhibitor) as control, since SP gets remitted from the dot plot in verapamil pre-treated cells.

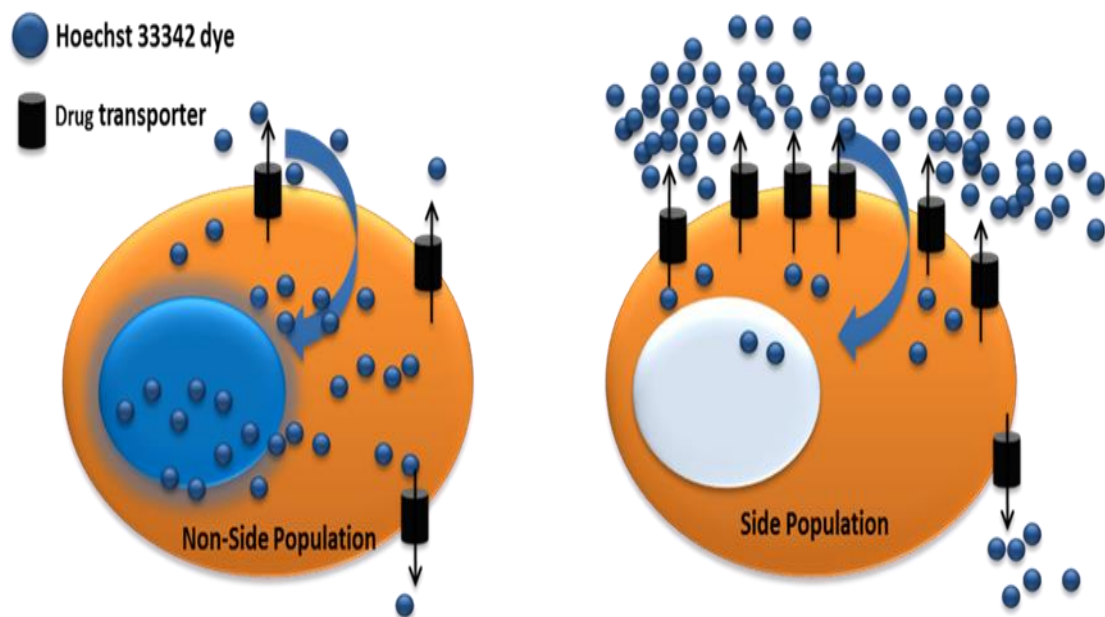


Figure 10: Side Population and non-side population: In side population (SP) fraction due to overexpression of efflux membrane transporters retains very low number of Hoechst dye hence lesser molecules bind to DNA. In contrary in non-side population (NSP) due to less number of membrane transporters most of the dye binds to the DNA. This differential binding of the dye separates SP from NSP population.

Presence of SP cells in ovarian cancer is well documented and reports showed that SP fraction significantly increases in chemoresistant ovarian cancer cell lines [94]. Shinji Hosonuma and Yoichi Kobayashi (2011) have shown that SP could be contained more in recurrent and metastatic tumors than in primary tumors, therefore these SP could be the real culprits for recurrence in ovarian cancer [94, 95].

SP cells have unique drug evading phenotype which resembles the characteristics of a cancer stem cell. SP population when compared with Non Side Population (NSP) are more proliferative, more tumorigenic, less apoptotic and have self-renewal capabilities. It has been well established that such cells do not respond to conventional chemotherapy and radiotherapy, resulting in development of chemoresistance and radioresistance and thus tumor relapse [96,

97]. Various groups working in this field have reported high expression of the ABC transporter MDR1, Bcrp1/ABCG2 proteins on the membrane of SP cells [92, 93, 98]. But association of SP population with acquired resistance is less studied. Thus more detailed study is required to get functional details of SP cells, their characterization and cohesiveness with CSC which would help us to understand the basic mechanism lying behind the chemoresistance and tumor relapse.

Aldehyde dehydrogenase (ALDH) activity: This method of CSCs isolation is based on its phenotype attributed by its high Aldehyde dehydrogenases (ALDH) activity. Aldehyde dehydrogenases are group of enzymes that catalyzes dehydrogenation (oxidation) of aldehydes to carboxylic acids and are mainly involved in the detoxification of process. ALDFELOR assay is performed through FACS for the isolation of ALDH positive cells. Similar to SP assay, an ALDH inhibitor, diethyl amino benzaldehyde (DEAB) is used for proper gating [99]. High level of ALDH activity has been observed in many cancer types. Cancer stem cells often have high level of ALDH activity which bestows their inherent drug resistance. Various investigators are now exploiting this ALDH activity to identify and isolate CSCs [100-102]. Wang et al (2011) have shown that as few 100 ALDH positive cells isolated from osteosarcoma cell line (OS99-1) were able to generate tumor in NOD/SCID mice where as ALDH negative cells could not form tumor [103].

All of the above mentioned techniques to isolate CSCs are not self-sufficient, rather it needs functional validation through its capability to form tumor xenograft in immunocompromised mouse. Till date researchers have shown that CSCs isolated from different tissue type could initiate and recapitulate the primary tumor when implanted in immune-compromised mice. However the kinetics of tumor growth from these CSCs is not fully investigated. A powerful method to monitor CSC mediated tumor development in real time is non-invasive molecular

imaging technique which utilizes reporter genes and reporter probe and compatible imaging modalities.

Cancer Stem Cells in different EOC subtypes:

Since HGSOC is the most predominant subtypes of epithelial ovarian cancer worldwide, majority of the research study on ovarian CSC are performed from this subtype (Figure 9, page 20). However, several researchers have tried to isolate and characterise CSC from other subtypes of EOC. Using ALDH high cells Kuroda et. al., isolated CSCs from Clear cell subtype of ovarian carcinoma and showed that these CSCs possessed higher sphere forming and tumorigenic ability. They also proposed high ALDH expression in clear cell type ovarian cancer to be a poor prognostic marker [104]. Increased expression of CD133 has been correlated with endometrioid cancer stem cells with an ability to self-renew in culture and also to differentiate into cells that recapitulated the primary tumor [105]. Furthermore, SP/ADLH(Br) population showed higher sphere-forming ability, cisplatin resistance, adipocyte differentiation ability and expression of SOX2 than those of SP/ALDH(Low), MP/ALDH(Br) and MP/ALDH(Low) cells suggesting that this could be a better prognostic marker for endometrioid cancer stem cells [106]. Mucinous subtype specific CSCs show over expression of CD24 with higher levels of Nestin, Beta catenin, Bmi-1, Oct4, Oct3/4, Notch1 and Notch4 than the matched CD24 negative cells. These CSCs possessed increased tumorigenic potential in immunocompromised mice [107].

Molecular imaging methods:

Molecular imaging is one of the powerful tools in the field of diagnosis and treatment of cancer. It can provide real time monitoring of different events (one, two or three) simultaneously. Non-invasive molecular imaging of living animals in pre-clinical studies with reporter genes has opened up new avenues to understand different molecular pathways and their association.

On the basis of the spectrum and source of energy used for detection, molecular imaging techniques could be broadly classified into five categories [108].

- I. Optical imaging –fluorescence/bioluminescence imaging
- II. Radionuclide imaging – positron emission tomography (PET) and single photon emission computed tomography (SPECT)
- III. X-ray computed tomography imaging (CT)
- IV. Magnetic resonance imaging (MRI)
- V. Ultrasound

Among all these techniques, bioluminescence imaging has the highest sensitivity and specificity and therefore is suitable to capture subtle molecular/cellular dynamics. Light is generated during catalysis of luciferin/coelenterazine substrates by luciferase enzymes which can be captured using high end CCD camera from small animals [108]. Multimodality bi-fusion construct was generated by Ray et al (2003) where two reporter genes (Fl2-Firefly luciferase and Tdt-Tandem Dimer Tomato) were joined together with short linkers and driven by CMV promoter [109]. CSCs labelled with such bi-fusion construct could be longitudinally monitored after xenotransplantation, giving the details of tumor growth/regression kinetics.

Use of bioluminescence imaging to understand the kinetics of CSC driven disease manifestation is still in infancy and only few such reports are available in literature. In one such study, Liu *et. al* (2010) investigated the role of breast cancer stem cells (BCSCs) in metastasis in real time using optical imaging [110]. They generated human-in-mouse breast cancer orthotopic models using patient derived tumor specimens labelled with optical reporter fusion genes, firefly luciferase (Luc) for whole-body tracking of cells via bioluminescence imaging (BLI) This approach led them to monitor BCSC growth and dissemination, at very early stage

and also permits both macroscopic and microscopic analysis of cancer progression [110]. Therefore, both in vitro and in vivo techniques for isolation and monitoring CSC biology are important to understand the association of chemoresistance and recurrence.

Molecular Signalling pathways in chemoresistance:

Like CSCs, that inherently confer drug resistance to the tumors, several signalling pathways required for normal functioning of an organ may get deregulated in cancer and confer drug resistance. Insulin like growth factor receptor (IGF-1R) mediated signalling is one of such known pathway that has been implicated in normal growth and deregulated growth of cancer cells and in drug resistance [16, 111-113].

IGF-1R Signaling:

Insulin Like Growth factor-1 Receptor (IGF-1R), is a receptor tyrosine kinase (RTK) that contains two extracellular ligand binding α -subunits and two cytoplasmic β -subunits. The β -subunits possess the tyrosine kinase catalytic domains that are activated upon ligand binding [111, 114].

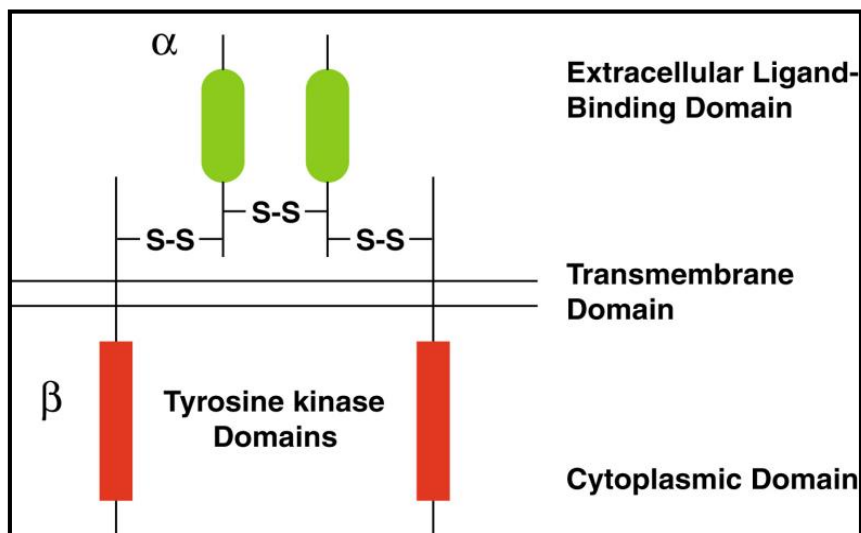


Figure 11: Tetrameric Structure of Insulin Like Growth factor 1 Receptor (IGF-1R): IGF-1R is a tetrameric structure with extracellular ligand binding domain having two α subunits, a

transmembrane domain spanning in the membrane and cytoplasmic domain with two β subunits which contains tyrosine kinase domains.

IGF-1R is activated by its ligands IGF-I and IGF-II, which are produced by the liver and also by many extra hepatic sites including tumor cells and stromal fibroblasts [113]. Binding of the ligand to its receptor (IGF-1R), leads to auto phosphorylation of tyrosine residues 1131, 1135 and 1136 in the kinase domain of the receptor [115]. The IGF-1R activity has been implicated in several different human malignancies, including various epithelial cancers, sarcomas, multiple myeloma, melanoma, and childhood cancers [116, 117]. Binding of ligand to the IGF-1R receptor transmits signals through a battery of signaling molecules which relays its signals via pathways like MAPK and PI3KCA leading towards acquire of chemoresistance. In colon cancer cells, resistance to 5-fluoro-uracil or oxaloplatin showed IGF-1R activation, and treatment with an IGF-1R antibody demonstrated significant growth inhibition of the resistant tumors [118, 119]. IGFs and their receptors play key roles in regulating the normal biology of ovarian epithelial cells and have been implicated in the transformed phenotype of ovarian carcinoma cells [120]. Eckstein et. al. (2009) for the first time showed that IGF-1R is hyper activated during acquirement of cisplatin resistance and AG 1024, an IGF-1R inhibitor could sensitize these resistant cells to cisplatin [16]. This Cisplatin resistance was mediated by the activated PI3K/Akt pathway but not by the MAPK/ERK pathway. In another study, a taxol resistant ovarian cancer cell line (Hey-T30) showed increased expression of IGF-II and activated IGF signaling [17]. Inhibition of IGF-1R (by a small molecule) or IGF-II (by siRNA) led to the reversal of taxol resistance. Though IGF ligands or the inhibition of IGF-1R kinase could sensitize platinum or taxol resistant ovarian cancer cells to the respective drugs, none of these studies had attempted to monitor the combinatorial effects of cisplatin/taxol with these inhibitors based on IGF-1R expression status. The crucial role of IGF/IGF-1R signaling in malignant transformation has attracted attention as promising therapeutic targets either by

developing antibodies or small molecule inhibitors against the receptor or ligands. A few of such antibodies and small molecules have already entered clinical trials [121]. Physiologically IGF-1R expression is regulated by either transcriptional activators (SP1, Foxo3) or repressors (WT1, P⁵³, BRCA1) through direct and co-operative binding to IGF-1R promoter in a context dependent manner [122, 123]. In addition, IGF-1R function can be modulated by ubiquitination and proteasomal degradation through binding of MDM2-E3 ligase [124]. A number of studies identified the IGF system as an important player in the development of gynaecologic tumours as well. Hirano et al. (2004) reported significantly higher expression of IGF-1R in 46 endometrial, 32 cervical, and 20 ovarian cancers [125]. IGF-I, IGF-II, and the IGF-1R have also been shown to be produced in vitro by ovarian cancer cell lines and various ovarian cancer cell lines display autocrine growth loops mediated through the IGF-1R [126, 127]. Using qRT-PCR, Sayer et al. (2005) found significantly higher IGF-II mRNA levels in 109 epithelial ovarian cancers compared with eight normal ovaries [128]. Moreover, high IGF-II gene expression was associated with high-grade advanced stage disease of ovarian cancer with poor survival. All of these investigations suggest that like other cancers, ovarian cancer has deregulated IGF-1R signaling axis which might results in chemoresistant phenotype. Recently Zhao et al (2011) showed that IGF-1R has a possible link between IGF-1R signaling and epithelial mesenchymal transition (EMT) where there has been a strong correlation with increased EMT phenotype with active IGF-1R signalling in hepatocellular carcinoma cell line OSI-906 [129].

Though independent studies revealed association of OCSC with cisplatin or taxol resistance and association of IGF-1R signalling in acquired cisplatin and taxol resistance in ovarian cancer cells, none of them investigated the association between CSC and IGF-1R signalling during acquirement of chemoresistance in ovarian cancer. Additionally relevance of CSC and IGF-1R signalling in platinum-taxol resistance was never investigated. Thus using indigenously

developed chemoresistant (cisplatin, paclitaxel and cisplatin-paclitaxol) cellular models and naturally occurring cisplatin resistance cells, in this study we aimed to investigate the role of CSC and IGF-1R signalling during acquirement of chemo resistance and to look for the possibility of early detection of chemoresistance. In order to answer, how the chemoresistance is generated in ovarian cancer and whether chemoresistance generation can be detected early, we have framed three objectives. Each objective has been described in detail in successive chapters that includes an introduction, results and discussion.

Objective 1: *Isolation and characterization of cancer stem cells (CSC) from chemosensitive & chemo resistant ovarian carcinoma cell lines.*

Objective 2: *Longitudinal monitoring of tumorigenicity of cancer stem cells in living subjects by non-invasive bioluminescence imaging.*

Objective 3: *To study the role of IGF-1R in maintenance of OCSC biology and epithelial mesenchymal transition.*

Chapter 2

Isolation and characterization of cancer stem cells (CSCs) from ovarian cancer cell line

Introduction:

There is an accumulating evidence of initiation, maintenance and recurrence exhibited by different types of human cancer caused by a sub population of cells residing within the tumour termed as cancer stem cells (CSCs) or cancer initiating cells (CICs)[130]. For the rest of the thesis, these cells will be referred as CSCs. With growing understanding about the potential of this small population in tumorigenesis, investigators are now largely focussed on correct identification and isolation of these CSCs to judge their therapeutic potential and for improving targeted therapy. With the advancement of research in the field of cancer stem cell biology, different tools have been developed to isolate CSCs from a heterogeneous population of tumor cells as mentioned briefly in the previous chapter (chapter 1). Different set of various biomarkers have been reported for the isolation of cancer stem cells. However a better understanding is needed to identify and isolate CSCs by making the use of correct biomarker or battery of biomarkers accompanied with other functional assays. As mentioned earlier in the introduction that CSCs play a crucial role not only during tumour initiation but also in therapy resistance and relapse. Hence it is even more important to study the characteristic features and behaviour of these cancer stem cells during tumour growth and acquirement of chemo resistance. In this chapter special emphasis has been made for the identification, isolation and characterization of ovarian cancer stem cells from chemosensitive and chemoresistant cells (indigenously developed against cisplatin, paclitaxel and dual drugs in our lab).

Ovarian Cancer Stem Cells (OCSCs):

A major landmark was made in the field of ovarian cancer in the year 2005, when Bapat and her group for the first time isolated two immortal clones (OCSCs) from the ascitic fluid of the epithelial ovarian carcinoma patients [77]. These clones showed anchorage independent spheroidal structure under *in vitro* condition. They also showed enriched cancer stem cell markers such as CD117, CD44 and nestin. These clones also recapitulated the primary tumor

morphology in tumor xenograft study. Another study led by Szotek group in 2006 found that a sub-population of dye-excluding cells known as side population (SP) exists within the tumour bulk that were highly tumorigenic in nature [80]. Later they confirmed these SP cells to be enriched with CSCs like phenotype by showing the high expression of CD44 and CD117 which were absent in NSP fraction. Zhang et. al (2008) isolated ovarian cancer initiating cells from primary human tumors on the basis of sphere forming ability of the cells [78]. They also showed that 100 dissociated spheroids were capable of recapitulating the primary tumor. The ALDH1A1 is another cancer stem cell marker which defines normal hematopoietic stem cells. Using the ALDEFLUOR assay, which is a functional flow cytometric based assay that identifies cells with higher ALDH1A1 activity, Landen et al (2010) for the first time showed that ALDEFLUOR assay could be used for isolation of ovarian cancer stem cells [131]. Since then there are mounting evidences showing occurrence of ovarian cancer stem cells in different cell lines and patient samples (Table 2.1).

S. No.	Marker	Reference
1	CD44	[77, 86, 132, 133]
2	CD133	[82, 83, 134, 135]
3	ROR1	[84]
4	CD117/C-kit	[136]
6	ALDH	[83, 131, 134, 137, 138]
7	Side Population	[139-142]

Table 2.1: Ovarian Cancer Stem Cells (OCSCs) markers: List of biomarkers used either alone or in combination for the isolation of ovarian cancer stem cells. ALDH and side population assays are the functional assays used to isolate OCSCs.

It has been observed that CSCs residing in the tumour bulk are resistant towards conventional radio and chemotherapy. Therefore during chemotherapy, while non-CSC tumor cells undergo apoptosis, these CSCs become enriched giving rise to recurrence and relapse of the disease. Thus most effective anticancer strategy would be to target both tumour bulk and OCSCs. In this line of treatment various researchers have tried cancer stem cell targeted therapy to achieve maximum efficacy of the treatment. Few of such therapies targeting ovarian cancer stem cells are listed below (Table 2.2).

Targeting Molecule	Target	Reference
VS-5589	Pi3K/mTOR	[143]
Oncolytic viruses	CXCL12/CXCR4	[144]
SGI-110	Epigenetic target of OCSC	[145]
Notch Inhibitor	Notch Signaling	[146]
Niclosamide	OCSCs	[147]
SiRNA	ALDH1	[148, 149]
Metformin	Ovarian cancer stem cells	[150]

Table 2.2: *Different molecular targets identified for ovarian cancer stem cells: List of druggable targets and their respective targeting molecules for ovarian cancer stem cells.*

Even though certain molecules have been identified that could specifically target ovarian cancer stem cells, none of them has reached the clinic. This suggests that there is an imperative need for understanding the biology and chemoresistant features of ovarian cancer stem cells.

Cancer stem cells and chemoresistance:

In spite of having considerable advancements in the field of cancer stem cell biology we still do not fully understand the association of cancer stem cells and chemo resistance. Since the

identification of CSCs in acute myeloid leukaemia in 1997, they have been reported by many investigators in different types of cancer. It has been very well documented that CSCs, irrespective of the tumor type are resistant towards chemotherapeutic drugs with increased levels of detoxifying enzymes e.g. ALDH, enhanced DNA repair abilities, increased drug efflux capacity, reduced drug influx and quiescent nature[66, 130]. In majority of the advanced stage ovarian carcinoma, recurrence and relapse of the disease are the major concerns. Thus OCSCs present a formidable obstacle against effective chemotherapy. In order to monitor the role of OCSCs during the development of chemoresistance, we developed *in vitro* cellular resistant models against cisplatin, paclitaxel and combination of cisplatin and paclitaxel in ovarian cancer cells (Figure 1). Using these resistant models we investigated the association of ovarian cancer stem cells with acquired chemo resistance. Given that there could be many targets against ovarian cancer stem cells, we focused on oct4 because of its indispensable role in maintenance of both stemness and chemoresistant phenotype [151-153]. Knockdown of oct4 results in decreased expression of other core transcription factor like sox2 and nanog [154].

Methodology:

Sphere formation assay:

Spheroid forming assays were performed using serum devoid of DMEM supplemented with a cocktail of growth factors and serial passaging was performed for monitoring long term self-renewal ability. Detailed protocol has been mentioned in the materials and methods section.

Antibodies and western blotting:

The protein lysates were prepared by using passive lysis buffer and concentration of proteins were estimated by Bradford assay. The proteins were resolved in SDS PAGE and transferred to nitrocellulose membrane. Membrane was probed with the appropriate primary antibodies (Oct4A, CD133 and beta actin) and HRP-conjugated secondary antibodies. The immune

complexes were detected using Pierce ECL systems according to instructions supplied by the manufacturer. Detailed protocol has been mentioned in the materials and methods section.

Quantitative real-time PCR (qRT-PCR):

Quantitative real time PCR was performed from 10ng of cDNA using SYBR Green method (Invitrogen). GAPDH expression was used as an internal control. The relative expression levels of mRNAs were calculated by the Δ Ct for relative quantification and $\Delta\Delta$ Ct method for fold change measurement. Primer sequences and the detailed protocol have been mentioned in the materials and methods.

Side population assay:

Side population assay protocol was adapted from Telford et al (2007). It was performed with some modification, where cells were incubated with verapamil 50uM for 20 minutes. SP and NSP fraction was sorted from 100 gauze nozzle at 4 degrees Celsius. Detailed protocol has been mentioned in the Appendix (materials and methods) section.

Construction of shOct4 knockdown clone: Target sequence against Oct4 (AACATGTGTAAGCTGCGGCC) was adapted from Zares et al. (2005)[155]. It was cloned in P13.7 lentilox vector using Hpa1 and Not 1 sites. Clones were validated with restriction digestion and transient transfection in 293FT cells. Detailed protocol has been mentioned in the materials and methods section.

Lentiviral mediated gene silencing:

For stable integration of shRNA construct against *Oct4* gene, lentiviruses were produced in 293FT cells. Virus was collected post 60 hours of transfection and concentrated with ultracentrifugation at 30,000 RPM for 90 minutes. Concentrated viruses were used for transducing the cells and 48 hrs post transduction high GFP positive cells (cells with shOct4 construct) were sorted through FACS. Western blotting and RT-PCR was performed to observe

the knockdown efficiency. Detailed protocol for the production of viruses and transduction procedure has been mentioned in the materials and methods section.

Results:

1. Development of chemoresistant model against cisplatin, paclitaxel and cisplatin+paclitaxel:

In order to monitor the early and late events taking place during the acquirement of drug resistance (cisplatin, paclitaxel and cisplatin + paclitaxel), our lab developed isogenic drug resistant models from two different EOC cell lines e.g. A2780 and OAW42 (Serous epithelial ovarian carcinoma). Later these resistant models were categorized into early resistant (ER) and late resistant (LR) stages depending upon their survival fraction at IC_{50} of sensitive cells. Early resistant cells showed 60-65 percent viability and late resistant cells showed >90 percent viability (figure 2.1) [156].

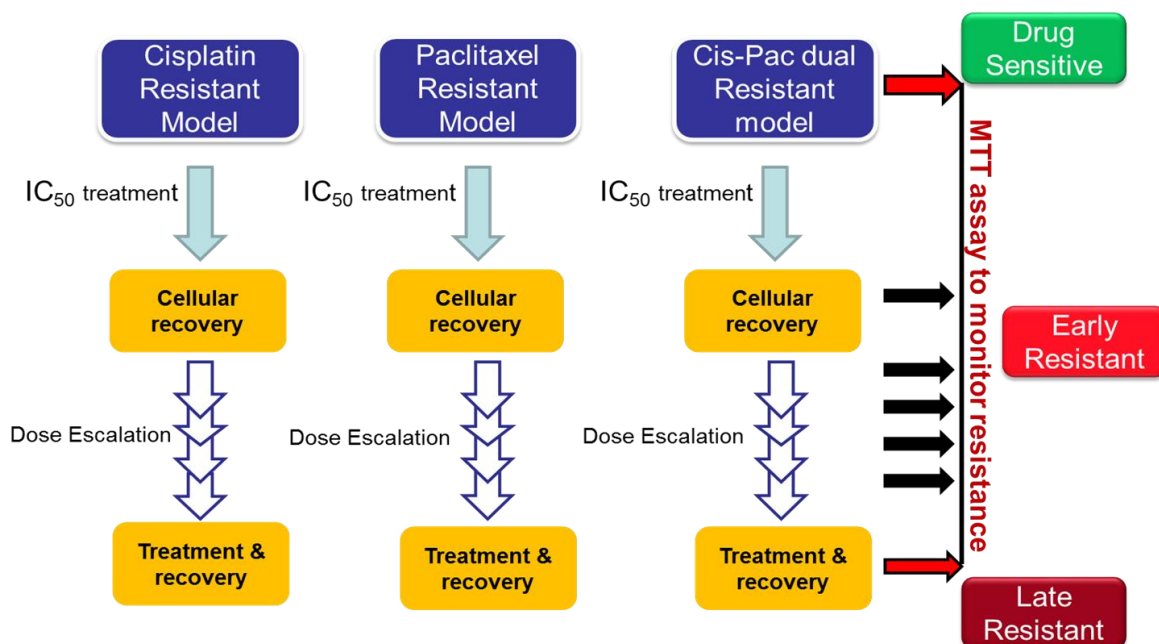


Figure 2.1: Schematic representation of development of A2780 resistant model: Chemo naïve A2780 cells were challenged against escalating doses of cisplatin, paclitaxel and

combination followed by recovery period. The whole model was categorized into early (Cis^{ER}, Pac^{ER} and Combi^{ER}) and late (Cis^{LR}, Pac^{LR} and Combi^{LR}) resistant cells.

The entire process of development of resistant cells took 6-7 months followed by its validation through MTT assay, where percentage viability of resistant cells after every treatment was monitored. These isogenic resistant cells were used as our model system to study the role of CSCs during the acquirement of chemoresistance where we isolated and characterized the CSCs from different stages of resistance.

2. Isolation of ovarian cancer stem cells from chemo sensitive, Early and Late resistant cells:

As mentioned in the introduction section, there lies a lot of discrepancy for the use of cell surface biomarkers to isolate ovarian CSCs from cell lines and patient samples. Thus we used two isolation strategies which are not based on cell surface markers rather they represent the functional property of cancer stem cells e.g. Side Population assay and Spheroid formation assay which would be common to all cell lines used and are more relevant for resistance study. We have also evaluated presence of certain biomarkers. In this present section we used SP assay for isolating ovarian CSCs from A2780 cell line. When analysed in sensitive, early and late resistant stages of Cisplatin, Paclitaxel and dual resistant models, we observed a gradual increase in SP fraction from sensitive to early and from early to late resistant cells across all the three resistant models. (A2780 = 1.4%±0.05, Cis-ER=2.4%±0.08; Cis-LR=5.73%±0.42; Pac-ER=4.06%±0.38; Pac-LR=6.8%±0.10; Combi-ER=5.05%±0.65; Combi-LR=17.6%±0.74) as shown in the figure 2.2 A-C.

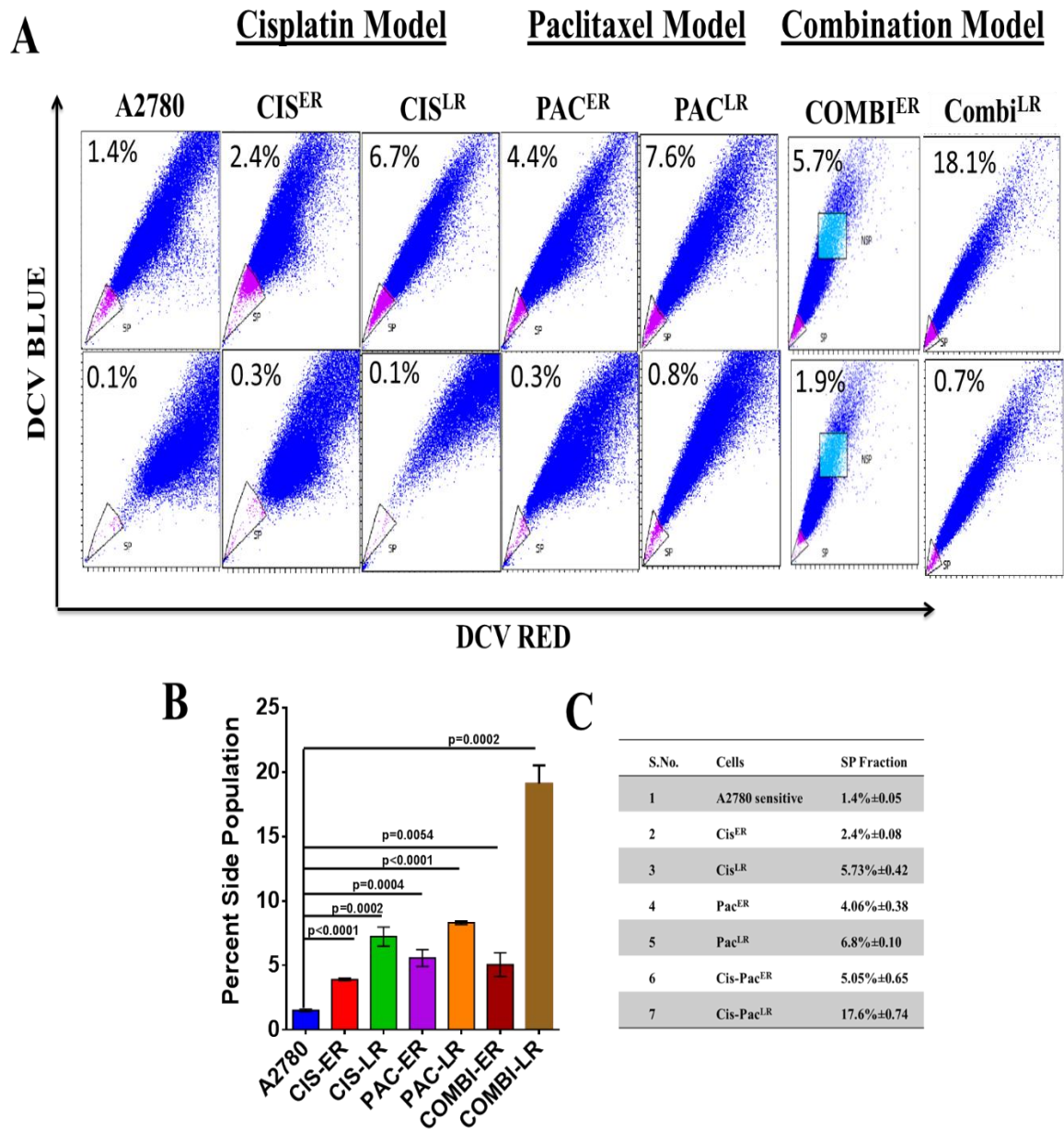


Figure 2.2: Side Population assay across the resistant models: (A) FACS dot plot analysis showing significant increase in SP fraction with increasing resistance across the resistant models. (B-C) Graphical and tabular representation of fold enrichment of SP fraction with increasing resistance across the resistant models ($p < 0.01$).

These SP and NSP cells were further characterized for CSC phenotype (self-renewal property and stemness gene expression) and resistance phenotype in the later part of this chapter.

3. Characterization of chemoresistant and ovarian cancer stem cells isolated from early and late resistant stages.

3.1 Biomarker based analysis across the resistant model:

We analysed a set of three biomarkers in A2780 resistant models mainly CD44, CD133, and CXCR4 to monitor if these CSC markers also increases with increasing resistance by FACS and western blot. It was observed that compared to sensitive A2780 cells, there was significant increase in the levels of CD44, CD133 and CXCR4 (Figure 2.3A). We also performed western blotting for CD133 which is a very well reported biomarker for ovarian cancer stem cells to investigate the enrichment at protein level. Increased expression of CD133 was observed in all the models irrespective of the drug used (Figure 2.3B)

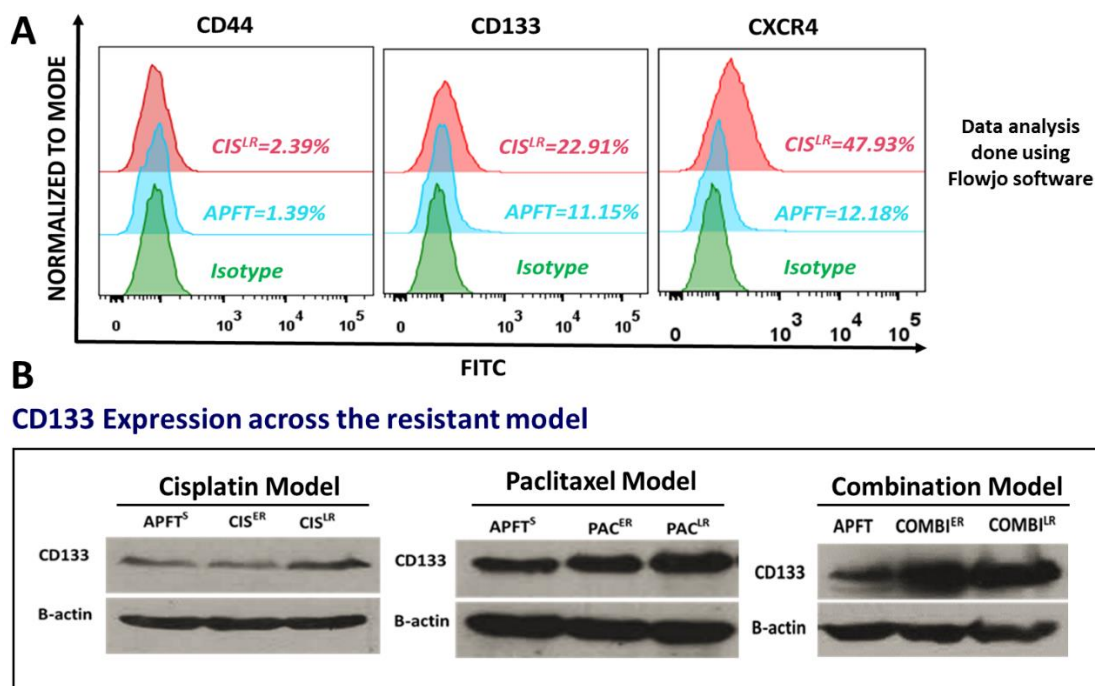


Figure 2.3: Biomarker expression analysis across the resistant models: (A) Expression of CD44, CD133 and CXCR4 was analysed in cisplatin resistant model with FACS. Increased expression of CD44, CD133 and CXCR4 was observed in Cis^{LR} cells compared to the sensitive cells. (B) Expression of CD133 was analysed through western blotting in cisplatin, paclitaxel

and dual resistant model which showed a gradual increase in the expression of CD133 with increasing resistance.

3.2 Sphere forming assay in sensitive and drug (cisplatin, paclitaxel and dual) resistant cells:

As mentioned earlier in the introduction that spheroid formation is one of the crucial assay that determines the self-renewal property of any stem cell or cancer stem cell. Here we sought to monitor the self-renewal property of SP and NSP fraction along with the main population (MP). Total 2000 viable SP/NSP/MP cells/well were seeded for spheroid culture. From these two thousand cells, A2780 chemo sensitive cells formed only 16 spheroids (0.81%) however, Cis^{ER} formed 30 spheroids (1.5%) showing a 1.8 fold increase at early stage of cisplatin resistance. In late resistant cells (Cis^{LR}) 46 spheroids were observed (2.3%) with 2.8 fold increase as compared to the sensitive cells. All the spheroids for data evaluation were counted at passage three. Similar findings were also observed in Paclitaxel and dual resistant model where Pac^{ER} cells were able to form 40 spheroids (2%) i.e.2.4 fold higher and Pac^{LR} formed 64 spheroids (3.2%) i.e. 3.9 fold increase; Combi^{ER} cells formed 77 spheroids (3.8%) i.e. 4.8 fold higher and Combi^{LR} cells formed 85 number of spheroids (4.25%) i.e 5.3 fold increase as compared to that of sensitive cells. (Figure 2.4A).

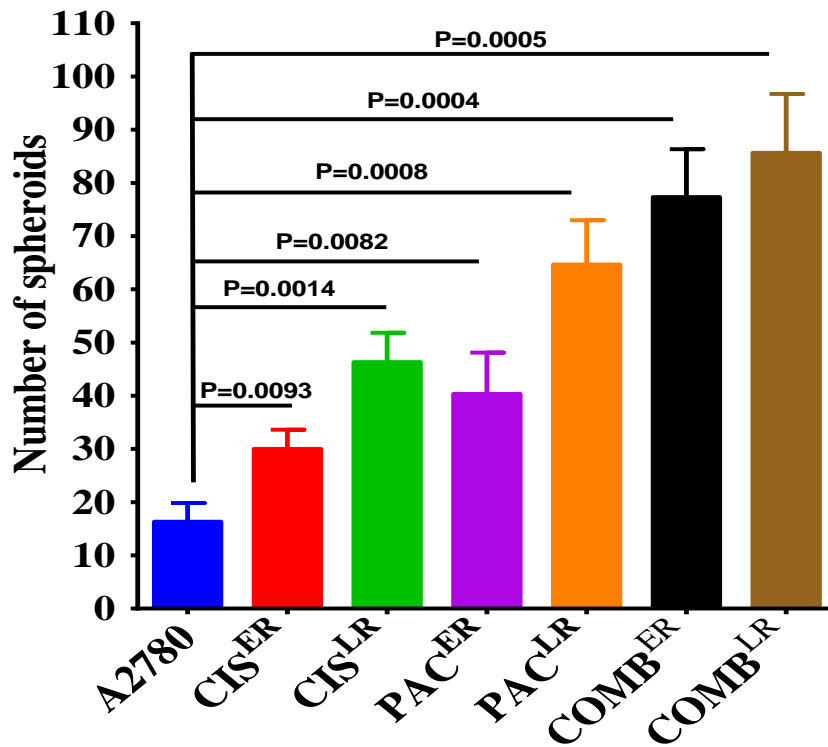


Figure 2.4: Quantification of spheroids across the resistant model: Monitoring the number of spheroids formed at 3rd passage showed that with increasing resistance there was significant increase in the sphere forming ability of early and late resistant cells. $Cis^{ER} = 1.8$ fold, Cis^{LR} showed 2.8 fold; $Pac^{+} = 2.4$ fold, $Pac^{LR} = 3.9$ fold; $Combi^{ER} = 3.8$ fold, $Combi^{LR} = 5.3$ fold

5. Characterisation of SP and NSP fraction for their self-renewal property and resistant phenotype

We investigated the spheroid forming ability of SP and NSP fractions from A2780 sensitive, early and late resistant cells. The main population (MP) of cells were sorted for their SP and NSP fraction and trypan blue staining was performed to count the viable cells. Precisely 2000 cells/well were seeded in a low adherent culture dishes and monitored till spheroid formation. The spheroids were then serially passaged till 3rd generations to count the number of spheroids. It was observed that NSP cells were highly compromised for their spheroid forming ability and showed significantly less number of spheroids compared to SP cells (Figure 2.5B).

Chemoresistance property of SP and NSP cells were also monitored with MTT assay and a comparison was made between MP, SP and NSP fractions for their chemoresistant behaviour at IC_{50} drug concentration of A2780 sensitive cells. A2780 sensitive, Cis^{LR}, Pac^{LR} and Combi^{LR} cells at their respective IC_{50} showed approximately 50 percent viability. However corresponding SP fraction showed marked increase in percent survival (A2780 = 68.7%, Cis^{LR} = 63.9%, Pac^{LR} = 72.49% and Combi^{LR} = 70.45%). Corresponding NSP fractions showed similar viability to respective parental population for resistant cells but the A2780 sensitive and Cis^{LR} cells showed marked decrease (A2780 = 24.4, Cis^{LR} = 35.7, Pac^{LR} = 48.4 and Combi^{LR} = 51.2) (Figure 2.5B). This suggests that resistant cells despite being NSP fraction can still maintain certain features of resistant phenotype. Next we wanted to monitor whether SP cells can differentiate into NSP cells and NSP cells could revert back to SP fraction. In order to execute this experiment we sorted SP and NSP fraction from both A2780 sensitive and Cis^{LR} cells, cultured them and performed SP assay at 3 consecutive passages (Figure 2.5C-D). Interestingly it was observed that in both sensitive and resistant cells there was an enrichment in the SP phenotype at consecutive passage (A2780 Sensitive; Passage1 = 1.5%, Passage2 = 5.8% and passage 3 = 27.3%; In Cis^{LR} cells, Passage1 = 7.3%, Passage2 = 11.9% and passage 3 = 49.3%) and rest of the cells differentiate into NSP fraction. However there was no SP fraction formed during 3 passages from NSP cells (Figure 2.5E). This suggests that SP cells can form both SP and NSP cells but NSP cells failed to form any SP cells up to 3 passages.

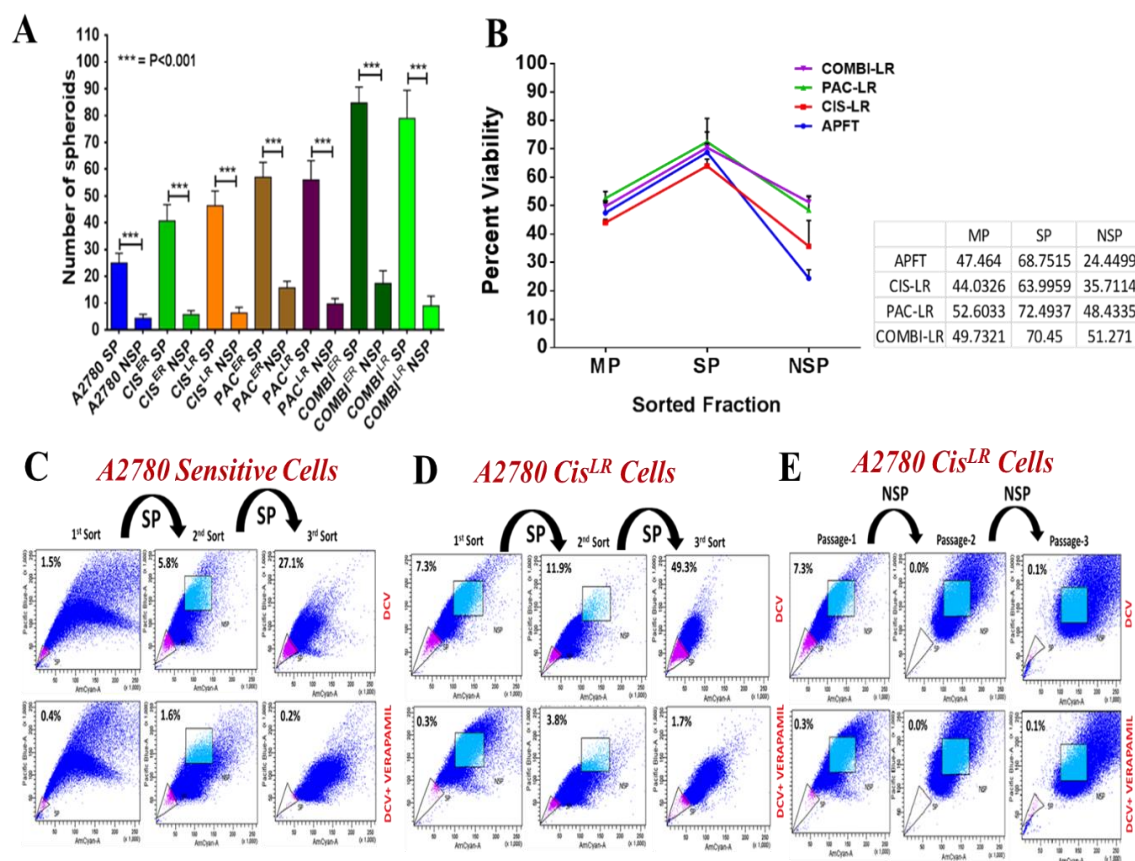


Figure 2.5: Characterisation of SP and NSP cells: (A) Spheroid formation assay was performed from 2000 cells showing an increase in the sphere forming ability from SP cells however drastic decrease in the sphere forming ability of NSP fraction was observed as compared to their respective SP fraction. (B) Comparison of survival fraction at IC₅₀ was monitored between SP and NSP cells, showing marked increase in the survival fraction of SP cells (A2780 SP = 68.75%, Cis^{LR} = 63.99%, Pac^{LR} = 72.4% and Combi^{LR} = 70.45%) compared to main population (MP) and NSP cells. (C-D) FACS analysis of DCV stained A2780 sensitive and Cis^{LR} cells at consecutive passage showed enrichment of SP fraction (A2780 Sensitive; Passage1 = 1.5%, Passage2 = 5.8% and passage 3 = 27.3%; In Cis^{LR} cells, Passage1 = 7.3%, Passage2 = 11.9% and passage 3 = 49.3%). (E) FACS analysis of DCV stained NSP fraction at different passage showing no SP phenotype (Passage1 = 7.3%, Passage2 = 0% and passage 3 = 0.1%)

Since we observed higher self-renewal ability from chemoresistant and SP cells we intended to monitor the expression of core transcription factors which maintains the pluripotency of cancer stem cells.

6. Expression of pluripotent genes across the resistant models.

In order to monitor the CSCs like feature of SP cells and chemoresistant cells which are enriched with SP cells, we monitored the transcript levels of *Oct4*, *Sox2* and *Nanog* across the resistant models as well as in SP and NSP fraction isolated from A2780 and OAW42 cells.

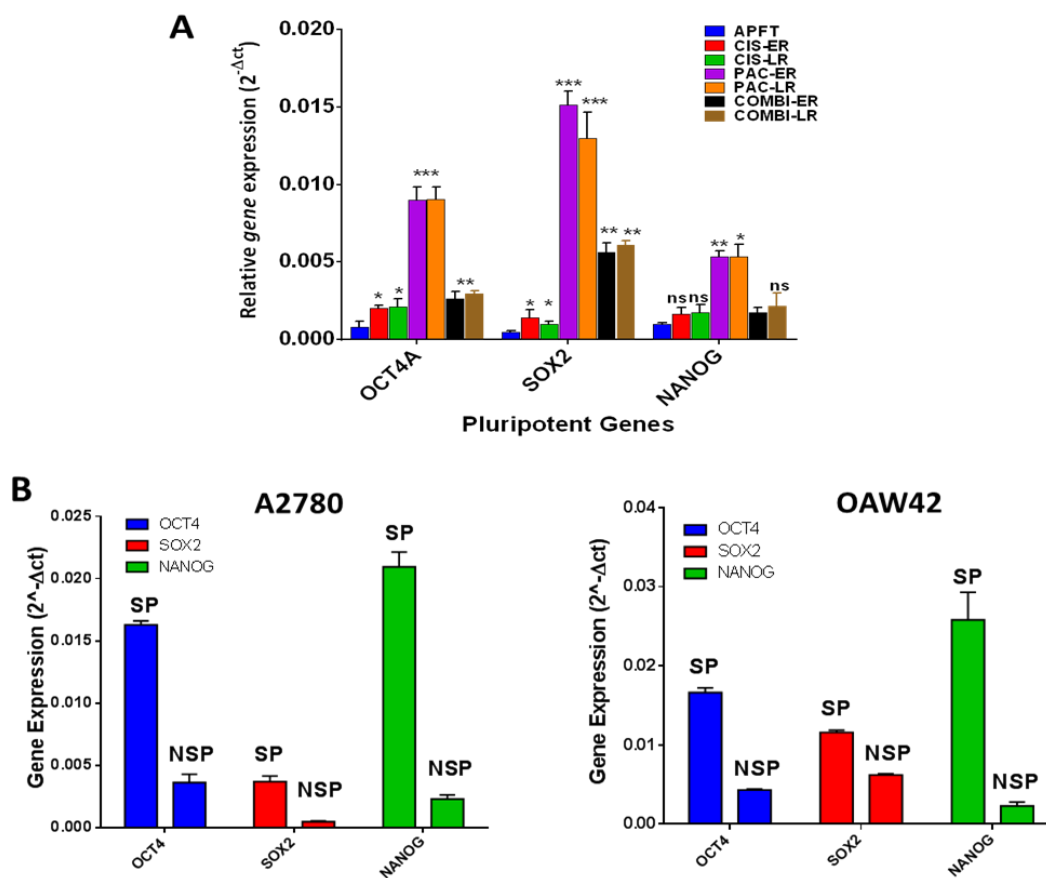


Figure 2.6: Quantitative analysis of pluripotent genes in SP, NSP and resistant cells: (A) Real time PCR analysis showing significant increase in the expression of *Oct4* and *Sox2* in cisplatin and paclitaxel resistant model. In dual resistant model only paclitaxel resistant cells showed significant increase in the expression of *nanog*. (B) Real Time PCR analysis of *Oct4*,

Sox2 and *nanog* from SP and NSP cells isolated from A2780 and OAW42 cells showed significantly higher transcripts in the SP fraction than NSP fraction.

In cisplatin, paclitaxel and combinatorial resistant models, transcript levels of both *Oct4* and *Sox2* showed a significant increase compared to the A2780 sensitive cells (Expression of *Oct4*: Cis^{ER} = 2.63 fold, Cis^{LR} = 2.76 fold; Pac^{ER} = 11.68 fold, Pac^{LR} = 11.78 fold; Combi^{ER} = 3.4 fold, Combi^{LR} = 3.8 fold. Expression of *Sox2*: Cis^{ER} = 2.9 fold, Cis^{LR} = 2.0 fold; Pac^{ER} = 32 fold, Pac^{LR} = 27 fold; Combi^{ER} = 11.9 fold, Combi^{LR} = 12.9 fold.) only at the early stages which then plateaued for late resistant cells. However, *nanog* was found to be significantly upregulated only in Pac^{ER} and Pac^{LR} cells (Pac^{ER} = 5.52 and Pac^{LR} = 5.55 fold) (Figure 2.6A). Next we monitored the transcript levels of *Oct4*, *Sox2* and *nanog* in the sorted SP and NSP fraction from A2780 and OAW42 cells. It was observed that SP cells had higher transcript levels of *Oct4*, *Sox2* and *nanog* compared to the NSP cells (Figure 2.6B).

Next we wanted to study the role of stemness genes in the maintenance of cancer stem cells and chemoresistant phenotype. From our previous results it was observed that the expression level of *Oct4* and *Sox2* increased significantly across all the resistant models. In addition in sensitive cells, *Oct4* gene expression was significantly higher in SP fraction. This suggested that *Oct4* might be one of the key players for the maintenance of SP phenotype. Therefore we monitored effect of *Oct4* gene silencing upon SP and chemoresistant phenotype using gene knockdown strategy.

7. Lentiviral mediated stable knockdown of *Oct4* gene:

To monitor the effect of *Oct4* gene we used lentiviral mediated *Oct4* knock down in all the resistant models. We cloned the sh*Oct4* sequence in PII 3.7 U6 linker plasmid. *Oct4* target sequence was adapted from the paper by Zaheres et al. (2005) which has shown significant silencing of *Oct4* in human embryonic stem cells [157]. The oligos were firstly annealed and checked on 20% PAGE (figure 6B) for their integrity. The annealed oligos were then cloned

under HpaI and NotI restriction sites in pLL3.7 U6 linker plasmid and the positive clones were screened with colony PCR and validated with restriction digestion (figure 6D-E).

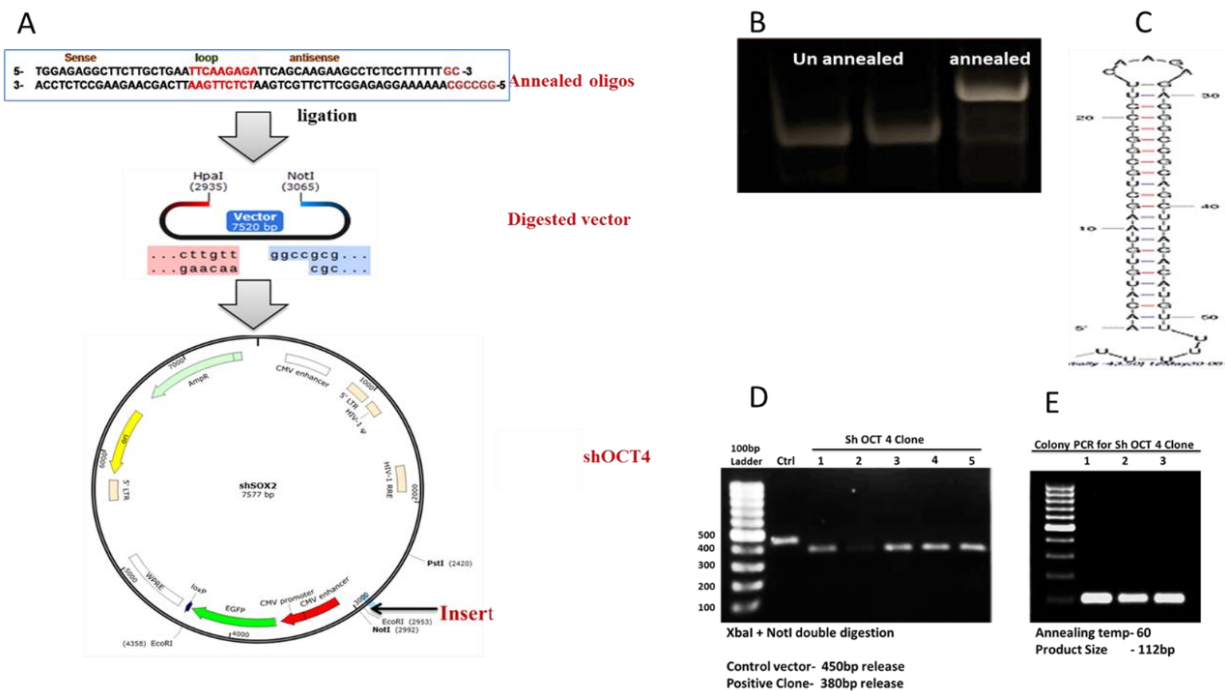


Figure 2.7: sh RNA mediated knock down cloning strategy: (A) Schematic diagram describing cloning of sh RNA in pLL3.7 plasmid. (B) Annealed oligos were checked on 20% PAGE; a shift was observed in case of double stranded annealed oligos compared to heat denatured forward and reverse oligos. (C) Oligos were checked through mFold server for its intrinsic property to form a hair pin loop structure which is a prerequisite condition for efficient knockdown of any gene. (D) Positive clones were firstly screened by colony PCR having specific forward and reverse primers with amplicon size = 112bp. Later validation was performed with restriction digestion using two unique sites, XbaI and notI, with release of 380 bp fragment in the positive clones and vector control gives a release of 450 bp and also PCR amplification with 112 bp amplicon size.

Before lentivirus production we first validated the knock down effect by transient transfection of the positive clone in 293FT cells at both transcript and protein level. Cells were first

transfected with shOct4 clone and only vector (Mock control) and then GFP positive cells harbouring the shRNA construct were sorted using FACS (figure 2.8A,B). These cells were cultured and used for quantitative PCR and western blotting. Significant decrease in the levels of *Oct4*, both at transcript and protein levels were observed compared to mock control (figure 2.8 C-E).

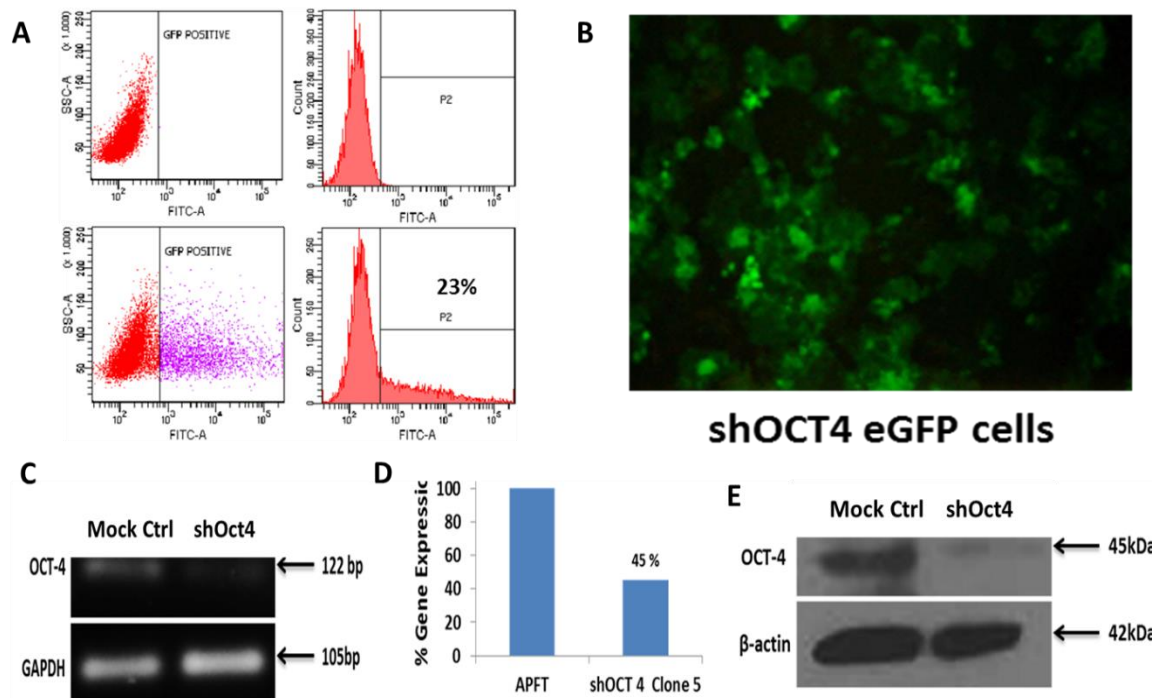


Figure 2.8. Transient validation of *Oct4* knockdown clone: (A) FACS analysis showing 23 percent high GFP positive cells after transient transfection of shOct4 clone in 293FT cells (B) Representative image of the sorted 293FT cells showing eGFP expression under fluorescence microscope (C). Semi quantitative PCR from GFP positive cells showed decreased *Oct4* expression in the knockdown cells compared to the mock control (D) quantitative real time PCR analysis showed 55 percent decrease in the transcript level of *Oct4* gene. (E). Western blotting analysis show significant knock down of oct 4 protein compared to the mock control

8. Generation of stable knockdown of *Oct4* in all the resistant cells:

To create stable *Oct4* knockdown cells, lentiviruses were generated by co-transfection of Envelope Plasmid (Env), Packaging Plasmid (PΔ), Transfer Vector (shOCT4) in 1:2:3 ratio. Post 60 hours of infection viruses were collected and concentrated using high speed ultracentrifuge. Later all the resistant cells were infected with lentiviruses harboring shOct4 oligos in presence of polybrene (1ug/ml). High GFP cells were sorted which showed a higher degree of knockdown in the A2780 sensitive and resistant cells. (Figure 2.9).

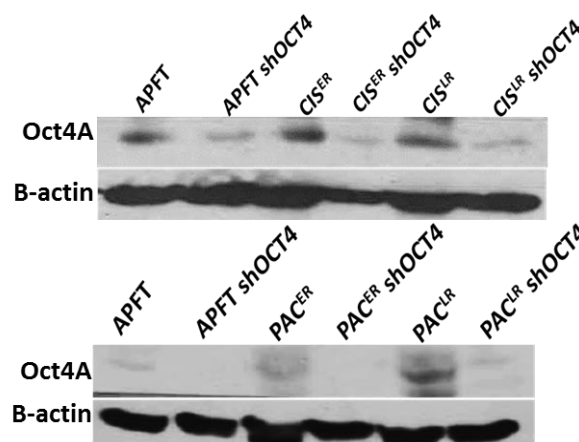


Figure 2.9: Validation of stable knockdown of *Oct4*: Western blot analysis showing significant decrease in the expression of *Oct4* protein in A2780 sensitive, Cis^{ER}, Cis^{LR}, Pac^{ER} and Pac^{LR} cells with stable knockdown of *Oct4* gene..

As shown by the western blot, significant decrease in the levels of *Oct4* protein in A2780 sensitive, Cis^{ER}, Cis^{LR}, Pac^{ER} and Pac^{LR} cells were observed. Due to some unavoidable circumstances, knockdown clones in dual resistant cells could not be generated and they are under progress now.

9. Monitoring the effect of *Oct4* gene knockdown on CSC phenotype and chemoresistance:

In order to understand the role played by *Oct4* gene in the maintenance of CSC phenotype, we examined SP phenotype, Self-renewal ability, Chemoresistance property in *Oct4* knockdown cells. DCV staining in Cis^{ER}/Cis^{ER} shOct4 and Cis^{LR}/Cis^{LR} shOct4 cells showed decrease in the

SP fraction (3 fold decrease in Cis^{ER} Oct4 knockdown cells and 2.4 fold in Cis^{LR} Oct4 knockdown cells) (Figure 2.10). Self-renewal ability of these knockdown cells was also monitored by spheroid formation assay (by counting the number of spheroids formed and assessing the number of passages as well). The knockdown cells formed significantly lower number of spheroids compared to their respective parental cells (Figure 2.10 B, Table2.2). All of the SP and NSP spheroids were counted at passage 2 because NSP cells were incapable of forming the spheroids beyond passage 2 suggesting that NSP cells are highly compromised for their self-renewal ability.

Long term spheroid forming ability was also monitored in the control cells and the knockdown cells where A2780, Cis^{ER}, Cis^{LR}, Pac^{ER} and Pac^{LR} showed spheroid forming ability beyond passage 4 however A2780 shOct4, Cis^{ER} shOct4, Cis^{LR} shOct4, Pac^{ER} shOct4, Pac^{LR} shOct4 cells were found to be incapable of forming spheroids beyond passage 2 (Figure 2.10 C). Chemoresistance property was also monitored with MTT assay in the *Oct4* knockdown cells using IC₅₀ drug concentration of A2780 sensitive cells (500ng/ml) where Cis^{LR} and Pac^{LR} cells showed marginal decrease in percent viability after *Oct4* knockdown, however Cis^{LR} cells showed significant decrease (Figure 2.10D).

Oct4 knockdown cells	Fold decrease in sphere forming ability
A2780	6.2 fold
Cis ^{ER}	5 fold
Cis ^{LR}	3.2 fold
Pac ^{ER}	6.3 fold
Pac ^{LR}	5.7 fold

Table 2.2: Fold decrease in sphere forming ability of Oct4 knockdown cells.

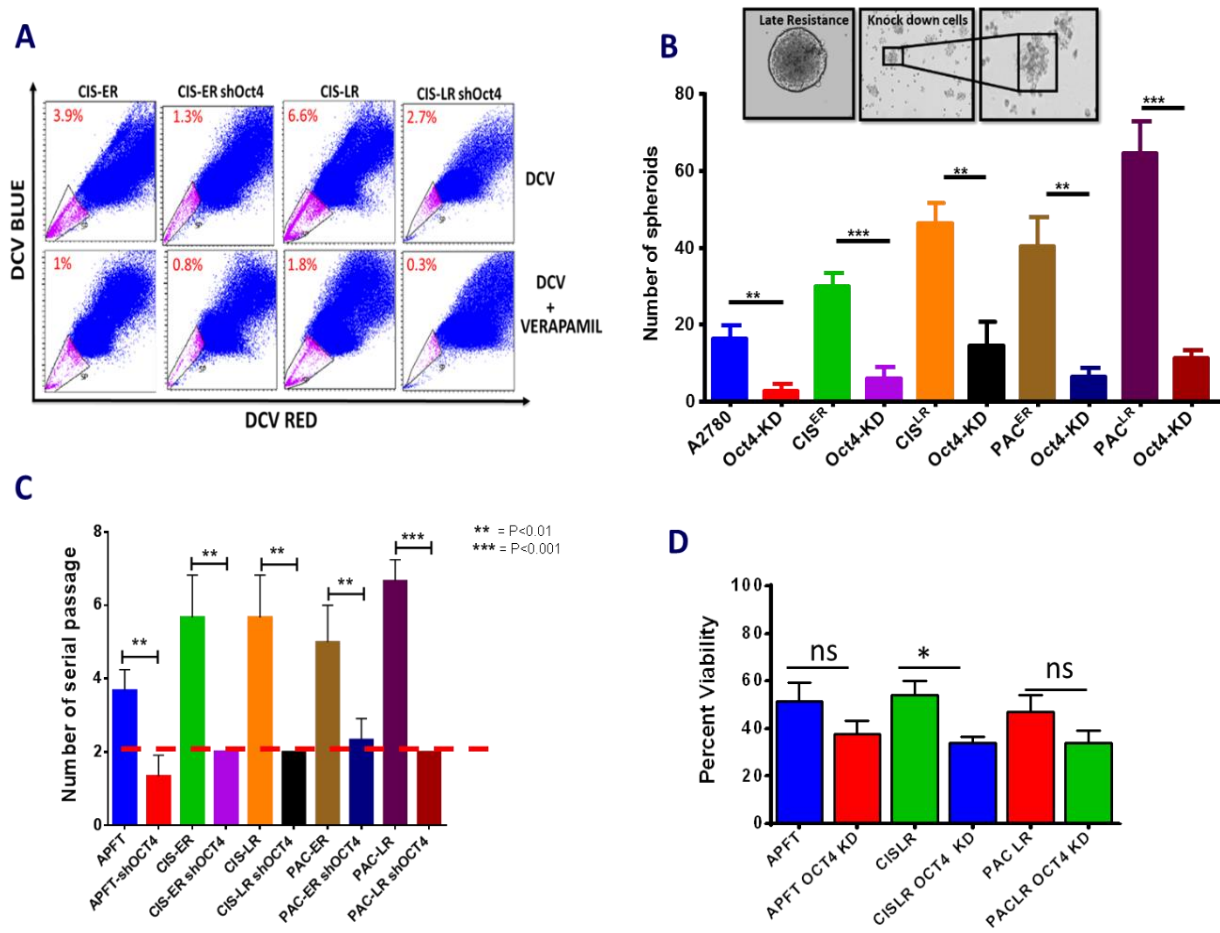


Figure 2.10: Consequence of Oct4 silencing: (A) FACS analysis showing, decrease in the SP fraction after Oct4 knockdown in the cisplatin early and late resistant cells; Cis^{ER} shOct4= 3 fold decrease and Cis^{LR} shOct4 = 2.4 fold decrease. (B) Bar graph showing significant decrease in spheroid forming capacity of Oct4 KD cells (A2780 shOct4, Cis^{ER} shOct4, Cis^{LR} shOct4, Pac^{ER} shOct4, Pac^{LR} shOct4 with 6.2, 3.2, 6.3 and 5.7 fold respectively). Inset shows the disrupted morphology of spheroids formed by Oct4 KD cells. (C) Serial passaging of spheroid cells showing A2780 shOct4, Cis^{ER} shOct4, Cis^{LR} shOct4, Pac^{ER} shOct4, Pac^{LR} shOct4 cells could not form spheroids after 2nd passage compared to the parental cells. (D) MTT assay showing percent viability at IC₅₀ of control cells.

Overall this study showed that with increasing drug resistance there was increased stemness gene expression and enrichment in SP fraction phenotype and higher propensity to form three

dimensional multicellular spheroids having higher self-renewal property. All these functions were compromised upon knockdown of *Oct4* with marginal effect on chemoresistance.

Discussion:

Acquirement of chemoresistance is a major therapeutic hurdle that delimits successful treatment outcomes for many human cancers. This is particularly evident in ovarian cancer, where the development of resistance is a common occurrence[158]. In past few decades there has been an enormous growth in our understanding of the mechanisms that can generate and sustain chemoresistance. This could be due to existence of cancer stem cells or possible enrichment of MDR transporter proteins, efficient DNA repair, and increased cell survival in cancer cells. In the present work we have tried to find the association between generation of chemoresistance and cancer stem cell features like SP phenotype, spheroid formation and biomarkers. To monitor this we used an indigenously developed cellular resistant model against different chemotherapeutic drugs (cisplatin, paclitaxel and combination) which were categorized into A2780 sensitive, early resistant (Cis^{ER}, Pac^{ER} and Combi^{ER}) and late resistant stages (Cis^{LR}, Pac^{LR} and Combi^{LR}). Interestingly a gradual increase in the SP fraction with increasing resistance was observed which suggest that escalated resistance in due course of time led to increase in the proportion of cancer stem cells like SP cells. We also observed that these SP cells could differentiate into both SP and NSP phenotype but the NSP cells could not form any SP phenotype, suggesting that these SP cells have differentiating property, an essential character of cancer stem cells. In order to monitor whether this SP phenotype is accompanied with higher self-renewal ability, we investigated the self-renewal ability of these resistant cells with spheroid formation assay. Compared to A2780 sensitive cells, all the early and late resistant cells showed significant increase in sphere forming ability irrespective of the chemotherapeutic drugs used for resistance development. This data indicates that with acquired resistance the CSC fraction is enriched with higher self-renewing ability which might provide

increased tumorigenic ability to these resistant cells. Since we saw an increased SP phenotype and self-renewal ability in these resistant cells we also analysed levels of the key transcription factors that maintain the pluripotency of a normal stem cells as well as of cancer stem cells. These core transcription factors are *Oct4*, *Sox2* and *nanog*. Interestingly we found that transcript levels of *Oct4* and *Sox2* were significantly upregulated in all the early resistant cells which then plateau in late resistant cells. This indicates that upregulation of Oct4 and Sox2 are critical for maintaining stemness features from very early events of resistance development. However the expression of *nanog* showed significant increase only in paclitaxel resistant cells and marginal increase in cisplatin and combination resistant model. This indicates that there could be differential regulation of these transcription factors in different resistant models. We also sorted SP and NSP fractions from two sensitive cell lines A2780 and OAW42 using FACS. SP cells showed significantly upregulated expression of *Oct4*, *Sox2* and *nanog* in both the cell lines A2780 and OAW42 suggesting that SP fractions are enriched with the cells possessing higher stemness property. Spheroid formation assay was also performed to monitor the self-renewal property of SP and NSP cells, where it was observed that SP cells from all of the resistant cells showed increased sphere forming ability at multiple passages however NSP cells were highly compromised for their sphere forming ability and could not form spheroids beyond 2nd passage. Since cancer stem cells are known to have higher chemoresistant property we compared the resistant phenotype in SP and NSP cells. As expected it was observed that SP cells showed higher percentage viability compared to NSP cells. However there was marginal difference between main population and NSP cells except A2780 sensitive cells and Cis^{ER} cells, indicating that NSP fraction can maintain the resistance phenotype, but are unable to self-renew or differentiate. Next we monitored if Oct4 plays any role in the self-renewal and chemoresistance by stable knockdown of *Oct4* gene in the resistant cells. After Oct4 knockdown, cells showed not only decreased SP phenotype but also decrease in the self-

renewal ability suggesting that Oct4 can regulate both SP and self-renewal property in these resistant cells. However we observed only marginal decrease in its resistant phenotype indicating that *Oct4* might not directly contribute to the resistance properties in these chemoresistant cells.

In the present study Early and late resistance stages imply the gradual changes occurring in a chemo naïve cell after being exposed to repeated doses of chemotherapeutic drugs. Cells belonging to early resistant stages still show reversible alterations in chemoresistant phenotype and cells that attain irreversible alterations after a long period of increased drug exposure are designated by late resistance. We believe that such entities might exist in patients as well but are beyond our current detection ability due to unavailability of any specific biomarkers or signatures. Also the heterogeneous background of a tumor could bar accurate identification of a specific stage.

The gold standard for measuring the differentiation and self-renewing ability of CSCs is to monitor tumor development in immune compromised mice. In the preceding chapter we have attempted to monitor the tumorigenic ability of SP and spheroid cells. Using non-invasive bioluminescence imaging, we monitored the tumor growth dynamics from SP/NSP and spheroid/adherent cells isolated from different stages of resistance in real time.

Chapter 3

Longitudinal monitoring of tumorigenicity of cancer stem cells in living subjects by non-invasive bioluminescence imaging

Introduction:

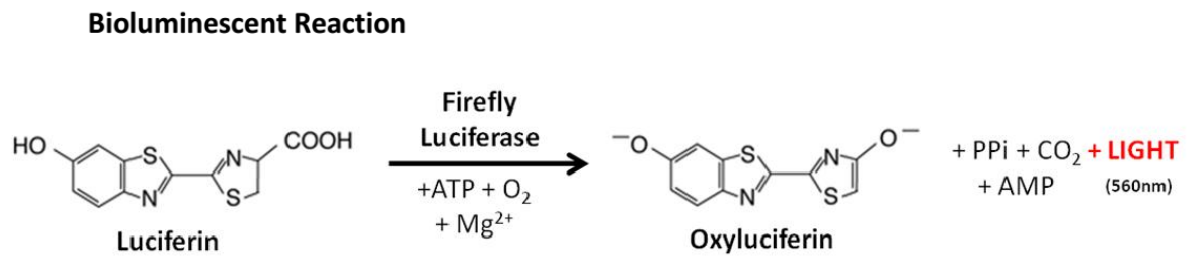
Generation of chemoresistance in due course of treatment is a major challenge for ovarian cancer patients that lead to recurrence and relapse of the disease. A probable cause for resistance acquirement is the presence and enrichment of cancer stem cells that are able to overcome drug toxicity [159]. In the previous chapter (chapter 2) identification and characterization of these CSC population based on the expression of cell-surface markers, functional assays like spheroid formation and SP assay from chemoresistant cells have been described in detail. However the most important characteristics which is also a gold standard for functional validation of CSCs is the ability to generate tumours from a very low number of cells in immune competent mice. Traditionally, a large (>1 million) number of cancer cells are implanted to develop tumor xenografts in immunocompromised mice. However, due to their self-renewal and differentiating properties, theoretically as few as ten CSCs could give rise to a primary tumour under appropriate conditions [110]. It is therefore important to assess putative CSC like populations for their tumorigenic ability.

Physical appearance and volume measurement are the two classical methods to monitor tumor growth in small animals. These measurements are only possible when the tumors are palpable, however *in vivo* bioluminescence imaging would allow us to monitor tumor growth in real time.

Bioluminescence Imaging

Bioluminescence is a biological phenomenon of an enzymatic reaction between luciferase enzyme and its respective substrate in the presence of ATP, O₂ and Mg²⁺. As a result of this enzymatic reaction emission of light occurs in a wide range of visible light (480-640 nm) [160]. Some luciferases can also catalyze their substrate in absence of ATP. This emitted light can be captured by CCD camera and the light signal could be quantified. This biological phenomenon

of bioluminescence has been used as an indirect method to monitor the activity of any gene or promoter by cloning the luciferase gene under any gene/promoter of interest.



The most commonly used bioluminescent reporter for biological research is firefly luciferase (*fluc/FLUC*) isolated from *Photinus pyralis* and further mutagenized for better expression in mammalian cells. Other luciferases used as reporters are:

- Renilla luciferase (Rluc) isolated from *Renilla reniformis*.
- Guassia luciferase (Gluc) isolated from copepod, *Guassia princeps*.
- Metridia luciferase (Mluc) isolated from marine copepod *Metridia longa*.

Some luciferases which are obtained from click beetle (*Pyrophosrus plagiophthalmus*), corals (*Tenilla*) and several bacterial species (*Vibrio fischeri* and *V. harveyi*) [161, 162].

Fluc, which have no post translational modification, is a heat labile enzyme that has a half-life of approximately 2-3 hours. Fluc produces photons in a reaction that is mediated by ATP, magnesium, and benzothiazoyl–thiazole luciferin. The light emitted from the firefly luciferase is an enzyme-catalyzed reaction which is recorded by a CCD camera with a broad-band i.e. 480–640 nm range of wavelength.

BLI is an important tool for non-invasive imaging with low cost and easy experimental procedures. It facilitates real-time analysis of the disease progression at a molecular level in living organisms without killing the experimental animal. Fluc mediated imaging has been

used in pre-clinical models of ovarian cancer to monitor the tumor burden during the course of chemotherapy and also to monitor the metastasis [156, 163, 164].

In Vivo Molecular imaging of cancer stem cells:

Liu et al (2010) have shown that Cancer stem cells from human breast tumors are involved in spontaneous metastasis in orthotopic mouse models [110]. In their study they have shown that as few as ten Breast Cancer Stem Cells (BCSCs) stably expressing firefly luciferase could be monitored for subsequent tumor growth and spontaneous metastasis in NOD/SCID mice. Similarly, Jauffret *et. al.*, (2010), showed that CD44⁺/CD24⁻ breast cancer stem cells have overlapping properties with high ALDH⁺ cells [165]. They performed *in vivo* bioluminescence imaging of ALDH-FLUOR-positive cells from the tumor xenograft which displayed CSC phenotype and mediated systemic metastasis[166]. In another study, Sun *et. al.*, (2010) showed that 1×10^3 ALDH^{high} cells from adenoid cystic carcinoma initiated the tumor formation and micro metastasis to distant organs like lungs and liver in live mice. However, no tumor formation was seen by same number of ALDH^{low} cells [167]. This suggests that CSCs even if in a very low number could be imaged non-invasively in the preclinical models with higher resolution and sensitivity.

In the present chapter we attempted to use BLI for the first time to monitor tumor growth kinetics of ovarian cancer stem cells isolated from different stages of chemoresistance. We implanted low number of SP and corresponding NSP population as well as spheroid and adherent cells in nude mice and monitored their tumor formation property over time.

Methodology:**Bioluminescence imaging vector and chemicals:**

For monitoring tumor growth kinetics, we used A2780 and resistant models (cisplatin, paclitaxel and combination) stably expressing PIK3CA-FL2-TDT reporter as described by Gaikwad et al (2013) [163]. D-Luciferin potassium salt, substrate for firefly luciferase was procured from Biosynth (Naperville, IL). Working stock of 30mg/ml D-luciferin was prepared in sterile PBS.

Cell Lines and culture condition:

A2780-PIK3CA-FL2-TDT cells were cultured in Dulbecco's modified Eagle's medium with 10% FBS and 1% penicillin-streptomycin (GIBCO, Carlsbad, CA).

Side Population assay:

Side population assay was performed to isolate both SP and NSP fraction from Pac^{ER} and Cis^{LR} cells through FACS. While sorting the cells, temperature was maintained at 4⁰C. Post sorting cell counting was performed with trypan blue staining and desired number of cells were resuspended in 50ul of chilled PBS. Detailed protocol for SP assay has been described in the materials and methods section.

Spheroid formation assay: Spheroid forming assays were performed using DMEM devoid of serum, supplemented with a cocktail of growth factors. Serial passaging was performed for monitoring long term self-renewal ability. Detailed protocol has been described in the materials and methods section.

Tumor xenograft assay and bioluminescence imaging.

Fifty thousand SP and NSP cells were resuspended in 50 µl PBS and injected subcutaneously into six to seven week-old NOD/SCID mice (n=5). In an another set of experiment, tumor

xenograft assay was performed with 10,000 spheroid and adherent cells isolated from early and late resistant cells. These cells were resuspended in 50 μ l PBS and injected subcutaneously into NOD/SCID mice (n=7). To perform *in vivo* imaging, mice were first administered with 100 μ l of D-luciferin (30mg/ml) intraperitoneally followed by anesthetization. After 10 minutes, mice were imaged till the maximum signals were observed. Imaging data consists of grey scale photographs superimposed on bioluminescence signals as an over lay depicting the site of injection and tumor growth. LIVINGIMAGE software was used to analyse the data points where ROIs (Region Of Interest) were drawn over the signals and respective ROI was measured as maximum photons/sec/cm²/sr. Tumor volume was measured using Vernier caliper applying the formula; Tumor volume = $\frac{1}{2}$ x Length x (Width)². All experiments were approved by the ACTREC Animal Ethics Committee.

Results:

Since it is difficult and time consuming to examine the tumorigenic potential of early and late resistant cells of each (cisplatin, paclitxel and dual drug) models in mice, we randomly selected one early (paclitaxel) and one late (cisplatin) resistant model from where we isolated both SP & NSP fraction for tumor xenograft study. Using similar randomisation one early and late resistant model was used for spheroid formation.

In vivo imaging of tumor xenograft from SP & NSP cells isolated from Pac^{ER} cells:

Side population assay was performed as described in chapter 2, followed by sorting of both SP and NSP fraction from the main population (Pac^{ER} cells). Sorted cells were counted with trypan blue dye and precisely 5 X 10³ SP and NSP cells were implanted subcutaneously in a cohort of NOD/SCID mice (n=5) on their left flank. Mice were imaged for Fluc activity on the day of cell implantation (day 0). Follow up imaging was performed to monitor the tumor development at regular intervals until they form a palpable tumor. During longitudinal monitoring of tumor xenograft, interestingly it was observed that in case of Pac^{ER} SP cells, tumor formation initiated

from day 15 showing an enhanced signal from day 0 (from $8.44 \times 10^6 \pm 5.08 \times 10^6$ to $3.44 \times 10^7 \pm 5.0 \times 10^7$ p/sec/cm²/sr). From day 15 to day 40 there was steep increase in the BLI signal obtained from the tumor xenograft ($3.44 \times 10^7 \pm 5.0 \times 10^7$ to $1.88 \times 10^{10} \pm 2.2 \times 10^{10}$ p/sec/cm²/sr) (Figure 3.1A&B). However there was a decrease in the BLI signal from the cohort of mice where NSP cells were implanted. Bioluminescent signal from NSP cells decreased from day 0 to day 40 ($3.92 \times 10^7 \pm 1.75 \times 10^7$ to $1.04 \times 10^4 \pm 4.66 \times 10^3$ p/sec/cm²/sr). Unfortunately, two mice from the cohort of mice bearing NSP tumor xenograft died in between the experiment. Along with Fluc imaging, we also measured the tumor volume and the graph was plotted (Figure 3.1C-D) showing increase in the tumor volume with increasing BLI signal from day 15 to day 40 ($0.04 \pm 0.03 \text{cm}^3$ to $0.98 \pm 0.80 \text{cm}^3$) in Pac^{ER} SP cells.

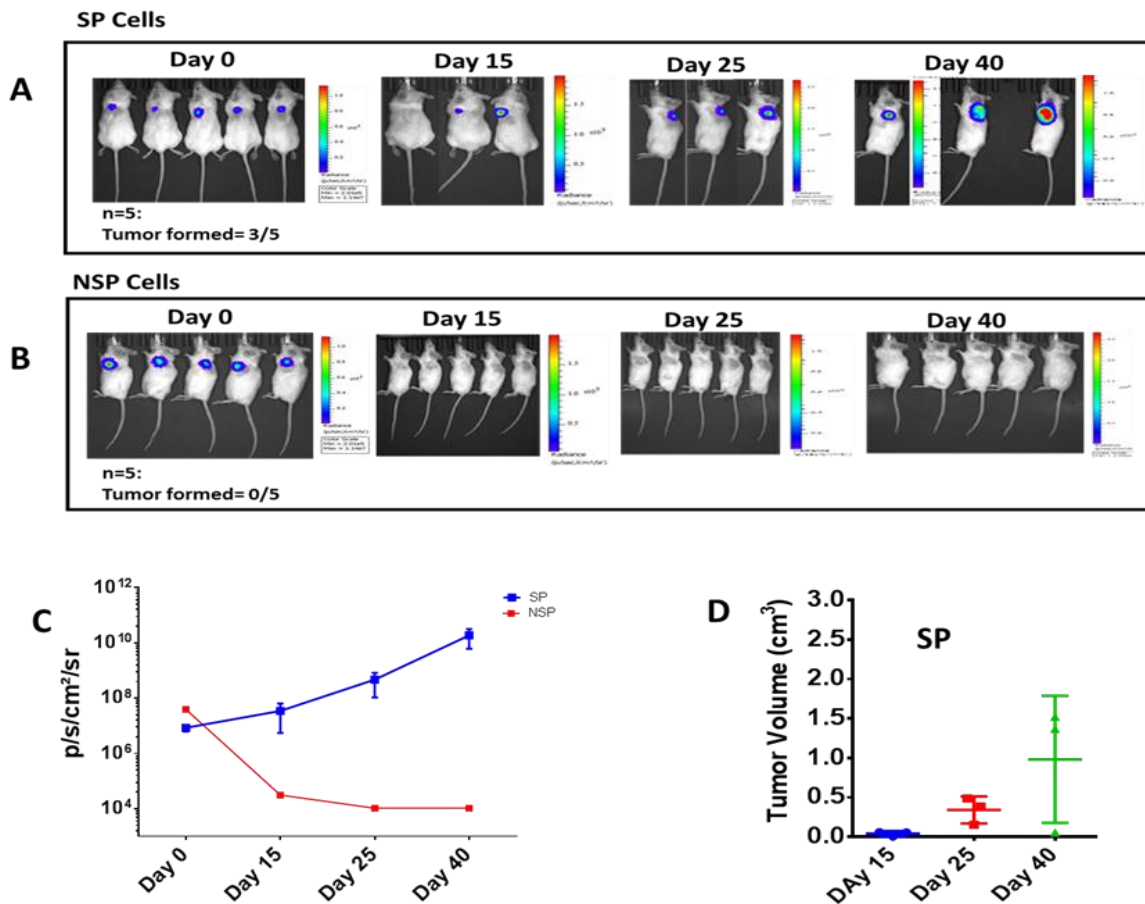


Figure 3.1: Monitoring tumorigenic potential of paclitaxel early resistant SP & NSP cells: (A-B) Representative bioluminescence images of Pac^{ER} SP & NSP tumor xenograft where 50,000 SP and NSP cells were implanted in NOD/SCID mice on day 0 ($n=5$). Real time monitoring of the tumor xenograft through non-invasive imaging showed increased bioluminescent signal from tumor xenograft with SP cells within day 15 to day 40 however tumor xenograft with NSP cells did not show any signal. (C) Graphical representation of the quantified signal for FL activity from mice with tumor xenograft implanted with SP & NSP cells from day 0 to day 40. Tumor xenograft from SP cells showed increased signal from day 15 to day 40 however NSP cells showed a steep decline in the signal till day 40. (D) Graphical representation of tumor volume measured by vernier caliper for Pac^{ER} SP cells ($n=3$) showing increase in the tumor volume from day 15 to day 40.

In vivo imaging of tumor xenograft from SP & NSP cells isolated from Cis^{LR} cells:

Using side population assay, SP and NSP fractions were sorted from Cis^{LR} cells. Post sorting cell counting was performed with trypan blue stain. Precisely 50,000 viable cells from both SP and NSP fractions were implanted subcutaneously on the right flank of NOD/SCID mice (n=5). Bioluminescence imaging of the tumor xenograft was performed on the day of cell implantation and the data was recorded as day 0. Follow up imaging was done at regular intervals to monitor the tumor growth kinetics from SP and NSP cells. It was observed that from day 0 to day 50 there was no increase in the bioluminescence signal both from SP & NSP cells. Interestingly, unlike Pac^{ER} cells where tumor formation started from day 15, Cis^{LR} SP cells initiated the tumor formation from day 80 where the BLI signal recorded from the tumor xenograft of Cis^{LR} SP cells increased from day 50 with $2.2 \times 10^5 \pm 5.35 \times 10^4$ p/sec/cm²/sr up to $4.03 \times 10^6 \pm 3.23 \times 10^6$ p/sec/cm²/sr by day 80 and $1.95 \times 10^{10} \pm 4.05 \times 10^9$ on day 110. However there was decrease in the BLI signal in NSP cells from day 50 to day 80 ($1.18 \times 10^5 \pm 1.07 \times 10^4$ to $9.70 \times 10^4 \pm 1.41 \times 10^4$ p/sec/cm²/sr to). At day 110, three mice in the cohort of five mice were showed palpable tumor (1.73 ± 0.74 cm³) but NSP cells did not form tumor even after 110 days (Figure 3.2B-C).

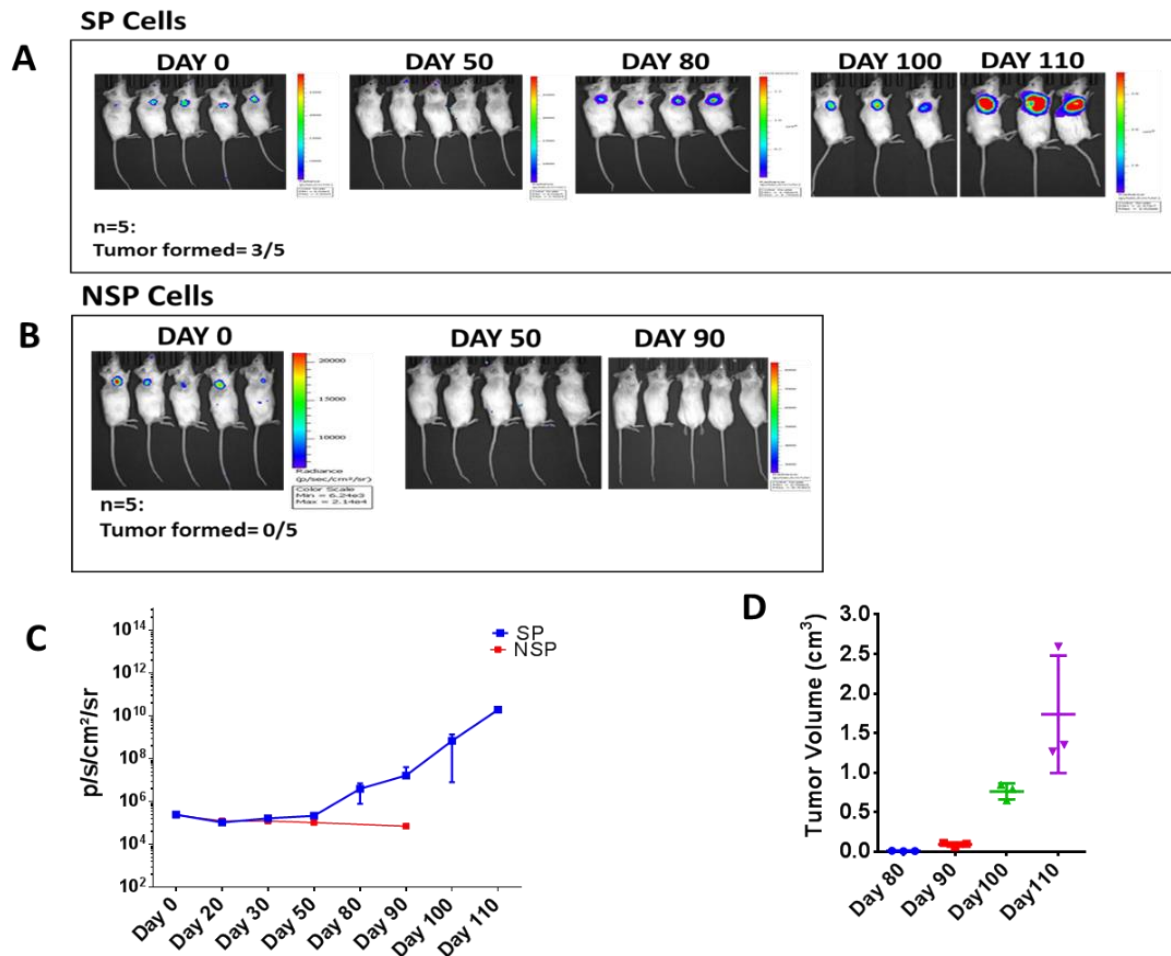


Figure 3.2: Longitudinal Monitoring of tumorigenic potential of cisplatin late resistant SP & NSP cells: (A-B) Representative bioluminescence images of Cis^{LR} SP & NSP tumor xenograft where 50,000 SP and NSP cells were implanted in NOD/SCID mice on day 0 (n=5). Real time monitoring of the tumor xenograft through non-invasive imaging showed an increase in the bioluminescent signal from tumor xenograft with SP cells from day 80 until day 110. However, tumor xenograft with NSP cells showed decrease in the signal from day 0 to day 90. (C) Graphical representation of the quantified signal for FL activity from the cohort of tumor xenograft implanted with Cis^{LR} SP & NSP cells from day 0 to day 110. Tumor xenograft from SP cells showed an increase in the signal from day 80 until day 110, however tumor xenograft from NSP cells showed decrease in the signal from day 0 to day 90 (D) Graphical

representation of tumor volume measured by vernier caliper for Cis^{LR} SP cells (n=3), showing an increase in the tumor volume from day 80 until day 110.

In vivo monitoring of tumor growth kinetics from Pac^{ER} spheroid and adherent cells:

Formation of spheroid under serum free condition is one of the functional property of cancer stem cells [77, 168]. Spheroid forming cells have higher self-renewal property as shown in the previous chapter where sphere forming cells from the resistant models showed an increased self-renewal ability and higher stemness gene expression (*Oct4*, *Sox2* and *nanog*). In this part of study, we intended to monitor the tumorigenic ability of these spheroid cells in comparison to the adherent cells. Since results from SP/NSP study demonstrated an early development of tumors from Pac^{ER} cells, we wanted to investigate further with this model. Both early and late resistant cells were allowed to form spheroids in serum free media in a low adherent plate and were serially passaged until the third generation. From the third passages of spheroid culture, 10,000 viable cells were implanted on the left flank and 10,000 adherent cells on right flank of NOD/SCID mice (n=7). Bioluminescence imaging of the tumor xenograft was performed on the day of cell implantation and the data was recorded as day 0. (Spheroid: $5.43 \times 10^6 \pm 1.36 \times 10^6$ p/sec/cm²/sr; Adherent: $9.9 \times 10^6 \pm 3.93 \times 10^6$ p/sec/cm²/sr). Follow up imaging was performed at regular time intervals to monitor the tumor growth kinetics. It was observed that mice implanted with 10,000 adherent cells showed a decrease BLI signal from day 0 to day 40 ($9.9 \times 10^6 \pm 3.93 \times 10^6$ to $2.12 \times 10^5 \pm 1.76 \times 10^5$ p/sec/cm²/sr) (Figure 3.3B, C). However, three mice from the cohort bearing tumor xenograft from spheroid cells showed an increase in the bioluminescence signal from day 0 to day 40 ($5.43 \times 10^6 \pm 1.36 \times 10^6$ to $9.01 \times 10^7 \pm 1.16 \times 10^8$ p/sec/cm²/sr). (Figure 3.3 A, C). Data was collected from the group of 4 mice since three mice from both the cohort died during experiment.

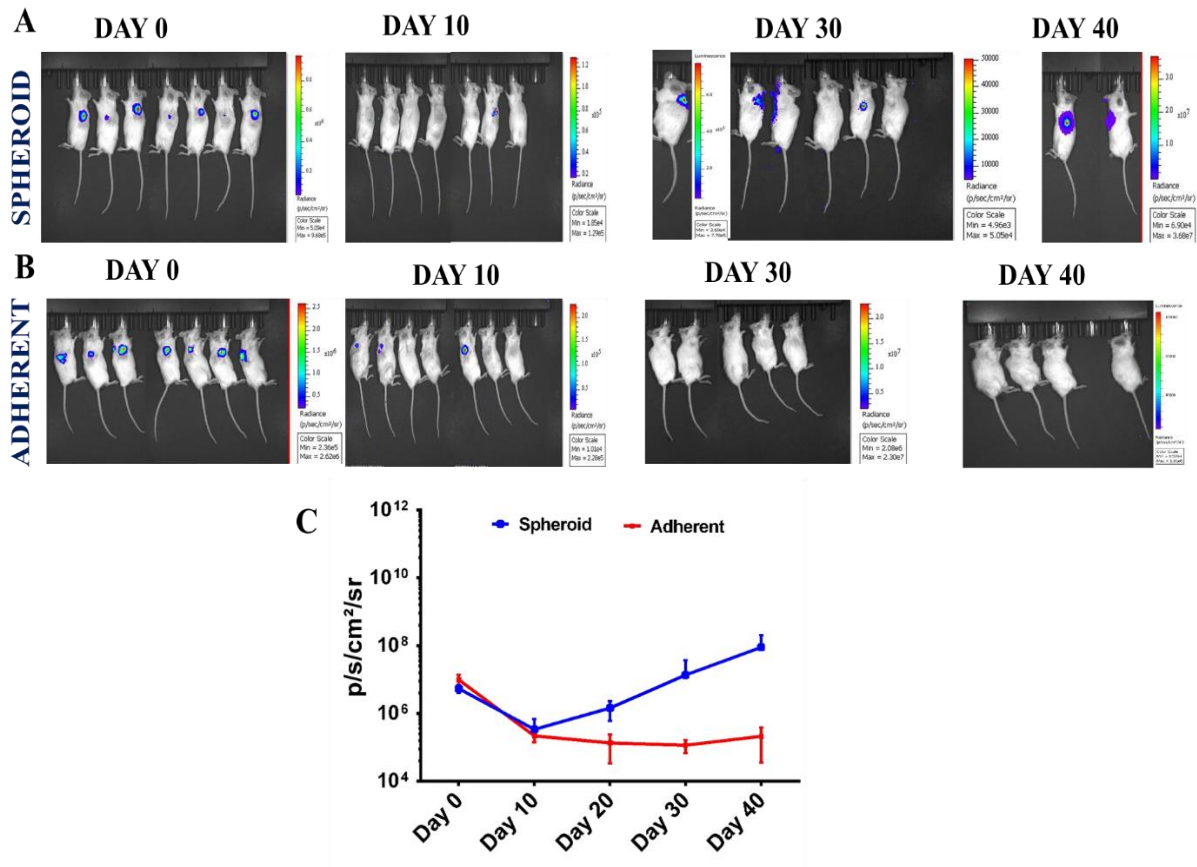


Figure 3.3: Longitudinal monitoring of Tumorigenic potential of spheroid and adherent cells from Pac^{ER} stage: (A-B) Representative bioluminescence images of tumor xenograft from Pac^{ER} spheroid and adherent cells where 10,000 spheroid and adherent cells were implanted in NOD/SCID mice on day 0 ($n=7$). Real time monitoring of the tumor xenograft through non-invasive imaging showed that tumor xenograft from Pac^{ER} spheroid cells showed a gradual increase in the signal from day 10 to day 40. However, tumor xenograft with Pac^{ER} adherent cells did not show any signal. (C) Graphical representation of the quantified signal for FL activity from the cohort of tumor xenograft implanted with Pac^{ER} spheroid and adherent cells from day 0 to day 40. Tumor xenograft from the spheroid cells showed an increased signal from day 10 to day 40. However NSP cells showed a decrease in the signal until day 40.

In vivo imaging of growth kinetics of Pac^{LR} tumor xenograft developed from spheroid and adherent cells:

Here we intended to monitor both tumorigenic ability and growth kinetics of Pac^{LR} spheroid cells versus adherent cells. In order to perform this experiment firstly spheroids were cultured under serum free media in low adherent plates up to three passages. Later 10,000 viable cells from both spheroids and adherent culture were implanted on the left and right flank region of NOD/SCID mice respectively (n=8). Longitudinal monitoring of the tumor xenograft was performed using Fluc activity. *In vivo* bioluminescence imaging was performed on the day of cell implantation and the data was recorded as day 0. Follow up imaging of tumor xenograft was performed at regular intervals (every 20 days) to monitor tumor growth. During monitoring of tumor growth through BLI, four mice from the cohort where 10,000 spheroid cell were implanted showing an increase in the bioluminescence signal from day 0 to day 120 ($1.84 \times 10^5 \pm 2.42 \times 10^4$ to $1.53 \times 10^9 \pm 1.26 \times 10^9$ p/sec/cm²/sr) (Figure 3.4 B, C). However we did not observe any increase in the bioluminescence signal from the adherent cells (Figure 3.4A, C). Surprisingly sudden increase in bioluminescent signal was observed from day 80 for spheroid group. At the end of the study (day120) we observed palpable tumor in three mice.

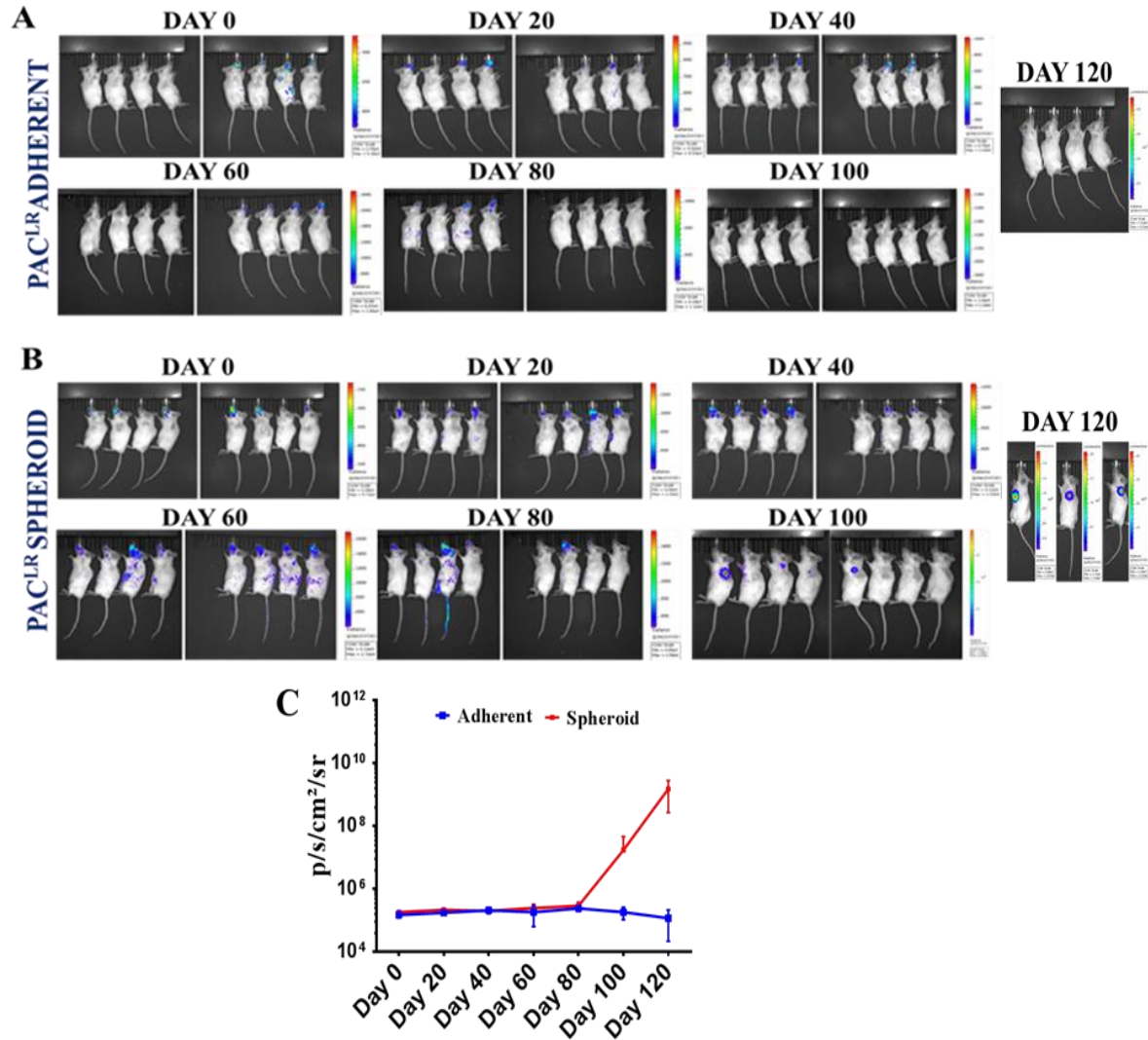


Figure 3.4: Monitoring Tumorigenic potential of spheroid and adherent cells from paclitaxel late resistant stage: (A-B) Representative bioluminescence images of tumor xenograft from Pac^{LR} spheroid and adherent cells where 10,000 spheroid and adherent cells were implanted in NOD/SCID mice on day 0 (n=8). Real time monitoring of the tumor xenograft through non-invasive imaging showed that tumor xenograft from Pac^{LR} spheroid cells showed an increase in the signal from day 100, however tumor xenograft from adherent cells did not show any increase in the signal. **(C)** Graphical representation of the quantified signal for FL activity from the cohort of tumor xenograft implanted with Pac^{LR} spheroid and adherent cells from day 0 to day 100. Tumor xenograft from spheroid cells showed an increased signal from day 100; however NSP cells did not show any increase in the signal.

Discussion:

Even though cancer stem cells from different tumor types have been investigated extensively in past decades, still they are not very well characterized under *in vivo* condition. *In vitro* studies may not sufficiently depict the complex behaviour of CSC biology in terms of its tumorigenic ability, stem cell plasticity and metastasis. However *in vivo* imaging techniques allow CSCs tracking to obtain valuable information such as tumor initiation from CSC population, stem cell plasticity and metastasis [110, 164]. Non-invasive imaging of different molecular events in pre-clinical model has become a standard practice for the evaluation of new drugs and monitoring molecular events in real time [169]. Various reporter genes have been utilized to assess various molecular events with varying depth inside the body of small animal. In this study for the first time we are showing the use of BLI to track down low number of ovarian SP, NSP, spheroid and adherent cells from different stages of resistance. We have shown the real time monitoring of tumor initiating property and growth kinetics of cancer stem cell like SP and spheroid cells isolated from early and late chemoresistant stage. In the previous chapter we have demonstrated *in vitro* identification and characterization of CSCs from different stages of resistance, where SP fraction showed an increased sphere forming ability with increased stemness gene expression. All of the *in vitro* assays performed earlier depicts that with increasing resistance there is an enrichment of ovarian cancer stem cells irrespective of the drug used to develop the resistant model. In this chapter we validated SP and NSP, spheroid and adherent cells for their tumorigenic property and showed that the tumor initiating event only could occur from the SP and spheroid cells but not from the NSP and adherent cells. Another aspect we were interested was to look into the tumor growth kinetics of CSCs isolated from early and late resistant stages of A2780 cells. To execute this experiment, we isolated SP and NSP fraction from all the resistant stages and randomly chose one early (Pac^{ER}) and one late (Cis^{LR}) resistant cells for tumor xenograft study. Interestingly we observed a differential

tumor growth kinetics from early and late resistant cells where Pac^{ER} SP cells initiated the tumor formation from day 15, and at the end of day 40, palpable tumors were formed. However SP fraction from the Cis^{LR} cells showed delay in the tumor initiation i.e. after day 80 tumor initiation started and by the end of day 110 a palpable tumor was observed. We also performed tumor xenograft experiment with spheroids and adherent cells from Pac^{ER} and Pac^{LR} stages. Similar to the previous findings Pac^{ER} spheroid cells initiated tumor formation from day 30 however spheroid cells from Pac^{LR} stage initiated the tumor formation around day 100. This suggests that SP fraction and spheroid cells from the same resistant cell line at early and late stages might have different tumorigenic potential. This intriguing behaviour of the cancer stem cell like population from different stages of resistance could be due to activation/inactivation of different signalling cascades that might have resulted in differential growth kinetics of the tumor development. Standard diagnosis of ovarian cancer in clinic is performed by MRI, CT and PET/CT imaging. Same imaging modality (MRI, CT and PET/CT) has also been used to differentiate ovarian cancer and benign adnexal lesion [170]. In another study, Prakash and Jagaru et al., showed FDG PET/CT in ovarian cancer as a critical tool for the preoperative evaluation of women with primary ovarian cancer and for postoperative follow-up assessment for evidence of recurrence in the patients [171, 172]. Hence available clinical imaging modalities are utilized to monitor ovarian cancer management routinely. However multiple imaging to monitor kinetics of tumor progression is not quite possible till now as we have shown in our preclinical set up. We believe that if ovarian cancer specific biomarkers or probes could be identified and developed in future, it would strengthen the diagnosis and disease management in ovarian cancer. Next we wanted to monitor if there is any differential gene regulation at early and late resistant stages of cisplatin, paclitaxel and combination model. This part of work has been detailed in the next chapter.

Chapter: 4

***Studying role of IGF-1R in maintenance of
ovarian cancer stem cell (OCSC) biology and
epithelial mesenchymal transition***

Introduction:

Insulin Like Growth Factor-1 Receptor (IGF-1R) tyrosine kinase is a member of the IGF axis that mediates growth, differentiation, metabolic activities and developmental processes [111, 113, 173]. Deregulation of IGF axis is associated with many pathologic conditions ranging from metabolic disorders, insufficient growth to cancers [174-176]. Activation of IGF-1R is well known for its crucial role in the process of tumorigenesis, chemo resistance and metastasis [5, 16, 113, 177-180]. This signalling constitutes a network of cellular and secreted proteins with multiple ligands (IGF-1, IGF-2, Insulin and Insulin like growth factor binding proteins (IGFBPs)). Strong homology with Insulin receptor adds another level of complicity on the function and regulation of IGF-1R. Among all these ligands, IGF-1 and IGF-2 are the most potent growth factors (ligands for IGF-1R) playing vital role in the developmental process and tight regulation of tissue growth and wound healing [181, 182]. IGF-1 and IGF-2 ligands are secreted from hepatocytes in an endocrine fashion to their respective cells and tissues. IGF-1 is known for years as a crucial mitogenic hormone and its overexpression has been strongly correlated with cancer [183-185]. The expression of IGF-1 is not constitutive, rather its level increases from prenatal to adult stage i.e. 20ng/ml to 100-200ng/ml in blood [186]. On the other hand IGF-2 is more important during foetal growth and development of certain organs like brain, liver and kidney. Though the levels of IGF-1 are 2-6 folds lower than IGF-2, yet IGF-2 alone is not sufficient for malignant transformation, however IGF-1 can independently lead towards transforming events [187]. Both these ligands transmit their signal for the complex cellular network through type 1 IGF receptor.

Structure and function of IGF-1R:

IGF-1R is a tetrameric receptor tyrosine kinase primarily localized on the membrane. The receptor is synthesized as a single polypeptide chain of 180 kDa having a 30 amino acid long signal peptide which guides the nascent IGF-1R polypeptide chain to endoplasmic reticulum where disulphide linkage occurs with simultaneous glycosylation and cleavage [188]. This yields a mature α and β subunits of IGF-1R which later assemble to form fully functional receptor in the membrane. IGF-1R is a non-canonical RTK which unlike other RTKs where ligand binding is an essential event for dimerization, remains as tetramer on the membrane. Ligand binding the activates the receptor activation by auto phosphorylation at Tyr1135, Tyr1131 and Tyr 1136 amino acid residues that lie within the kinase domain of activation loop [189]. (Figure 4.1). Auto phosphorylation of these tyrosine residues leads to conformational change for different docking proteins, such as Src homology 2 domain-containing (Shc) protein and insulin receptor substrates (IRS1–4). These substrates are further recruited within phosphorylation sites in the cytoplasmic domain. Binding of the ligand to IGF-1R leads to IRS phosphorylation and recruitment of regulatory (p85) and catalytic (p110) subunits of PI3K followed by phosphorylation of AKT at threonine 308 and Serine 473 [111, 113, 114]. Activated AKT then promotes cell survival through multiple mechanisms that include inhibition of apoptosis and induction of prosurvival gene expression via phosphorylation of several downstream target proteins e.g. IKK α and CREB [190]. The other parallel pathway, mediated by activated IGF-1R activation by IRS or Shc proteins is the RAS-RAF-MAPK or JNK that results in increased cell survival, cell growth and proliferation [191, 192]. Recently VM Macualay et al (2011) showed that IGF-1R can localize into nucleus through clatherin mediated endocytosis, binds with Leukemia Inhibitory Factor (LEF) transcription factor and increases expression of LEF downstream target genes like *cyclin D1* and *axin 2* [193, 194]. Another study by Sarfstein et al, (2012), using DNA affinity chromatography and ChIP showed

that in breast cancer cells, IGF-1R translocates into the nucleus and auto regulates IGF-1R expression in estrogen receptor (ER) negative cells but not in ER positive cells [195]. Thus IGF-1R could perform its function both as RTK when present on the membrane and as a transcriptional regulator when localized to the nucleus. All these actions exerted by IGF-1R have a strong relation with generation of chemoresistance either by activating the cell survival proteins or by upregulating the antiapoptotic machinery. Kurrey et. al. (2009) showed that acquisition of EMT phenotype via upregulation of snail and slug could lead to generation of chemoresistance and radioresistance in ovarian cancer [196]. In this study they have also reported that snail and slug may indirectly upregulate the self-renewal programme and acquisition of stem cell like phenotype. Though role of IGF-1R in promotion of drug resistance is well researched in various malignancies (as detailed below), whether IGF-1R activation is required for development of chemoresistance and EMT in ovarian cancer cells has not been explored in detail. In this section, an attempt was made to explore potential role and underlying mechanisms driven by IGF-1R in generation of chemoresistance in ovarian cancer cells. Simultaneously association between activated IGF-1R signalling, EMT and cancer stem cells were investigated.

Role of IGF-1R in chemo resistance and Cancer Stem Cells:

Generation of chemo resistance involves multiple events occurring sequentially and at the same time as well. Activation of IGF-1R signalling through PI3K/AKT or MAPKs promotes chemo resistance in tumour cells [111, 113]. IGF-1R has been extensively studied for its role and for the specific mechanisms through which it promotes resistance against various chemotherapeutic drugs. There are three major ways through which IGF-1R can lead to chemo resistance;

1. Enhancement in the tumour growth and inhibition of apoptosis through upregulating surviving signals: With increased IGF-1R signalling, rate of proliferation increases which results in enhanced tumor growth. Additionally, active IGF-1R signaling protects several cell types from a variety of apoptotic insults. IGF-1R-mediated protection from apoptosis primarily depends upon the activation of PI3K, Akt/protein kinase B, and phosphorylation and inactivation of BAD (member of the Bcl-2 family of proteins)[197]. There is also mitochondrial translocation of Raf1 and nedd4 in response to the interaction of IGF-1R with 14.3.3 protein which result in BAD phosphorylation and thus evading the mechanism of apoptosis[198].
2. Increased DNA repair mechanism: Several independent studies show that IGF-1R signalling gets activated in response to ionizing radiations and inhibition of IGF-1R either through IGF-1R deletion or using IGF-1R kinase mutant or antisense strategy act as radio sensitizer[199, 200]. This modulation in radio sensitivity was achieved majorly through IGF-1R interaction with ATM kinase and Ku DNA binding proteins. Macaulay et al (2001) have shown that ATM can directly regulate IGF-1R expression[199] and Peruzzi et al (2001) showed that tumour cells with defective ATM kinases expressed low levels of IGF-1R and were found to be more radiosensitive[201].
3. Increased expression of multi-drug resistant (MDR) gene: MDR gene encoded ATP-dependent drug efflux pump has broad substrate specificity. Its overexpression leads to decreased drug accumulation in resistant cells. Guo et al (1998), showed that in colorectal carcinoma, IGF-1R could lead to chemoresistance via the increased expression of MDR1 [202].

Since hyper activation of IGF-1R has found to be a crucial pre-requisite for malignant transformation in majority of the cancers like breast, prostate, lung, central nervous system, gastrointestinal, bone & soft tissue, Head & neck and in haematological malignancy [111, 113,

114, 203-205]. Several inhibitors comprised of antibodies, small molecule kinase inhibitor or ligand inhibitors are developed and used in clinical trials [121]. A comprehensive list of the monoclonal antibodies and small molecule inhibitors of IGF-1R kinase[206] are listed below.

Examples of antibodies that target the extracellular domain of IGF-1 R		
Antagonistic and/or neutralizing antibody	Company	Phase of development
CP-751,871	Pfizer	Phase I
EM164	ImmunoGen and Sanofi-Aventis	Preclinical
IMC-A14	ImClorie	Preclinical
h7C 10 (F50035)	Pierre Fabre and Merck	Preclinical
19D12	Schering-Plough	Preclinical
Examples of small molecule inhibitors that target IGF-1 R kinase		
Small molecule kinase inhibitor	Company	Phase of development
INSM18	Insmed	Phase I
PPP	Karolinska Cancer Institute and Biovitrum	Preclinical
NVP-ADW742	Novartis Pharma	Preclinical
NVP-AEW541	Novartis Pharma	Preclinical
BMS-536924	Bristol-Myers Squibb	Preclinical
BMS-554417	Bristol-Myers Squibb	Preclinical

Table 4.1: A comprehensive list of monoclonal antibodies and small molecule inhibitors of IGF-1R kinase.

However, none of these inhibitors till date is adapted in clinical practice indicating further validation on the mechanism, exact time of implementation and efficacy for single or combinatorial treatment is required.

As mentioned earlier in the introduction (chapter 1), cancer stem cells have higher chemoresistant property. However, role of IGF-1R signalling in maintainence of CSC phenotype is less investigated. Till date there are only two reports available describing the role of IGF-1R in CSC biology. Chang et al (2013) for the first time demonstrated that expression of

phosphorylated IGF-1R was greater in Breast Cancer Stem Cells (BCSCs) than in non-BCSCs from xenograft models of human breast cancer[207]. In another study, Hart et al (2011) reported that post IGF-1 treatment there was an enrichment in the colon cancer stem cells and anti IGF-1R monoclonal Ab (CP-751,871) can specifically target CSC population[208, 209].

IGF-1R and Ovarian Cancer:

The insulin-like growth factor (IGF) family proteins play a vital role in the the development of tissues or organs and postnatal growth, and maintenance of normal function of many cell types of the body including ovary [210-212]. IGF-1R axis is largely active during ovulatory process when constant rupture and repara of surfce epithelium takes place. Liu et al (2007) showed that Foxo3 (downstream target of IGF1) gene disruption in mice leads to inappropriate oocyte activation and premature entry of primordial follicles into the growing pool leading to infertility [213]. As expected that abnormal growth and carcinogenesis in ovary would be associated with deregulation in IGF-1R signaling, several investigators found an active IGF-1R signaling in Serous Epithelial ovarian carcinoma [214, 215].

However, very few reports exist to suggest that IGF-1R could be a crucial player in imparting resistance against cisplatin and paclitaxel in ovarian cancer. Eckstein et al (2009) showed that hyperactivation of IGF-1R signalling is required for gaining cisplatin resistance through incremental increase in IGF-1R transcript levels with increasing resistance. AG 1024 (IGF-1R inhibitor) could sensitize these resistant cells towards Cisplatin [16]. They also found that this Cisplatin resistance was mediated by the activated PI3K/Akt pathway but not by the MAPK/ERK pathway. In another study performed bu Huang et al., (2010) a taxol resistant ovarian cancer cell line (Hey-T30) showed higher expression of IGF-II and activated IGF signaling. Inhibition of IGF-1R (by a small molecule inhibitor) or IGF-II (by siRNA) led to the reversal of taxol resistance [17]. These two reports clearly indicated that IGF-1R has a vital

role in acquirement of resistance towards both cisplatin and paclitaxol. Patel et al (2011) showed indispensable role of IGF-1R signaling in the maintenance of colon cancer stem cells [118]. IGF-1R was also reported to play a crucial role in the maintenance of breast and hepatic cancer stem cells [118, 207, 216]. But nothing was known about IGF-1R signalling in ovarian cancer stem cell biology. This prompted us to investigate the role of IGF-1R signalling during the acquirement of chemoresistance and maintenance of ovarian cancer stem cell phenotype.

Role of IGF-1R during epithelial to mesenchymal transition:

A hallmark of EMT is loss of E-cadherin, a key mediator of cell–cell junctions and the gain of vimentin. Down regulation of E-cadherin is mostly governed by transcriptional repression, mediated by zinc finger forkhead domain and bHLH transcription factors including Zeb1/TCF8/DEF1, Zeb2 (Sip1), Snail, Slug, FOXC2 and Twist [217]. Lorenzatti et al (2011), showed that CCN6 is a secretory protein that modulates insulin-like growth factor-1 (IGF-1) signaling pathway and knockdown of CCN6 in benign mammary epithelial cells triggers an epithelial to mesenchymal transition via upregulation of transcription factor ZEB1[218]. Zhao et al., (2011) showed that in a panel of six hepato cellular carcinoma cell lines exhibiting up regulated IGF-1R and IR levels, treatment of OSI-906 (IGF1-R/IR dual inhibitor) resulted in decreased expression of two epithelial markers E-cadherin and ErbB3 and up regulation of two mesenchymal markers i.e. vimentin and zeb[129]. This suggested that IGF-1R and IR plays a crucial role in the maintenance of EMT phenotype. Kajiyama et. al., (2007) established paclitaxel resistant EOC cell lines to investigate the changes in the cellular morphology, motility and EMT[219]. They found decreased expression of the epithelial adhesion molecule (E-cadherin) and increased mesenchymal markers (vimentin and fibronectin) in the paclitaxel resistant cells. Rosano et. al., (2011) showed that activation of Endothelin-1 (ET-1) and Endothelin A receptor (ETAR) not only leads to the acquirement of EMT phenotype but also resistance against cisplatin and paclitaxel suggesting that acquisition of EMT phenotype might

lead towards generation of chemoresistance[220]. Role of IGF-1R has been linked to acquirement of resistance against cisplatin and paclitaxel but its role in generation of EMT phenotype in chemoresistant cells is still unknown. Since we know that IGF-1R axis is significantly upregulated at an early resistant stages we intend to monitor the association of IGF-1R in the regulation of epithelial and mesenchymal transition in chemoresistant cells.

Methodology:

Cell cultures and treatments

Ovarian carcinoma cells (A2780) were cultured in Dulbecco's modified Eagle's medium with 10% FBS and 1% penicillin-streptomycin (GIBCO, Carlsbad, CA). For PPP (Calbiochem, Germany) alone or combinatorial (cisplatin+PPP/paclitaxel+PPP/cisplatin-paclitaxel+PPP) treatments, cells starved for 12hrs were then treated with required concentrations of PPP for 48hrs and further processed.

Western blotting

Western blotting was performed as described earlier with antibodies against IGF-1R β -subunit, AKT, pAKT and beta actin were obtained from Cell Signaling Technology (Danvers, MA) and WT1, Vimentin from Abcam (Cambridge). Detailed protocol is given in materials and methods section.

Quantitative real-time PCR (qRT-PCR) from cell line, primary cells and tumor:

Total RNA was extracted from cultured cells using RNease kit (Qiagen, Netherlands). 1-2ug of total RNA was reverse transcribed using cDNA synthesis kit (Invitrogen, Carlsbad, CA). QRT-PCR analysis was performed using SYBR Green method (Invitrogen). GAPDH was used as an internal control. The relative expression levels of mRNAs were calculated by the ΔC_t for relative quantification and $\Delta\Delta C_t$ method for fold change measurement.

Immunofluorescence: Immunofluorescence study by confocal microscopy was performed as described earlier. Briefly, cells fixed with chilled methanol was probed with IGF-1R Ab for

overnight at 4⁰C followed by Secondary Ab (anti rabbit Dylight 633). Cells were counterstained with DAPI and mounted with vectashield medium. Images were observed under Carl Zeiss, LSM 710 microscope.

MTT assay: Cell viability was assessed using the standard thiazolyl blue tetrazolium bromide (MTT) method and percent viability was counted using the formula

$$[\{ \text{Absorbance}^{(\text{Test})} \div \text{Absorbance}^{(\text{Control})} \} \times 100]$$

Colony formation assay: Single-cell suspensions were plated in six well dishes at a density of 1000 cells/ well. Once adhered, cells were serum starved for 12 hours followed by cisplatin, paclitaxel, and Cis + Pac and PPP treatment either alone or in combination for 48 hours. The plates were further incubated for 7-8 days and colonies were stained with 0.01% crystal violet and counted under inverted microscope.

FACS: To monitor the membrane bound expression of IGF-1R at different resistant stages, FACS was performed using IGF-1R monoclonal Ab (Cell Signaling) at dilution 1:200 in PBS. Staining was performed in unfixed cells to monitor IGF-1R protein which is present only at the membrane. Secondary Ab against IGF-1R, anti-rabbit FITC (Abcam) was used at a dilution (1:200). Data analysis was performed using Flow-Jo software.

Statistical analysis: Assays were performed in triplicates and data were presented as the mean \pm standard deviation. Statistical significance was assessed by two-tailed Student's t-test.

Results:

Differential expression of IGF-1R at sensitive, early and late stages of drug resistance:

Acquirement of drug resistance is a multifactorial event driven via various mutations in resistance related genes, apoptosis and signalling pathways along with deregulated signalling cascade. While investigating modulation in IGF-1R signalling pathways in our cisplatin,

paclitaxel and dual resistant models, an interesting oscillatory pattern in IGF-1R expression was observed during the course of resistance development irrespective of the nature of drug. Significantly higher transcripts were found in Cis^{ER}, Pac^{ER} and Cis-Pac^{ER} cells that considerably decreased at Cis^{LR}, Pac^{LR} and Cis-Pac^{LR} stages in comparison to sensitive cells (Table 4.2 & Figure 4.1 A).

	Resistant Stage	Fold Change
Early Resistant cells	Cis ^{ER}	3.8
	Pac ^{ER}	5.4
	Combi ^{ER}	11
Late Resistant Cells	Cis ^{LR}	0.6
	Pac ^{LR}	0.7
	Combi ^{LR}	3.8

Table 4.2: Fold change in the levels of IGF-1R transcripts: *Quantitative PCR to measure IGF1R was performed and fold change was calculated by $2^{-\Delta\Delta Ct}$ method across the resistant models. Compared to the sensitive cells early resistant cells (Cis^{ER}, Pac^{ER} and Combi^{ER}) showed increased expression of IGF-1R (3.8, 5.4 and 11 fold in) however late resistant cells showed decreased expression in Cis^{LR} and Pac^{LR} (0.6 and 0.7 fold) except Combi^{LR} cells where 3.8 fold increase was observed.*

This oscillatory pattern of IGF-1R was also evident at protein level where early resistant cells from all the three resistant models showed high level of IGF-1R protein whereas at their respective late stages the levels of IGF-1R decreased (Figure 4.1F) [180]. The function of IGF-1R is mediated via auto phosphorylation of the kinase domains upon ligand binding. Therefore for proper and optimal activation to take place, membrane localization of IGF-1R is very

important. Hence we investigated the status of IGF-1R qualitatively and quantitatively through confocal microscopy and FACS (Figure 4.2 D-E).

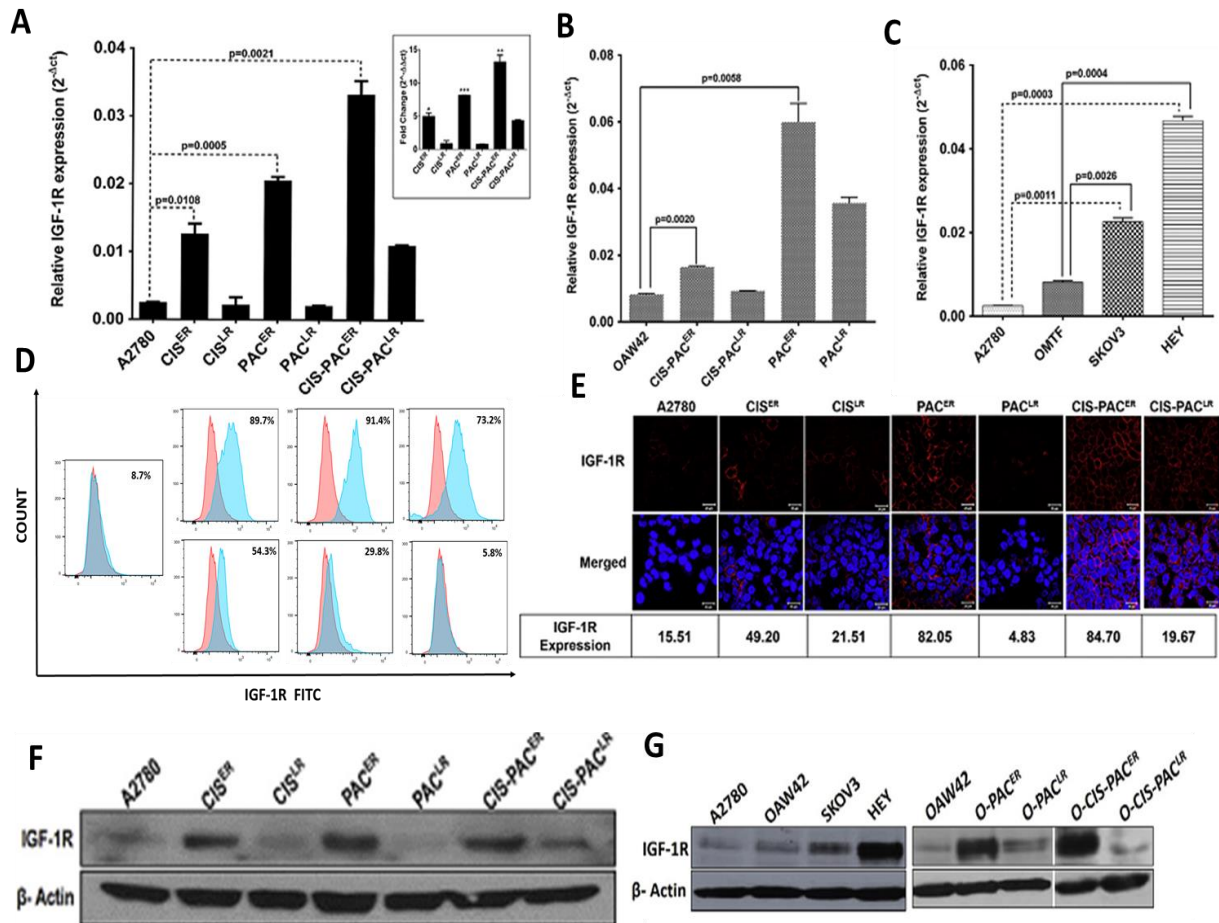


Figure 4.1. Expression analysis of IGF-1R at different stages of resistance in A2780 cells and intrinsically cisplatin resistant cells: (A) Real time quantification of IGF-1R transcripts in A2780, Cis^{ER}, Cis^{LR}, Pac^{ER}, Pac^{LR}, Cis-Pac^{ER} and Cis-Pac^{LR} cells using IGF-1R specific primers normalized to GAPDH showed high expression of IGF-1R at early and low expression at late resistant stages. Fold change in IGF-1R expression in resistant cells compared to control cells are shown graphically in the inset. (B) Real time quantification of IGF-1R transcripts in OAW42, OAW42-Pac^{ER}, OAW42-Pac^{LR}, OAW42-Cis-Pac^{ER} and OAW42-Cis-Pac^{LR} cells showed significant increase at early stages which decreased at late stages. (C). Basal level of IGF-1R transcripts in SKOV3 and HEY cells showed significant upregulation

compared to A2780 and OAW42 cells. (D) FACS analysis showing increased membrane staining in early resistant cells (89.7%, 91.4% and 73.2% in CIS^{ER} , Pac^{ER} $Cis-Pac^{ER}$ respectively) compared to late resistant cells (54.3%, 29.8% and 5.8% in Cis^{LR} , Pac^{LR} $Cis-Pac^{LR}$ respectively) (E) Immunofluorescence study by confocal microscopy in cells probed with an antibody against IGF-1R β demonstrated increased membrane localization of IGF-1R at early resistance (Cis^{ER} , Pac^{ER} $Cis-Pac^{ER}$) cells. Error bars represent SE for triplicate measurements. (F) Western blot analysis of IGF-1R showed an increased expression during early stage of resistance (CIS^{ER} , Pac^{ER} $Cis-Pac^{ER}$) compared to sensitive cells and late resistant cells. (G) Western blot analysis of IGF-1R during early stage of resistance in OAW42- Pac^{ER} and OAW42- $Cis-Pac^{ER}$ showed increased protein level compared to sensitive cells and late resistant cells. Both SKOV3 and HEY cells showed increased IGF-1R expression compared to A2780 and OAW42 cells at protein level.

In accordance with transcript and protein data, around 82.05% and 84% of the early paclitaxel and dual resistant cells and 49.2% of early cisplatin resistant cells showed membrane localization of IGF-1R in comparison to 15.5% in sensitive cells. A drastic reduction in membrane localization of IGF-1R was observed in paclitaxel late resistant cells than cisplatin and dual resistant cells (4.83% vs. 21.51% & 19.67%) (Figure 4.1E). Since microscopic analysis provides a more qualitative and semi quantitative measurement of gene expression, we checked the receptor level quantification by FACS in unfixed cells. Similar to microscopic data 89.7%, 91.4% and 73.2% cells of cisplatin, paclitaxel and dual resistance at early stages respectively were found positive in comparison to A2780 sensitive cells which showed only 8.7% positivity. Decrease in receptor positivity (54.3%, 29.8% and 5.8%) in cisplatin, paclitaxel and dual late resistant cells respectively were observed. This data indicates that acquirement of resistance to cisplatin, paclitaxel and dual drug actively requires hyper-

activation of IGF-1R only during early phase of acquirement of resistance which later becomes independent of IGF-1R signalling. For the biological relevance of this finding we investigated the expression levels of IGF-1R in two naturally resistant cells towards cisplatin (SKOV3 & Hey) and another endogenous cellular resistant model developed in OAW42 cells (Serous EOC). In OAW42 paclitaxel and dual resistant cells, IGF-1R expression was higher at early stage and decreased at late stage at both transcript and translational levels. SKOV3 and Hey cells showed higher IGF-1R expression compared to A2780 and OAW42 (cisplatin sensitive) (Figure 4.1C, G)

Transcriptional regulation of IGF-1R:

IGF-1R signaling is a complex event which involves various transcriptional activators and repressors. We performed string analysis using a software STRING V9.1 based on reported interactors to find out possible key regulators of IGF-1R (Figure 4.2). We then categorized these transcriptional regulators into transcriptional activators and repressors as per our analysis and established literature [122, 124, 221].

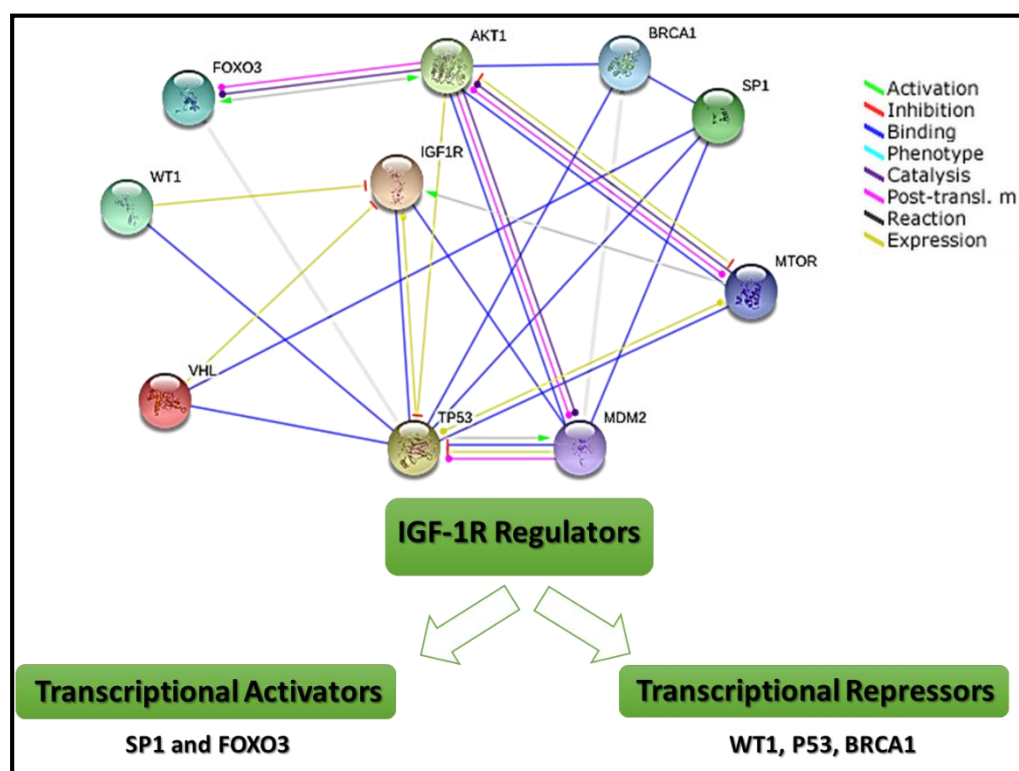


Figure 4.2. String analysis for IGF-1R and its possible interactors: Based on available literature, most probable interacting partners were used for the string analysis keeping the confidence level 90 percent. String of potential regulators for IGF-1R as transcriptional activators (SP1 and FOXO3) or repressors (WT1, P53 and BRCA1) were found where Blue lines show direct binding, Green lines activation and red lines inhibition of IGF-1R.

Since we observed that IGF-1R expression was significantly high during early phase of resistance, we intended to monitor the transcript levels of positive regulators; SP1 and FOXO3. It was observed that SP1, a known potential regulator of IGF-1R that has strong affinity towards GC rich region of IGF-1R promoter did not corroborate with the transcript levels of IGF-1R. However expression levels of Foxo3 did show positive correlation with up regulated Foxo3 transcripts at early stages of cisplatin and paclitaxel resistant cells but not in dual resistant cells. In dual resistant cells the transcriptional and translational regulators could be more complex and might be different which needs further investigation. WT1, a known transcriptional repressor for IGF-1R remained unaltered across the resistant models as shown in the figure 4.3. However, further studies are required to understand the level of activated Sp1, Foxo3 in these resistant cells to estimate the actual correlation with IGF-1R level.

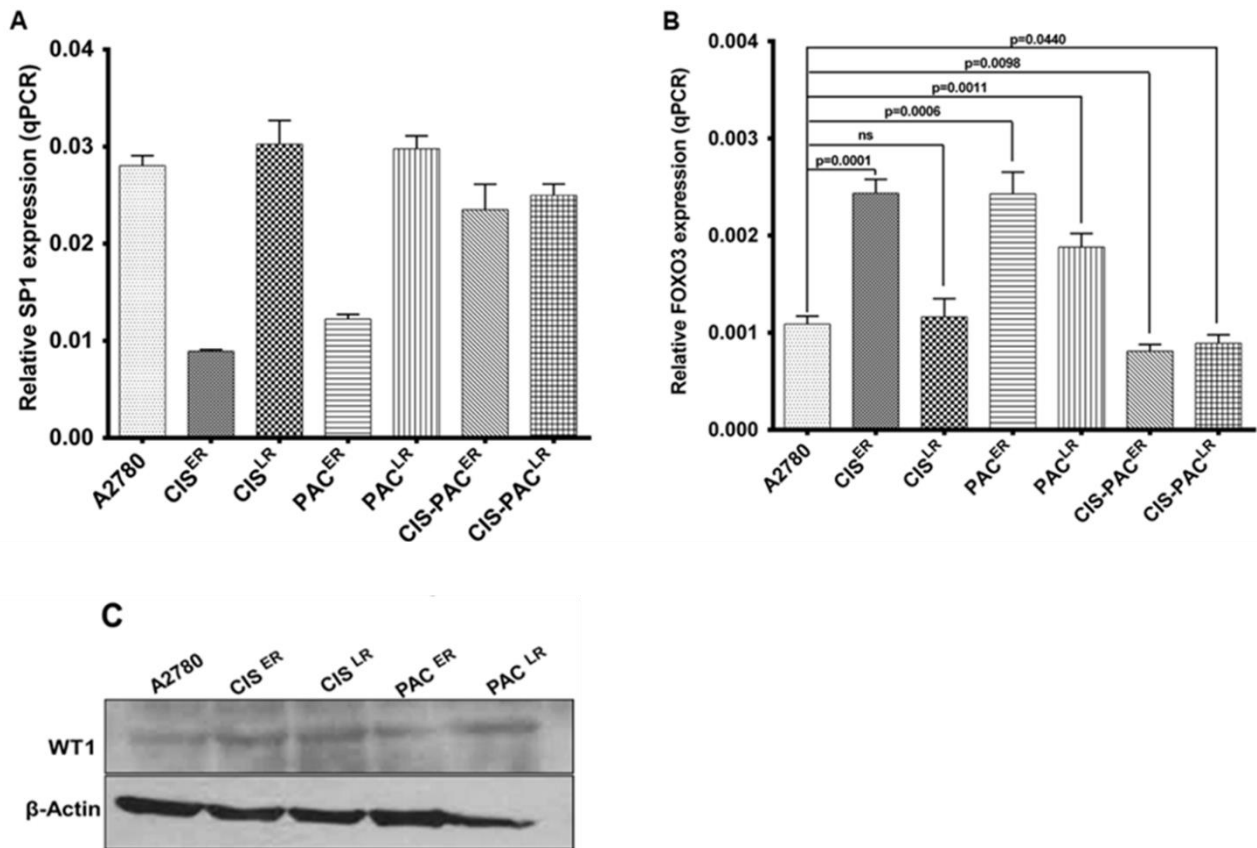


Figure 4.3. Transcriptional regulators of IGF-1R expression in the resistant models. (A) SP1 mRNA profile: Quantitative PCR with SP1 showed less expression in Cis^{ER} cells compared to Cis^{LR} cells. However Pac^{ER}, Pac^{LR}, Cis-Pac^{ER} and Cis-Pac^{LR} cells showed marginal increase in SP1 expression. **(B) FOXO3 mRNA profile:** Real time analysis of Foxo3 transcripts showed significantly high expression in Cis^{ER} and Pac^{ER} cells that decreased in Cis^{LR} and Pac^{LR} cells. However, Cis-Pac^{ER} and Cis-Pac^{LR} cells did not show differential expression pattern. **(C) WT1 expression:** Western blot analysis of total cell lysate did not exhibit any significant change across the resistant models.

Next we wanted to find the effect of IGF-1R inhibition on the resistant characteristics of these cells. Since IGF-1R has a strong homology with IR, we looked for specific inhibitors of IGF-1R in the available literature which have already entered in clinical trials (Table 4.3).

Agent	Company/Institute	Phase	Comments
IGF1R TKIs			
A-928605	Abbott	Preclinical	Pyrazolopyrimidine TKI
BMS-536924	Bristol-Myers Squibb	Preclinical	ATP-competitive, equipotent inhibition of IGF1R and IR
BMS-554417			
INSM-18 (NDGA)	Insmed	Phase I-II	Dual inhibitor of the IGF-I and HER2 receptor kinases Phase I data suggest modest PSA responses in patients with nonmetastatic prostate cancer
PPP	Karolinska Cancer Institute and Biovitrum	Preclinical	Inhibits phosphorylation of Y1136 in the kinase activation loop. Does not inhibit IR Preferentially inhibits PI3K-Akt pathway, blocks growth of a range of tumors <i>in vitro</i> and <i>in vivo</i> Induces IGF1R down-regulation via involvement of β -arrestin 1/MDM2
NVP-ADW742	Novartis Pharma	Preclinical	ATP-competitive inhibitor, shows ~ 15-fold selectivity for IGF1R relative to IR in intact cells In SCLC, inhibits PI3K-AKT and induces synergy in combination with chemotherapy
NVP-AEW541	Novartis Pharma	Preclinical	ATP-competitive inhibitor, shows ~ 27-fold selectivity for IGF1R relative to IR within intact cells Inhibits Akt/mTOR pathway, enhances growth inhibition of MM cells in combination with dexamethasone and bortezomib
OSI-906	OSI Pharmaceuticals	Phase I	Shows ~ 10-fold selectivity for IGF1R relative to IR. Synergistic antiproliferative effects in combination with erlotinib in CRC cell lines via blockade of AKT and ERK phosphorylation
XL-228	Exelixis	Phase I	Inhibitor of IGF1R, BCR-ABL and Src
Agent	Company/Institute	Phase	Comments
IGF1R antibodies			
AVE1642	Sanofi-Aventis	Phase I-II	Humanized version of murine EM164 IgG ₁ antibody. Phase I single agent in MM, with docetaxel in solid tumors, well-tolerated, no DLT. Planned combination with bortezomib in MM
SCH-717454 (19D12)	Schering-Plough	Phase I-II	Fully human monoclonal antibody Activity against IGF1R/IR hybrid receptors via interaction with the IGF1R component
CP-751,871	Pfizer	Phase I-III	Fully human IgG ₂ . Phase I: mild hyperglycemia, no DLT, MTD not achieved. At 20 mg/kg, 10 of 15 patients had SD. Phase II in adrenocortical carcinoma, sarcoma: SD in 60% patients. Phase II in NSCLC: RR 51% to CP-751,871 with TC vs. 36% on TC alone. Objective responses to TC with antibody in 72% of squamous tumors, including "striking" responses in bulky disease, and some PR/SD on CP-751,871 after PD on TC alone
IMC-A12	ImClone Systems, Inc.	Phase I-II	Recombinant human monoclonal IgG ₁ antibody, binds IGF1R and IGF1R/IR hybrid receptors but not IR alone. Stable disease in 46% of patients with solid tumors in phase I
BIIB022	Biogen Idec	Phase I-II	Fully human nonglycosylated version of IgG ₄ .P antibody lacking Fc-effector function
MK-0646	Merck	Phase I-III	Humanized monoclonal IgG ₁ . Phase I toxicity hyperglycemia and thrombocytopenia. Current studies: phase II in neuroendocrine tumors and NSCLC; phase II/III in metastatic CRC with cetuximab and irinotecan
R1507	Roche	Phase I-II	Human monoclonal IgG ₁ antibody. Phase I showed PR in four of eight patients with sarcoma
AMG 479	Amgen	Phase I-II	Fully human monoclonal IgG ₁ antibody. Phase I activity: CR in Ewing's, PR in neuroendocrine tumor. Phase IB with panitumumab or gemcitabine: one DLT (hyperglycemia)

Table 4.3: List of IGF-1R specific inhibitors and antibodies which are under clinical trial.

Girnit et al., in 2004 validated a small molecule inhibitor picropodophyllin (PPP) derived from picropodotoxin (PPT) as a specific inhibitor for IGF-1R kinase activity. We performed in silico modelling of the kinase domain specifically for the residues Y1131, Y1135 and 1136 responsible for auto phosphorylation of the RTK with PPP. Similar to previous reports PPP binds specifically in the docking pocket created by Y1135 and Y1136 (figure 4.4) in our model.

little change in viability and Pac^{LR} cells were completely refractory to PPP even at the highest dose (2.5 μ M) (figure 4.5B). We also monitored the effect of PPP on naturally resistant cells i.e. SKOV3 and Hey which has increased basal expression of IGF-1R showing dose dependent decrease in the percent viability as shown in the figure 6C.

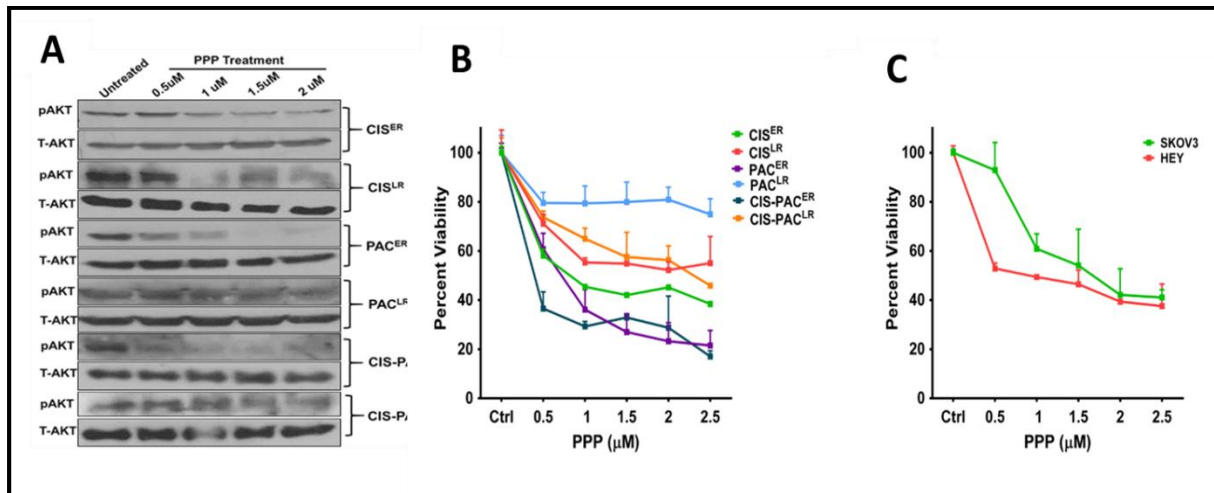


Figure 4.5. Effect of PPP treatment on chemoresistant models and intrinsically resistant cells: (A-B) Treatment with 0.5 μ M, 1 μ M, 1.5 μ M and 2 μ M PPP CIS^{ER}, Pac^{ER} and Cis-Pac^{ER} showed dose dependent decrease in pAKT levels with no change in tAKT; however, Cis^{LR}, Pac^{LR} and Cis-Pac^{LR} did not show much decrease. (B) Treatment with PPP at different concentrations (0.5 μ M, 1 μ M, 1.5 μ M, 2 μ M and 2.5 μ M PPP), CIS^{ER}, Pac^{ER} and Cis-Pac^{ER} showed most prominent effect where percent viability decreases in a dose dependent manner. However late resistant cells (Cis^{LR}, Pac^{LR} and Cis-Pac^{LR}) did not show any dose dependent decrease. (C) SKOV3 and Hey (intrinsically resistant to cisplatin) showed dose dependent decrease in percent viability in response to treatment with increasing concentration of PPP.

Since sole inhibition of a specific signalling may not exert maximum resistance reversal, we investigated combinatorial effect of PPP along with the drugs. To avoid the toxicity produced by each therapy, we chose to perform the combinatorial treatment at the lowest possible concentrations. We stringently determined the IC₁₀, IC₂₀, and IC₄₀ values for the

chemotherapeutic drugs ($IC_{10} = 250$ ng/ml, $IC_{20} = 500$ ng/ml and $IC_{40} = 1$ μ g/ml for Cis^{ER} ; $IC_{10} = 1$ μ g/ml, $IC_{20} = 2$ μ g/ml and $IC_{40} = 3$ μ g/ml for Cis^{LR} ; $IC_{10} = 10$ ng/ml, $IC_{20} = 20$ ng/ml and $IC_{40} = 40$ ng/ml for Pac^{ER} and $IC_{10} = 25$ ng/ml, $IC_{20} = 50$ ng/ml and $IC_{40} = 100$ ng/ml for Pac^{LR} ; $IC_{10} = 0.875$ ng/ml + 5 ng/ml, $IC_{20} = 1.16$ ng/ml + 6.66 ng/ml and $IC_{40} = 1.75$ ng/ml + 10 ng/ml for $Cis-Pac^{ER}$ and $IC_{10} = 2.33$ ng/ml + 13.33 ng/ml, $IC_{20} = 7$ ng/ml + 40 ng/ml and $IC_{40} = 17.5$ ng/ml + 100 ng/ml for $Cis-Pac^{LR}$) and IC_{10} , IC_{20} for IGF-1R inhibitor ($IC_{10} = 0.1$ μ M and $IC_{20} = 0.2$ μ M for CIS^{ER} ; $IC_{10} = 0.1$ μ M and $IC_{20} = 0.2$ μ M for CIS^{LR} ; $IC_{10} = 0.1$ μ M and $IC_{20} = 0.2$ μ M for Pac^{ER} and $IC_{10} = 0.2$ μ M, $IC_{20} = 0.4$ μ M for Pac^{LR} ; $IC_{10} = 0.1$ μ M and $IC_{20} = 0.2$ μ M for $Cis-Pac^{ER}$ and $IC_{10} = 0.1$ μ M and $IC_{20} = 0.2$ μ M for $Cis-Pac^{LR}$) as shown in the figure 4.6 A-B. All of the IC doses were calculated after 12 hours of serum starvation followed by 48 hours of respective drug treatment (PPP/Cisplatin/Paclitaxel/Cisplatin + Paclitaxel).

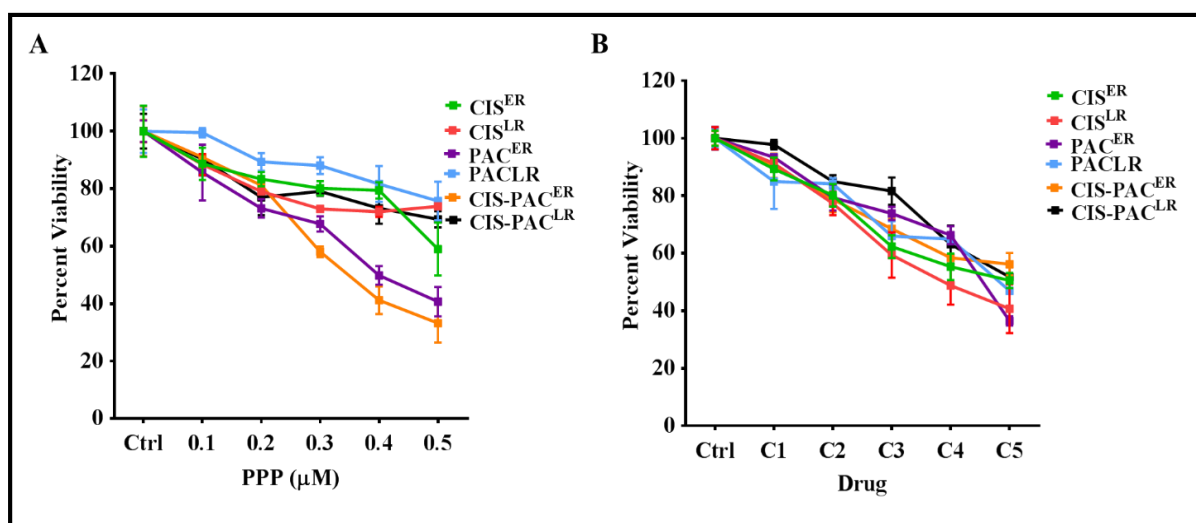


Figure 4.6. (A) *Determination of IC_{10} and IC_{20} for PPP in cisplatin, paclitaxel and dual resistant model.* MTT assay was performed to calculate the inhibitory concentrations of PPP for 90 and 80 percent viability: $IC_{10} = 0.1$ μ M and $IC_{20} = 0.2$ μ M for CIS^{ER} ; $IC_{10} = 0.1$ μ M and $IC_{20} = 0.2$ μ M for CIS^{LR} ; $IC_{10} = 0.1$ μ M and $IC_{20} = 0.2$ μ M for Pac^{ER} and $IC_{10} = 0.2$ μ M,

$IC_{20} = 0.4 \mu M$ for Pac^{LR} ; $IC_{10} = 0.1 \mu M$ and $IC_{20} = 0.2 \mu M$ for $Cis-Pac^{ER}$ and $IC_{10} = 0.1 \mu M$ and $IC_{20} = 0.2 \mu M$ for $Cis-Pac^{LR}$ cells. **(B) Determination of IC_{10} , IC_{20} and IC_{40} for all the resistant models (cisplatin, paclitaxel and dual treatment):** MTT assay was performed to calculate the inhibitory drug concentrations for 90, 80 and 60 percent viability: $IC_{10} = 250 \text{ ng/ml}$, $IC_{20} = 500 \text{ ng/ml}$ and $IC_{40} = 1 \mu\text{g/ml}$ for Cis^{ER} ; $IC_{10} = 1 \mu\text{g/ml}$, $IC_{20} = 2 \mu\text{g/ml}$ and $IC_{40} = 3 \mu\text{g/ml}$ for Cis^{LR} ; $IC_{10} = 10 \text{ ng/ml}$, $IC_{20} = 20 \text{ ng/ml}$ and $IC_{40} = 40 \text{ ng/ml}$ for Pac^{ER} and $IC_{10} = 25 \text{ ng/ml}$, $IC_{20} = 50 \text{ ng/ml}$ and $IC_{40} = 100 \text{ ng/ml}$ for Pac^{LR} ; $IC_{10} = 0.875 \text{ ng/ml} + 5 \text{ ng/ml}$, $IC_{20} = 1.16 \text{ ng/ml} + 6.66 \text{ ng/ml}$ and $IC_{40} = 1.75 \text{ ng/ml} + 10 \text{ ng/ml}$ for $Cis-Pac^{ER}$ and $IC_{10} = 2.33 \text{ ng/ml} + 13.33 \text{ ng/ml}$, $IC_{20} = 7 \text{ ng/ml} + 40 \text{ ng/ml}$ and $IC_{40} = 17.5 \text{ ng/ml} + 100 \text{ ng/ml}$

Combination treatment of cytotoxic drugs with IGF-1R inhibitor:

In the combinatorial treatment study, IC_{10} and IC_{20} doses of PPP were combined with IC_{10} , IC_{20} and IC_{40} doses of cisplatin, paclitaxel and dual model for early and late resistant cells. In all three resistant models, combinatorial treatments with PPP showed potentiating effects which were more pronounced at lower doses and in early resistant stages (Figure 4.7 A-C). In Pac^{ER} cells, a combination of IC_{10} paclitaxel and IC_{10} PPP demonstrated marginal effect (11.72% cell kill) that increased to 25.6% reduction in viability ($p < 0.01$) with IC_{20} dose of PPP. This effect was more pronounced in combination of IC_{20} paclitaxel and IC_{10} & IC_{20} of PPP exhibiting a 20.15% and 34.92% reduction in cell viability. With higher concentration of paclitaxel (IC_{40}) we did not observe further reduction in cell viability rather the survival plot became more flattened. In contrast, the Pac^{LR} cells showed trivial response (2-8%) to

treatments with all concentrations of paclitaxel (IC₁₀, IC₂₀ & IC₄₀) combined with PPP (IC₁₀ and IC₂₀). Thus paclitaxel and PPP induced significantly higher cell death in Pac^{ER} cells than in Pac^{LR} cells (p>0.0005). In cisplatin resistant model, the Cis^{ER} cells did not demonstrate any significantly higher lethal effect than Cis^{LR} cells by combinatorial treatments of cisplatin and PPP. While the IC₁₀ cisplatin with IC₁₀ and IC₂₀ of PPP in Cis^{ER} cells showed 43% and 54% cell death respectively, similar treatments in Cis^{LR} cells showed 42% and 45% cell death which did not meet significance between the two groups. A similar trend was also observed with at IC₂₀ dose of cisplatin when combined with IC₁₀ and IC₂₀ doses of PPP in both Cis^{ER} and Cis^{LR} cells. The combinatorial model interestingly showed similar response like the cisplatin model. In Cis-Pac^{ER} cells, IC₁₀ dose of dual drugs with IC₁₀ and IC₂₀ doses of PPP induced 46% and 52% cell death and IC₂₀ dose of dual drugs with same doses of PPP induced 56% and 69% cell kill. The Cis-Pac^{LR} cells exhibited 22-37% cell death for IC₁₀ and IC₂₀ doses of dual drugs in combination with IC₁₀ and IC₂₀ doses of PPP. The IC₄₀ dose of dual drug however showed severe cytotoxicity (76-83%) in the early but mild response (2-10%) in late resistant cells after combinatorial treatments.

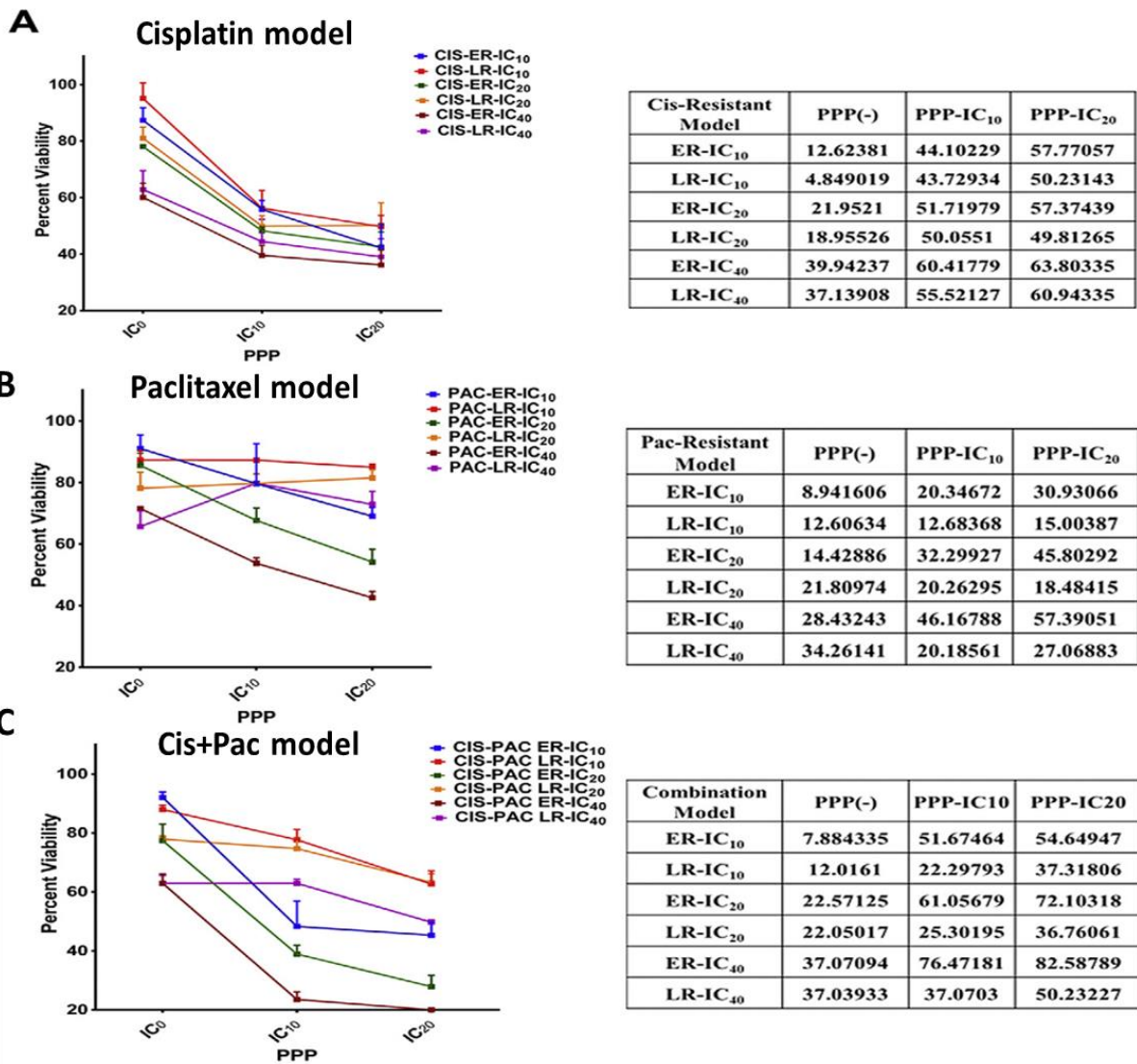


Figure 4.7. Effect of combinatorial treatments of Cisplatin and Paclitaxel with PPP. (A) Combinatorial treatment in Cisplatin resistant cells: Graphical representation of MTT assay of the combinatorial treatments of Cisplatin demonstrated potentiated cell killing effects which was more pronounced in Cis^{ER} than Cis^{LR} cells. Maximal effect was found at IC₂₀ of Cisplatin and IC₁₀ and IC₂₀ of PPP in Cis^{ER} cells when compared with Cis^{LR} cells. Table represented the percent cell killing by different combinations of Cisplatin and PPP in early and late resistant stages. (B). Combinatorial treatment in Paclitaxel resistant cells: Graphical representation of MTT assay of the combinatorial treatments of Paclitaxel demonstrated potentiated cell killing effect in Pac^{ER} cells. The Pac^{LR} cells showed negligible toxicity at all

these combinatorial treatments. Table represented the percent cell killing by different combinations of Paclitaxel and PPP in early and late resistant stages. (C). Combinatorial treatment in Cis-Pac resistant cells: Graphical representation of MTT assay of the combinatorial treatments of Cisplatin + Paclitaxel demonstrated potentiated cell killing effect in Cis-Pac^{ER} cells. The Cis-Pac^{LR} cells showed lesser toxicity at all these combinatorial treatments. Tabular representation shows the percent cell killing of Cis-Pac^{ER} and Cis-Pac^{LR} cells under various combinatorial treatments

Effect of combinatorial treatments of PPP and cisplatin/paclitaxel on clonogenic potential:

Long term survival of the resistant cells was monitored with single and combinatorial regimens through clonogenic assay. Both cisplatin/paclitaxel (IC₂₀) and PPP (IC₂₀) in individual treatments resulted in ~75% surviving fraction (Figure 4.8A-B), however, PPP treatment resulted in reduced size of the colonies. The most significant effect was seen after combinatorial treatments with IC₂₀ doses of both cytotoxic drugs and PPP. The surviving fraction for Cis^{ER}, Pac^{ER}, Cis-Pac^{ER} cells with hyperactive IGF-1R signalling dropped to 20% after combinatorial treatments. Interestingly, Cis^{LR}, Pac^{LR}, Cis-Pac^{LR} cells did not exhibit any reduction in surviving fraction (0.7) even after combination treatment but colony size was significantly reduced (Figure 4.8B).

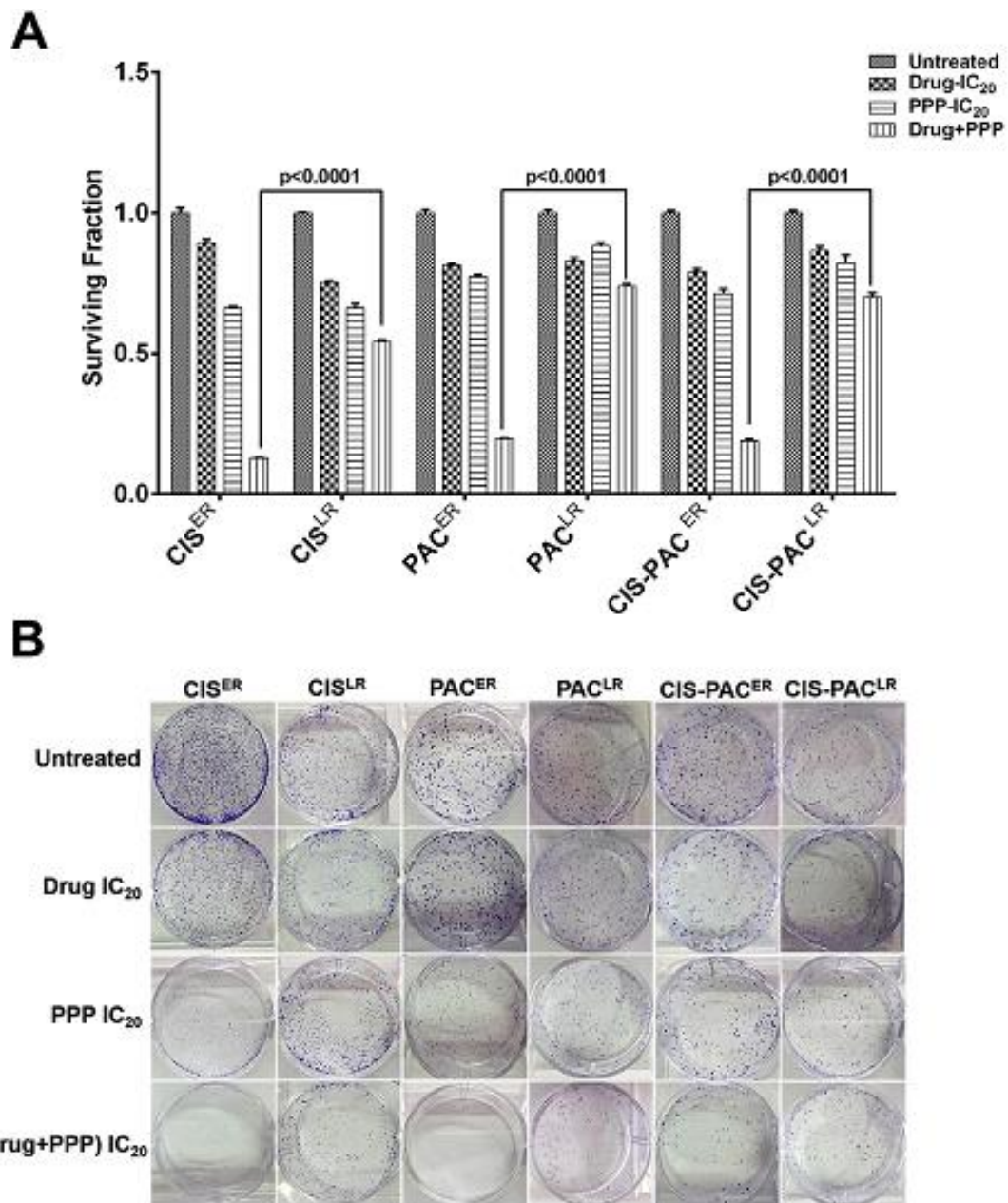


Figure 4.8. *Effect of combination treatment on clonogenic potential of resistant cells. A graphical representation showing surviving fraction of Cis^{ER}/Cis^{LR}, Pac^{ER}/Pac^{LR} and Cis-Pac^{ER}/Cis-Pac^{LR} cells treated with IC₂₀ of Cisplatin and Paclitaxel either alone or in combination with IC₂₀ PPP for 7 days. B. Representative images of colonies formed after individual and combination treatment.*

Role of IGF-1R signalling in maintenance of ovarian CSC phenotype:

In chapter 2 we have shown that with the acquirement of resistance against cisplatin, paclitaxel and dual treatment there was gradual enrichment in the CSC phenotype (SP fraction) in A2780 early and late resistant cells. We also observed that the transcript levels of core transcription factors (*Oct4*, *Sox2* and *nanog*) which are responsible for the maintenance of stemness phenotype increases from A2780 sensitive cells to early and late resistant stages of cisplatin, paclitaxel and dual resistant models. To investigate the role of IGF-1R in the maintenance of cancer stem cell phenotype in chemoresistant cells we monitored the levels of stemness genes (*Oct4*, *Sox2* and *nanog*) as a function of CSC phenotype after inhibition of IGF-1R with small molecule inhibitor (PPP). We investigated the expression levels of these stemness genes in paclitaxel early and late resistant cells after PPP treatment. In Pac^{ER} cells, 1.5uM PPP treatment resulted in 16.6, 18.1 and 17.2 fold decrease in the expression of *Oct4*, *Sox2* and *nanog* respectively. Pac^{LR} cells also showed significant decrease in the expression levels of *Oct4*, *Sox2* and *nanog* (2.9, 4.3 and 3.5 fold respectively) however the fold decrease was more significant in case of early resistant cells (Figure 4.9A-B). Spheroid formation assay was performed with IGF-1R inhibitor (PPP) at 1.5 uM concentration. Number of spheroids formed in the ER & LR cells were significantly lower after PPP treatment compared to their respective parental cells (Figure 4.9 C-D).

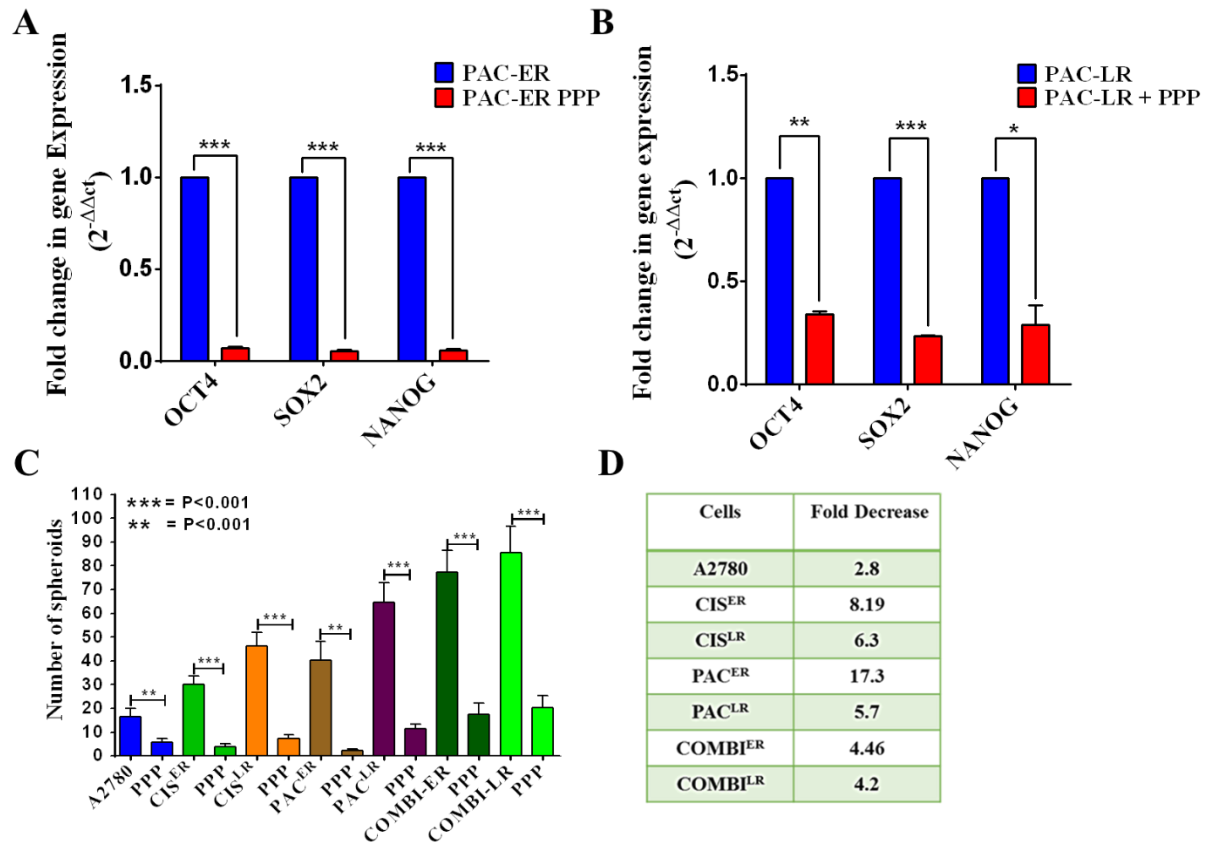


Figure 4.9. Effect of IGF-1R inhibitor (PPP) on CSC phenotype. (A-B). Quantitative real time PCR for Oct4, Sox2 and nanog was performed after PPP treatment (1.5μM) for 48 hrs, where Pac^{ER} cells showed highly significant decrease in the levels of Oct4, Sox2 and nanog expression (16.6, 18.1 and 17.2 fold respectively) however Pac^{LR} cells showed only 2.9, 4.3 and 3.5 fold decrease in the expression of Oct4, Sox2 and nanog respectively. (C-D) To monitor the effect of PPP on self-renewal property of sensitive and resistant cells, spheroid formation assay was performed with 2000 cells/well. Bar graph showing significant decrease in the number of spheroids in A2780 sensitive, cisplatin, paclitaxel and combination resistant cells after PPP treatment. A2780= 2.8 fold; Cis^{ER}= 8.19 fold, Pac^{ER}=17.3 fold, Combi^{ER}= 4.46 fold however Cis^{LR}= 6.3 fold, Pac^{LR}= 5.7 fold and Combi^{LR}= 4.2 fold

Role of IGF-1R in epithelial and mesenchymal transition (EMT):

Since EMT of the resistant cells enable them for distant metastasis, we wanted to investigate if IGF-1R has any role in the process of epithelial and mesenchymal transition. First we monitored the basal level of E-Cadherin (Epithelial marker) in A2780, OAW42 and MCF7 (Positive control) through immunofluorescence. It was observed that in comparison to MCF-7 which showed membrane localized E-Cadherin, A2780 showed no membrane staining for E-Cadherin however OAW42 did show membrane localized E-cadherin (Figure 4.10A). Next we monitored the expression of vimentin (a mesenchymal marker) in the A2780 resistant model. Interestingly it was observed that expression of vimentin increased from sensitive to early resistant stages and then becomes constant till late resistant stages (Figure 4.10B). To test the hypothesis if IGF-1R plays any role in EMT phenomenon, we treated Cis^{ER} cells with increasing concentration of PPP (0.5uM, 1uM, 1.5uM and 2uM) for 48 hours. A dose dependent decrease in the levels of pAKT with no change in the tAKT was observed as before. Interestingly the levels of vimentin also showed a dose dependent decrease with no change in the b-actin levels (Figure 4.10 C). This suggests that IGF-1R might play a crucial role in the process of epithelial and mesenchymal transition.

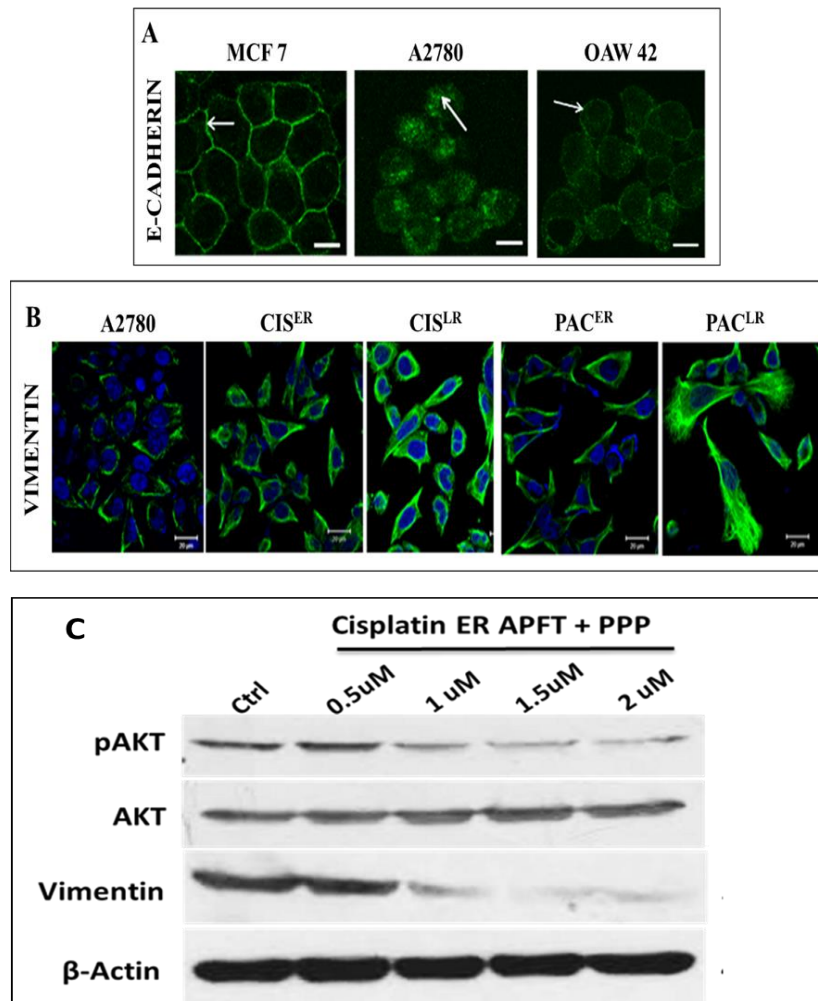


Figure 4.10. Expression analysis of E-Cadherin, Vimentin and pAKT (A) Confocal microscopy showing the localization of E-cadherin in MCF-7, A2780 and OAW42 cells. (B) Confocal imaging of expression and localization of vimentin in A2780 sensitive, Cis^{ER}, Cis^{LR}, Pac^{ER} and Pac^{LR} cells. (C) Western blot analysis showing the levels of pAKT, AKT, Vimentin and β-actin at different doses of PPP (0.5uM, 1uM, 1.5uM and 2uM) for 48 hours.

Since E-cadherin levels were very low in A2780 cells we sought to monitor the known transcriptional repressors for E-cadherin i.e. *snail*, *slug*, *twist* and *zeb1* in the resistant models. These transcriptional repressors are known to bind E-box region in the E-cadherin promoter and suppress the expression of E-cadherin favouring epithelial to mesenchymal transition. In our resistant models we performed quantitative transcript analysis for *snail*, *slug*, *zeb1* and *twist* through real time PCR (Figure 4.11 A-B).

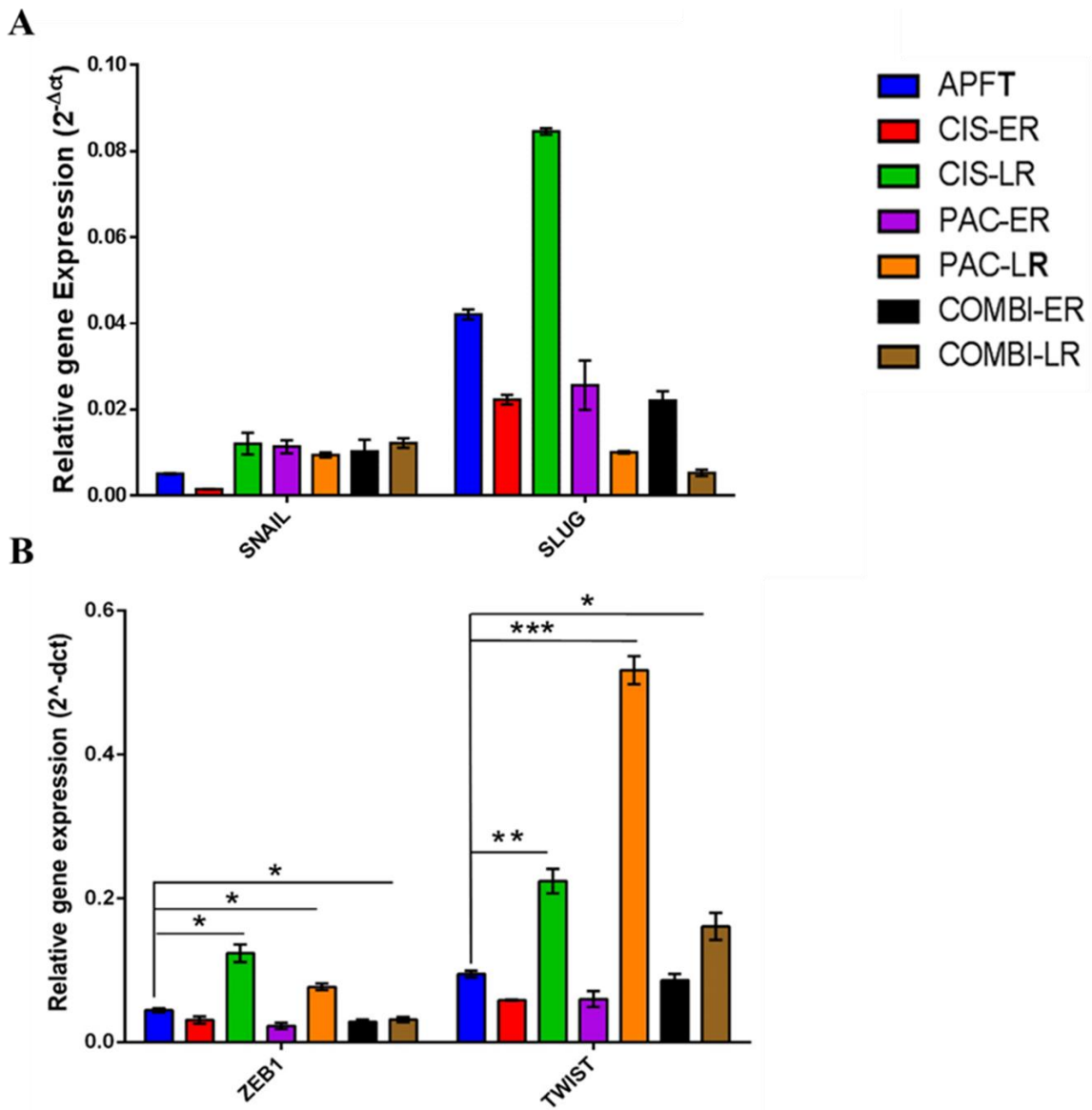


Figure 4.11. Quantitative PCR analysis for EMT genes: (A-B) Quantitative Real Time PCR was performed to monitor the transcript levels of EMT genes (snail slug, Zeb1 and twist) across the resistant models. Quantified data (relative gene expression) showed marginal increase in the expression of snail in all resistant stages (Cis^{LR}, Pac^{ER}/Pac^{LR} and Cis-Pac^{ER}/Cis-Pac^{LR}) except Cis^{ER} and the expression of slug showed increase only in Cis^{LR} cells. However expression of Zeb1 and twist was consistently and significantly higher in all of the late resistant cells except Cis-Pac^{LR}.

Quantitative PCR analysis across the resistant models (cisplatin, paclitaxel and combination) showed that there was marginal increase (>1.5 fold) in the level of snail except Cis^{ER} cells compared to A2780 sensitive cells, however there was no trend observed across the resistant model. Although the basal level of slug was higher in A2780 cells as compared with snail, there was decrease in the expression levels of slug across the resistant models, except Cis^{LR} which showed and increased expression. Expression of Zeb1 showed significant increase only in Cis^{LR} and Pac^{LR} cells however Cis-Pac^{LR} cells showed significant decrease. Among all of the mentioned EMT regulators (snail, slug, zeb1 and twist), only expression of twist followed a similar trend across all the models where its expression showed significant increase compared to the A2780 sensitive cells (2.4, 5.6 and 1.7 fold increase in Cis^{LR}, Pac^{LR} and Cis-Pac^{LR} respectively).

Discussion:

Ovarian cancer is the one of the deadliest gynaecological malignancy, where the recurrence and relapse of the disease are the major concern. Clinically, recurrent and the relapsed disease are chemo resistant in nature hence the basic understanding about mechanism for generation of chemo resistance is of higher priority in ovarian cancer management. There is an imperative need for the identification of chemoresistance generation at early stages. Identification of early molecular events in generating chemo resistance, would probably be beneficial for developing future therapeutic strategies for enhanced efficacy. In order to dissect the acquired chemoresistance into different stages we developed cellular resistant models (cisplatin, paclitaxel and cisplatin + paclitaxel) of ovarian cancer cells. These cells were divided into early and late stages of resistance based on their percent viability at IC₅₀ of sensitive cells. We found gradual increase in the SP phenotype and spheroid forming ability with the acquirement of resistance against cisplatin, paclitaxel and cisplatin+paclitaxel. However there was a prominent difference in tumorigenic ability between early and the late resistant cells as shown in chapter 3, where SP cells from early resistant cells (Pac^{ER}) initiated tumor formation much earlier (Day 15) compared to SP cells from late resistant cells (Cis^{LR}) (Day 50). This intriguing finding led us to investigate the statuses of major signalling pathways involved in cell proliferation and tumor growth. As discussed in the introduction, IGF-1R signalling plays an important role in normal ovarian function and dysregulation of this pathway is often associated with ovarian cancer.

In this chapter we monitored the expression of IGF1-R at transcript and protein level across the resistant models. Interestingly, it was observed that IGF-1R expression were significantly higher at all the early resistant stages. At later stages of chemoresistance the expression of IGF-R was significantly lower showing an oscillatory pattern of IGF-R signalling during the acquirement of chemoresistance. Confocal analysis of IGF-1R staining showed increased

membrane localization in early resistant cells, an essential event for ligand binding and activation of IGF-1R. At late resistant stages hyper-activation of Akt was observed in all of the resistant models. Hyper-activation of Akt is known to phosphorylate and negatively suppress the regulation of EGFR, IGF-1R and Her3 receptor tyrosine kinases. Thus it is possible that higher p-Akt level in late resistant cells might be suppressing the IGF-1R expression. Further investigation is required to investigate this feedback loop between Akt and IGF-1R. Transcript analysis of *Foxo3* corroborated with IGF-1R expression which also indicates a probable feedback loop between Akt, Foxo3 and IGF-1R in the cisplatin and paclitaxel resistant models where higher levels of pAKT might phosphorylate Foxo3 and sequester them in the cytoplasm. This would lead to inability of foxo3 to shuttle into the nucleus and upregulate the IGF-1R transcripts[223]. However such corroboration was not observed in the case of dual resistant model which could be due to more complex regulatory mechanism.

Since IGF-R expression was higher at early resistant stages, we used this stage as a therapeutic window to understand therapeutic potential of IGF-R inhibition in single and in combination with cytotoxic drugs. We used a small molecule inhibitor picropodophyllin (PPP) either alone or in combination with cisplatin and/or paclitaxel. Interestingly, PPP showed a dose dependent decrease in percent viability at early stages but had little effect at late stages. In combinatorial treatments of very low doses of PPP (IC_{20}) along with lowest possible doses of cisplatin and paclitaxel (IC_{20}) early resistant cells showed significant reversal of chemo resistance. Long term survival of the early and late resistant cells was also monitored through clonogenic assay under combinatorial treatment. Early resistant cells (Cis^{ER} , Pac^{ER} , $Cis-Pac^{ER}$) showed even more promising effects in terms of higher efficacy and lower toxicity compared to late resistant cells (Cis^{LR} , Pac^{LR} , $Cis-Pac^{LR}$) which did not shown promising cell killing. Till today, there were only two studies which reported about association of hyper activated IGF-1R signalling with platinum and taxol resistance in ovarian cancer cells. However the kinetics of IGF-1R

expression and its association with CSC and EMT phenotype at different resistant stages during the acquirement of chemoresistance has never been investigated.

In this chapter we for the first time are documenting the differential expression of IGF-1R expression at early and late resistant stages and its essential role in maintaining the CSC and EMT phenotype. To investigate if IGF-R plays any role in maintaining CSC and EMT phenotype we inhibited the IGF-R signalling with PPP. Interestingly we observed that spheroid forming ability and stemness gene expression of early resistant cells were highly compromised in response to PPP treatment suggesting that IGF-R might play a crucial role in the maintenance of CSC phenotype at early resistant stages. To investigate effect of IGF-1R on epithelial mesenchymal transition, we monitored the levels of snail, slug, zeb1 and twist across the resistant models but we did not see any corroboration with IGF-1R expression. However post PPP treatment in Cis^{ER} cells we did see a significant decrease in the levels of vimentin in a dose dependent manner. A2780 cells show more mesenchymal features like low and cytoplasmic e-cadherin and strong vimentin expression indicating that these cells might have passed the transition phase. Thus our data suggests that IGF-1R signalling might play an indirect role in epithelial mesenchymal transition in these A2780 cells that requires further investigation.

To the best of our knowledge, this is the first identification of a therapeutic window for IGF-1R expression in early chemo resistant ovarian cancer cells that could be utilized for potentiating the cytotoxic effects at lowest possible doses as an adjuvant chemotherapy.

Chapter 5

Summary and conclusion

Ovarian cancer is one of the deadliest gynaecological malignancy where early diagnosis and generation of chemoresistance are of major concerns. This disease is initially asymptomatic in nature and thus remains unnoticed while the cancer progresses. Unfortunately at the time of diagnosis, patient already attains stage III and stage IV disease. Another level of complexity in ovarian cancer is due to presence of different histological types namely Epithelial Ovarian Carcinoma (EOC); Ovarian Germ cell Carcinoma and stromal Cell Carcinoma. Among all mentioned types, epithelial ovarian cancer is the predominant one comprising of 80-85% of ovarian cancer cases. Among epithelial subtype high grade serous is the most predominant one which constitutes about more than 80 percent of the disease. Rest other subtypes constitutes mucinous, Clear Cell Carcinoma, endometrioid and transitional ovarian carcinoma. Clinical management of the disease largely depends upon surgery and chemotherapy where Platinum and Taxol based drugs like cisplatin, carboplatin, oxaloplatin, paclitaxel and docetaxel are the main line of chemotherapeutic drugs which are given to the patients either alone or in combination. However the module of treatment varies for upfront surgery and neoadjuvant chemotherapy depending upon the extent of disease. In an initiative made by group of scientist and clinicians at MD Anderson Centre under moon shot programme have developed an algorithm for defining a treatment plan with personalized surgical approach. This algorithm includes diagnostic laparoscopy followed by R_0 scoring performed by two independent surgeons. If there is disagreement in the R_0 scores 3rd surgeon does the scoring. Depending upon the R_0 score; if $R_0 < 8$, patient undergoes for upfront surgery and if $R_0 \geq 8$, patient undergoes three cycles of chemotherapy before surgery.

Apart from regular chemotherapy, few targeted therapies like PARP inhibitors (Olaparib), are available in the clinics against epithelial ovarian carcinoma which has shown a great promise in the patients specifically carrying mutations in either of BRCA1 or BRCA2 genes[44]. This targeted therapy has also been used in combination with platinum and taxol based drugs to

improve the therapeutic efficacy and improved progression free survival with acceptable and manageable tolerability profile [224, 225]. Bevacizumab targeted therapy has also been used in high grade advanced disease to overcome the angiogenesis with increased progression free survival [11]. However these targeted therapies cannot be used for all of the patients, it is restricted to only BRCA1/BRCA2 mutated and advanced ovarian carcinoma patients. Despite of all these efforts, the mortality rate is still very high in India and across the globe. The major reason behind higher mortality rate in ovarian cancer is late diagnosis and the acquirement of chemoresistance against both conventional chemotherapeutic drugs and targeted therapy which eventually leads to tumor recurrence. Even though patients show good response initially towards chemotherapeutic regimen but later they fail to respond to the same drugs. Thus acquirement of resistance towards platinum and taxol based drugs are very common and a major hurdle in combating this disease. Unfortunately, chemoresistance cannot be reversed by altering any single target because acquirement of resistance against these drugs involves multifactorial events occurring simultaneously to give rise to a chemoresistant phenotype. So it becomes more important to diagnose the acquirement of chemoresistance early. In recent time both from clinical and pre-clinical studies, it has been observed that a small population of cells (termed Cancer Stem Cells) residing in the heterogeneous tumor cells are intrinsically resistant towards chemotherapeutic drugs. During chemotherapy these cells remain unaffected and get enriched over a period of time and due to their higher propensity to initiate tumor formation, give rise to recurrence and relapse of the disease. However the time of relapse varies among individuals as in some of the disease has an early relapse and in others relapse occurs after a long period of time. Why does an early and late relapse of the disease happen is still enigmatic and an intensive area of research.

In this study, we aimed to longitudinally monitor acquirement of drug resistance and cancer stem cell properties against single drugs (cisplatin and paclitaxel) and in combination (cisplatin

+ paclitaxel) in ovarian cancer cells. We also attempted to identify differentially regulated signalling cascade/s during development of resistance. In order to monitor the early events for acquirement of resistance in real time, we used A2780 ovarian carcinoma cell line (undifferentiated cell type), stably expressing a bi-fusion reporter construct (Fl2-Tdt) and cellular resistance models were developed against cisplatin, paclitaxel and combinatorial treatment by giving escalated drug dosage[156]. Development of resistance was monitored after every cycle of treatment for its percent survival at IC50 dose of sensitive cells till it attained greater than 90 percent viability. Depending upon the survival fraction the whole resistant models were further categorized into sensitive (parental cells), early and late resistant stages according to resistance index. To investigate the association of CSCs during the course of resistance generation, we critically examined the CSC phenotype across the resistant models with different techniques which involved both functional assays and expression of surface biomarkers. It was observed that CD133, a well-known OCSC marker gradually increased with increasing resistance across all the resistant models, suggesting that there is enrichment of CSCs with increasing resistance irrespective of the drugs given. We also looked at other surface biomarkers e.g. CD44 and CXCR4 in A2780 sensitive and Cis^{LR} cells which showed that compared to A2780 sensitive cells cisplatin late resistant cells has marked increase in the expression of CD44 and CXCR4. We also chose two functional assays (Side population and spheroid formation assay) for isolation and characterization of these ovarian cancer stem cells from different stages of resistance against cisplatin, paclitaxel and combination. We majorly used side population assay for isolation of putative CSCs because the method is based on innate cellular ability to efflux the dye due to overexpression of multi-drug membrane transporters which play a very significant role for resistance development. Hence this isolation strategy was highly appropriate to study both chemoresistant and CSC phenotype. Secondly this isolation method is a functional assay which is more homogenous compared to the cell surface

biomarkers which are highly heterogeneous in nature and varies between cell lines. Spheroid formation assay is based on the self-renewal property of stem cells and cancer stem cells and thus determine a critical functional property of CSCs. In our study both SP fraction and spheroid forming ability significantly increased from sensitive to early and from early to late resistant stages of each chemoresistant models. However this enrichment was much higher in case of dual resistant cells compared to cisplatin and paclitaxel resistant cells. Suggesting the combination treatment (Cisplatin + Paclitaxel), which is a regular treatment modality in the clinics might have an adverse outcome in chemoresistance generation and tumor relapse. To monitor the CSC phenotype, one of the gold standards for the validation is to assay their differentiation property. In our study we critically monitored the differentiation ability of SP cells *in vitro*. Both SP and NSP cells sorted from A2780 sensitive and Cis^{LR} cells passaged longitudinally with interim FACS analysis for SP and NSP phenotype. Interestingly while SP cells were significantly enriched in successive passages, they were still able to differentiate into NSP cells. This result unequivocally proves that SP cells can divide asymmetrically to give rise to both SP and NSP phenotype. However the NSP fractions failed to form any SP population during serial passaging suggesting that NSP cells do not have further differentiation properties. These NSP cells did not form spheroids beyond 2nd passage and whatever spheroids formed were significantly smaller and distorted. The SP cells were able to form spheroids till passage seven. These results indicated that SP fractions were indeed enriched with CSC like cells and were able to self-renew and differentiate at multiple passages. Importantly, across the different resistant models, dual resistant cells showed maximum self-renewal ability compared to cisplatin and paclitaxel resistant cells. However when we compared the resistant properties of SP, NSP and MP cells isolated from A2780 sensitive and late resistant cells, only SP cells showed higher resistance but very little or no difference was observed between NSP and MP population. Thus our data suggests that a cancer non-stem cell population might remain

resistant towards drugs but does not possess self-renewal and differentiation properties. This is an important finding towards the contribution of CSC in disease recurrence.

Since there were increased SP phenotype and self-renewal ability, we also monitored the expression of pluripotent transcription factors (*Oct4*, *Sox2* and *nanog*) in resistant cells. The expression of *Oct4* and *Sox2* significantly increased from sensitive to early resistant stage and then remained constant at later stages. Thus we can imply that stemness gene expression is an early and essential event in CSC population during resistance acquirement. In order to find the association of cancer stem cell phenotype, chemoresistance and pluripotency, we sought to monitor the effect of *Oct4* knockdown in these resistant cells. *Oct4* was chosen as its expression has been well correlated with both CSC and chemoresistance phenotype both in cellular model and in patient samples (Samardzija et al., Journal of Ovarian Research, 2012). Additionally *oct4* also regulates the transcription of *sox2* and *nanog* (Chew et. al., Molecular and cellular Biology, 2005). Lentiviral mediated knock down resulted in significant decrease *oct4* levels at transcriptional and translational level in all the resistant cells (sensitive, ER and LR) compared to the mock control. Silencing of *oct4* led to significant decline in spheroid forming abilities in both sensitive and resistant cells. Interestingly marked decrease in the SP fraction was found in these *Oct4* silenced cells suggesting that this pluripotent transcription factor might regulate the SP and self-renewal properties in the resistant cells. However no significant effect of *Oct4* knockdown on the resistant phenotype was found which indicates that chemoresistance property is not be attributed by *Oct4* expression alone.

Tumorigenic ability and tumor growth kinetics of SP and spheroid cells in comparison to NSP and adherent cells were tested in immune-compromised mice. We implanted 50,000 cells from SP & NSP fractions and 10,000 cells from spheroid & adherent cells from early (*Pac*^{ER}) and late (*Pac*^{LR}, *Cis*^{LR}) resistant cells in NOD/SCID mice. Development of tumors in each group was monitored through *in vivo* bioluminescence imaging at regular time interval. Interestingly

we found that SP and spheroid cells were able to initiate and propagate the tumor formation, however, both NSP and adherent cells could not even initiate tumor formation. Most importantly it was found that SP and spheroid fraction from early resistant stages initiated the tumor formation much earlier (within 15-20 days) whereas SP and spheroid cells from late resistant stages showed much delay in the tumor initiation (within 80-90 days). This data showed existence of functional heterogeneity in the cancer stem cell population isolated at different stages. We believe existence of such functional heterogeneity in CSC ultimately govern the kinetics of tumor relapse and a detailed investigation this mechanism of functional heterogeneity is required in future to explain why some patients show early tumor relapse while others experience disease relapse years after. These intriguing results also pointed that there might be some differential gene regulation at early and late resistant stages, which had resulted in differential tumor growth and functional heterogeneity in these SP and spheroid cells.

IGF-1R signaling is one of the important signaling which is required for the normal development of ovary and its functioning. There are couple of reports which suggest that IGF-1R active signaling can give rise to cisplatin and paclitaxel resistance and help in the process of EMT. However the exact mechanism is still unknown how IGF-1R mediates resistance and EMT phenotype. We intended to monitor the role of IGF-1R during acquirement of chemoresistance and its association with EMT phenotype. Interestingly while monitoring the transcript level of IGF-1R at different stages of resistance we observed an oscillating expression pattern of IGF-1R. Increased levels of IGF-1R were observed at early resistant stages, which decreased at later stages. However levels of activated AKT were significantly higher at late resistant stages in all of the resistant models suggesting the presence of a feedback loop in the IGF1R/PI3KCA/Akt axis during development of chemoresistance which is independent of the nature of drugs. As expected higher membrane localisation of IGF1R were found in early resistant cells compared to the sensitive and late resistant stages.

This up regulated IGF-1R signalling at early stages of resistance provided a therapeutic window to investigate the plausibility of reversing resistant phenotype. We chose a specific tyrosine kinase inhibitor (PPP) which specifically inhibits IGF-1R but not Insulin Receptor. It was observed that with increasing doses of PPP, there was dose dependent decrease in the pAKT levels in early resistant cells but not in sensitive and late resistant cells. It is well recognized that many targeted therapy works better when combined with a cytotoxic drug. To investigate such potential of combination treatment strategy, we used very low concentrations of PPP and chemotherapeutic drugs (IC₁₀ and IC₂₀) to monitor cellular viability through MTT (short-term survival) and long term survival through clonogenic assay. Both the assays revealed that combinatorial treatment of PPP and chemotherapeutic drugs (cisplatin/paclitaxel alone or in combination) at their respective IC₁₀ and IC₂₀ had a drastic effect in cell killing only in the early resistant stages. Treatment of PPP also resulted in significant decrease in the stemness gene expression and spheroid forming ability. All these data suggests that IGF-1R signalling actively regulate chemoresistance and cancer stem cell properties in ovarian cancer cells acquiring resistance. Our study thus opens up a new horizon for testing IGF1R related inhibitors in neoadjuvant therapeutic settings in future.

Epithelial Mesenchymal Transition is yet another phenomenon which can give rise to resistance. Our cellular resistant model is developed in A2780 cells which show predominant mesenchymal state with no E-cadherin on the membrane and high vimentin expression. We monitored the expression of E-box binding proteins snail, slug, zeb1 and twist which supresses the expression of E-cadherin and favour EMT. Quantitative PCR data showed that neither snail nor slug showed any positive corroboration with the IGF-1R status. However expression of zeb1 and twist were significantly higher in late resistant stages. To check if IGF-1R inhibition can affect the mesenchymal phenotype we treated early resistant cells with PPP with increasing doses and performed western blotting for vimentin and found that IGF-1R inhibition lowered

down the level of vimentin in a dose dependent manner. Thus inhibition of IGF1R signalling might partially downregulate mesenchymal phenotype and thereby stalling metastatic potential of cancer cells. Further studies are ongoing with stable knockdown of IGF-1R which would provide more insight into the role of IGF-1R in maintaining the CSC and EMT phenotype

All together our study shows that acquirement of chemoresistance in ovarian cancer cells is highly dynamic in nature, require an active IGF1R signalling and associated with enhanced CSC phenotype. We also demonstrate that IGF-1R signalling is critical in early phases of resistance, however, cells at late resistance are independent of IGF-1R signaling. This provides a therapeutic window where IGF-1R inhibitors could possibly be used as combination therapy for ovarian cancer treatment.

Clinical relevance of our current findings:

- Enrichment of chemoresistant cells with higher CSC phenotype (chemoresistance, self-renewal and differentiation) during different cycles of chemotherapy unequivocally suggest contribution of CSC towards disease recurrence and relapse.
- Existence of heterogeneous CSC population (with differential tumorigenicity) might be the cause for early and late relapse which are assisted with increased IGF-1R signalling.
- Use of IGF-1R inhibitor during early resistance as a neoadjuvant chemotherapy provides a better therapeutic window for increased efficacy and lower toxicity.
- Use of umbrella trials for targeted therapy using IGF-1R and AKT inhibitor in combination with chemotherapeutic drugs.

Future Directions:

- To investigate and identify differential regulators of IGF-1R protein at early and late resistant stages.
- To monitor the role of IGF-1R in the maintenance of cancer stem cell phenotype by stable knockdown of IGF-1R followed by monitoring its tumorigenic ability.

References

1. Heintz, A., et al., *Carcinoma of the ovary*. International Journal of Gynecology & Obstetrics, 2006. **95**: p. S161-S192.
2. Griffiths, C.T., R.H. Grogan, and T.C. Hall, *Advanced ovarian cancer: Primary treatment with surgery, radiotherapy, and chemotherapy*. Cancer, 1972. **29**(1): p. 1-7.
3. Hicks, M.L. and G. Parham, *Can you screen for ovarian cancer?* Journal of the National Medical Association, 1995. **87**(2): p. 109.
4. Le Page, C., et al., *Signature of a silent killer: expression profiling in epithelial ovarian cancer*. Expert Rev Mol Diagn, 2004. **4**(2): p. 157-67.
5. Eckstein, N., *Platinum resistance in breast and ovarian cancer cell lines*. J Exp Clin Cancer Res, 2011. **30**: p. 91.
6. Mimeault, M., R. Hauke, and S.K. Batra, *Recent advances on the molecular mechanisms involved in the drug resistance of cancer cells and novel targeting therapies*. Clin Pharmacol Ther, 2008. **83**(5): p. 673-91.
7. Arora, A. and E.M. Scholar, *Role of tyrosine kinase inhibitors in cancer therapy*. Journal of Pharmacology and Experimental Therapeutics, 2005. **315**(3): p. 971-979.
8. Paul, M.K. and A.K. Mukhopadhyay, *Tyrosine kinase—Role and significance in Cancer*. International journal of medical sciences, 2004. **1**(2): p. 101.
9. Sharma, P.S., R. Sharma, and T. Tyagi, *Receptor tyrosine kinase inhibitors as potent weapons in war against cancers*. Current pharmaceutical design, 2009. **15**(7): p. 758-776.
10. Burger, R.A., et al., *Incorporation of bevacizumab in the primary treatment of ovarian cancer*. New England Journal of Medicine, 2011. **365**(26): p. 2473-2483.
11. Perren, T.J., et al., *A phase 3 trial of bevacizumab in ovarian cancer*. New England Journal of Medicine, 2011. **365**(26): p. 2484-2496.

12. Ferrara, N., et al., *Discovery and development of bevacizumab, an anti-VEGF antibody for treating cancer*. Nature reviews Drug discovery, 2004. **3**(5): p. 391-400.
13. Kamat, A.A., et al., *Metronomic chemotherapy enhances the efficacy of anti-vascular therapy in ovarian cancer*. Cancer Research, 2007. **67**(1): p. 281-288.
14. Perks, C., A. Peters, and D. Wathes, *Follicular and luteal expression of insulin-like growth factors I and II and the type I IGF receptor in the bovine ovary*. Journal of reproduction and fertility, 1999. **116**(1): p. 157-165.
15. Coppola, D., et al., *The insulin-like growth factor I receptor induces transformation and tumorigenicity of ovarian mesothelial cells and down-regulates their Fas-receptor expression*. Cancer research, 1999. **59**(13): p. 3264-3270.
16. Eckstein, N., et al., *Hyperactivation of the insulin-like growth factor receptor I signaling pathway is an essential event for cisplatin resistance of ovarian cancer cells*. Cancer Res, 2009. **69**(7): p. 2996-3003.
17. Huang, G.S., et al., *Insulin-like growth factor 2 expression modulates Taxol resistance and is a candidate biomarker for reduced disease-free survival in ovarian cancer*. Clin Cancer Res, 2010. **16**(11): p. 2999-3010.
18. Zahreddine, H. and K. Borden, *Mechanisms and Insights into Drug Resistance in Cancer*. Frontiers in Pharmacology, 2013. **4**.
19. Hazlehurst, L., R. Argilagos, and W. Dalton, *β 1 integrin mediated adhesion increases Bim protein degradation and contributes to drug resistance in leukaemia cells*. British journal of haematology, 2007. **136**(2): p. 269-275.
20. Wilson, T., D. Longley, and P. Johnston, *Chemoresistance in solid tumours*. Annals of Oncology, 2006. **17**(10): p. x315.
21. Moreno-Smith, M., et al., *ATP11B mediates platinum resistance in ovarian cancer*. J Clin Invest, 2013. **123**(5): p. 2119-30.

22. Wang, S., D. Yang, and M.E. Lippman. *Targeting Bcl-2 and Bcl-X L with nonpeptidic small-molecule antagonists*. in *Seminars in oncology*. 2003. Elsevier.
23. Ullah, M.F., *Cancer multidrug resistance (MDR): a major impediment to effective chemotherapy*. Asian Pac J Cancer Prev, 2008. **9**(1): p. 1-6.
24. Wattel, E., et al., *p53 mutations are associated with resistance to chemotherapy and short survival in hematologic malignancies*. Blood, 1994. **84**(9): p. 3148-3157.
25. Crea, F., R. Danesi, and W.L. Farrar, *Cancer stem cell epigenetics and chemoresistance*. Epigenomics, 2009. **1**(1): p. 63-79.
26. Chuthapisith, S., et al., *Breast cancer chemoresistance: emerging importance of cancer stem cells*. Surg Oncol, 2010. **19**(1): p. 27-32.
27. Suebwong Chuthapisith, M., *Cancer Stem Cells and Chemoresistance*.
28. Ma, L., et al., *Cancer stem-like cells can be isolated with drug selection in human ovarian cancer cell line SKOV3*. Acta Biochim Biophys Sin (Shanghai), 2010. **42**(9): p. 593-602.
29. Alvero, A.B., et al., *Molecular phenotyping of human ovarian cancer stem cells unravels the mechanisms for repair and chemoresistance*. Cell Cycle, 2014. **8**(1): p. 158-166.
30. Steffensen, K.D., et al., *Prevalence of epithelial ovarian cancer stem cells correlates with recurrence in early-stage ovarian cancer*. J Oncol, 2011. **2011**: p. 620523.
31. Torre, L.A., et al., *Global cancer statistics, 2012*. CA Cancer J Clin, 2015. **65**(2): p. 87-108.
32. Dikshit, R., et al., *Cancer mortality in India: a nationally representative survey*. The Lancet, 2012. **379**(9828): p. 1807-1816.
33. Santesson, L. and H. Kottmeier, *General classification of ovarian tumours*, in *Ovarian cancer*. 1968, Springer. p. 1-8.

34. Kaku, T., et al., *Histological classification of ovarian cancer*. Medical Electron Microscopy, 2003. **36**(1): p. 9-17.
35. Bankhead, C.R., et al., *Identifying symptoms of ovarian cancer: a qualitative and quantitative study*. BJOG, 2008. **115**(8): p. 1008-14.
36. Bankhead, C.R., S.T. Kehoe, and J. Austoker, *Symptoms associated with diagnosis of ovarian cancer: a systematic review*. BJOG, 2005. **112**(7): p. 857-65.
37. Jacobs, I., et al., *A risk of malignancy index incorporating CA 125, ultrasound and menopausal status for the accurate preoperative diagnosis of ovarian cancer*. BJOG: An International Journal of Obstetrics & Gynaecology, 1990. **97**(10): p. 922-929.
38. Moore, R.G., et al., *A novel multiple marker bioassay utilizing HE4 and CA125 for the prediction of ovarian cancer in patients with a pelvic mass*. Gynecologic oncology, 2009. **112**(1): p. 40-46.
39. Mohaghegh, P. and A.G. Rockall, *Imaging strategy for early ovarian cancer: characterization of adnexal masses with conventional and advanced imaging techniques*. Radiographics, 2012. **32**(6): p. 1751-1773.
40. Shepherd, J.H., *Revised FIGO staging for gynaecological cancer*. BJOG: An International Journal of Obstetrics & Gynaecology, 1989. **96**(8): p. 889-892.
41. Kurman, R.J. and I.-M. Shih, *Molecular pathogenesis and extraovarian origin of epithelial ovarian cancer—Shifting the paradigm*. Human Pathology, 2011. **42**(7): p. 918-931.
42. Kurman, R.J. and I.-M. Shih, *The Origin and pathogenesis of epithelial ovarian cancer—a proposed unifying theory*. The American journal of surgical pathology, 2010. **34**(3): p. 433.
43. Mendelsohn, J., et al., *The Molecular Basis of Cancer: Expert Consult-Online*. 2008: Elsevier Health Sciences.

44. Audeh, M.W., et al., *Oral poly (ADP-ribose) polymerase inhibitor olaparib in patients with BRCA1 or BRCA2 mutations and recurrent ovarian cancer: a proof-of-concept trial*. *The Lancet*, 2010. **376**(9737): p. 245-251.
45. Takahara, P.M., C.A. Frederick, and S.J. Lippard, *Crystal structure of the anticancer drug cisplatin bound to duplex DNA*. *Journal of the American Chemical Society*, 1996. **118**(49): p. 12309-12321.
46. Torigoe, T., et al., *Cisplatin resistance and transcription factors*. *Current Medicinal Chemistry-Anti-Cancer Agents*, 2005. **5**(1): p. 15-27.
47. Ardizzoni, A., et al., *Cisplatin-versus carboplatin-based chemotherapy in first-line treatment of advanced non-small-cell lung cancer: an individual patient data meta-analysis*. *Journal of the National Cancer Institute*, 2007. **99**(11): p. 847-857.
48. Dieras, V., et al., *[Oxaliplatin and ovarian cancer]*. *Bulletin du cancer*, 2006. **93**: p. S35-9.
49. Parmar, M., et al., *Paclitaxel plus platinum-based chemotherapy versus conventional platinum-based chemotherapy in women with relapsed ovarian cancer: the ICON4/AGO-OVAR-2.2 trial*. *Lancet*, 2003. **361**(9375): p. 2099-2106.
50. ten Bokkel Huinink, W., et al., *Topotecan versus paclitaxel for the treatment of recurrent epithelial ovarian cancer*. *Journal of Clinical Oncology*, 1997. **15**(6): p. 2183-2193.
51. Wani, M.C., et al., *Plant antitumor agents. VI. Isolation and structure of taxol, a novel antileukemic and antitumor agent from Taxus brevifolia*. *Journal of the American Chemical Society*, 1971. **93**(9): p. 2325-2327.
52. Trimble, E., et al., *Paclitaxel for platinum-refractory ovarian cancer: results from the first 1,000 patients registered to National Cancer Institute Treatment Referral Center 9103*. *Journal of clinical oncology*, 1993. **11**(12): p. 2405-2410.

53. Escobar, P.F. and P.G. Rose, *Docetaxel in ovarian cancer*. 2005.
54. Cottu, P.H., L. Mignot, and V. Diéras, *Docetaxel and ovarian cancer*. 2007.
55. Piver, M.S., et al., *The impact of aggressive debulking surgery and cisplatin-based chemotherapy on progression-free survival in stage III and IV ovarian carcinoma*. *Journal of Clinical Oncology*, 1988. **6**(6): p. 983-989.
56. Bristow, R.E., et al., *Survival effect of maximal cytoreductive surgery for advanced ovarian carcinoma during the platinum era: a meta-analysis*. *Journal of Clinical Oncology*, 2002. **20**(5): p. 1248-1259.
57. Neoplasm, C.I.O., *International Collaborative Ovarian Neoplasm trial 1 and Adjuvant ChemoTherapy In Ovarian Neoplasm trial: two parallel randomized phase III trials of adjuvant chemotherapy in patients with early-stage ovarian carcinoma*. *Journal of the National Cancer Institute*, 2003. **95**(2).
58. Mazzeo, F., et al., *Neoadjuvant chemotherapy followed by surgery and adjuvant chemotherapy in patients with primarily unresectable, advanced-stage ovarian cancer*. *Gynecologic oncology*, 2003. **90**(1): p. 163-169.
59. Robinson, W.R., G. Barnett, and A.S. Rogers, *Neoadjuvant chemotherapy prior to intraperitoneal chemotherapy in women with advanced ovarian cancer*. *Community Oncology*, 2008. **5**(7): p. 376-380.
60. Kehoe, S., et al., *Primary chemotherapy versus primary surgery for newly diagnosed advanced ovarian cancer (CHORUS): an open-label, randomised, controlled, non-inferiority trial*. *The Lancet*. **386**(9990): p. 249-257.
61. Nick, A.M., et al., *A framework for a personalized surgical approach to ovarian cancer*. *Nature Reviews Clinical Oncology*, 2015.

62. Godwin, A.K., et al., *High resistance to cisplatin in human ovarian cancer cell lines is associated with marked increase of glutathione synthesis*. Proceedings of the National Academy of Sciences, 1992. **89**(7): p. 3070-3074.
63. Boyerinas, B., et al., *Let-7 modulates acquired resistance of ovarian cancer to Taxanes via IMP-1-mediated stabilization of multidrug resistance 1*. International Journal of Cancer, 2012. **130**(8): p. 1787-1797.
64. Parker, R., et al., *Acquired cisplatin resistance in human ovarian cancer cells is associated with enhanced repair of cisplatin-DNA lesions and reduced drug accumulation*. Journal of Clinical Investigation, 1991. **87**(3): p. 772.
65. Isoyama, S., et al., *Establishment of phosphatidylinositol 3-kinase inhibitor-resistant cancer cell lines and therapeutic strategies for overcoming the resistance*. Cancer Sci, 2012. **103**(11): p. 1955-60.
66. Dean, M., T. Fojo, and S. Bates, *Tumour stem cells and drug resistance*. Nat Rev Cancer, 2005. **5**(4): p. 275-84.
67. Patrawala, L., et al., *Side population is enriched in tumorigenic, stem-like cancer cells, whereas ABCG2+ and ABCG2- cancer cells are similarly tumorigenic*. Cancer Res, 2005. **65**(14): p. 6207-19.
68. Beier, D., J.B. Schulz, and C.P. Beier, *Chemoresistance of glioblastoma cancer stem cells--much more complex than expected*. Mol Cancer, 2011. **10**: p. 128.
69. Dalerba, P., R.W. Cho, and M.F. Clarke, *Cancer stem cells: models and concepts*. Annu. Rev. Med., 2007. **58**: p. 267-284.
70. Dallas, N.A., et al., *Chemoresistant colorectal cancer cells, the cancer stem cell phenotype, and increased sensitivity to insulin-like growth factor-I receptor inhibition*. Cancer Res, 2009. **69**(5): p. 1951-7.

71. Bonnet, D. and J.E. Dick, *Human acute myeloid leukemia is organized as a hierarchy that originates from a primitive hematopoietic cell*. Nat Med, 1997. **3**(7): p. 730-7.
72. Lapidot, T., et al., *A cell initiating human acute myeloid leukaemia after transplantation into SCID mice*. Nature, 1994. **367**(6464): p. 645-8.
73. Collins, A.T., et al., *Prospective identification of tumorigenic prostate cancer stem cells*. Cancer research, 2005. **65**(23): p. 10946-10951.
74. Kim, C.F.B., et al., *Identification of bronchioalveolar stem cells in normal lung and lung cancer*. Cell, 2005. **121**(6): p. 823-835.
75. Dalerba, P., et al., *Phenotypic characterization of human colorectal cancer stem cells*. Proceedings of the National Academy of Sciences, 2007. **104**(24): p. 10158-10163.
76. Bapat, S.A., *Evolution of cancer stem cells*. Semin Cancer Biol, 2007. **17**(3): p. 204-13.
77. Bapat, S.A., et al., *Stem and progenitor-like cells contribute to the aggressive behavior of human epithelial ovarian cancer*. Cancer Res, 2005. **65**(8): p. 3025-9.
78. Zhang, S., et al., *Identification and characterization of ovarian cancer-initiating cells from primary human tumors*. Cancer Res, 2008. **68**(11): p. 4311-20.
79. Szotek, P.P., et al., *Normal ovarian surface epithelial label-retaining cells exhibit stem/progenitor cell characteristics*. Proc Natl Acad Sci U S A, 2008. **105**(34): p. 12469-73.
80. Szotek, P.P., et al., *Ovarian cancer side population defines cells with stem cell-like characteristics and Mullerian Inhibiting Substance responsiveness*. Proc Natl Acad Sci U S A, 2006. **103**(30): p. 11154-9.
81. Alvero, A.B., et al., *Stem-like ovarian cancer cells can serve as tumor vascular progenitors*. Stem Cells, 2009. **27**(10): p. 2405-13.

82. Curley, M.D., et al., *CD133 expression defines a tumor initiating cell population in primary human ovarian cancer*. Stem Cells, 2009. **27**(12): p. 2875-2883.
83. Silva, I.A., et al., *Aldehyde dehydrogenase in combination with CD133 defines angiogenic ovarian cancer stem cells that portend poor patient survival*. Cancer Res, 2011. **71**(11): p. 3991-4001.
84. Zhang, S., et al., *Ovarian cancer stem cells express ROR1, which can be targeted for anti-cancer-stem-cell therapy*. Proc Natl Acad Sci U S A, 2014. **111**(48): p. 17266-71.
85. Jiabo, D., et al., *Expression compilation of several putative cancer stem cell markers by primary ovarian carcinoma*. Journal of Cancer Therapy, 2010. **1**(04): p. 165.
86. Alvero, A.B., et al., *Molecular phenotyping of human ovarian cancer stem cells unravels the mechanisms for repair and chemoresistance*. Cell cycle, 2009. **8**(1): p. 158-166.
87. Johansson, C.B., et al., *Identification of a neural stem cell in the adult mammalian central nervous system*. Cell, 1999. **96**(1): p. 25-34.
88. Vermeulen, L., et al., *Single-cell cloning of colon cancer stem cells reveals a multi-lineage differentiation capacity*. Proc Natl Acad Sci U S A, 2008. **105**(36): p. 13427-32.
89. *Human Ovarian Cancer Stem Cells*.
90. Chiou, S.-H., et al., *Positive correlations of Oct-4 and Nanog in oral cancer stem-like cells and high-grade oral squamous cell carcinoma*. Clinical Cancer Research, 2008. **14**(13): p. 4085-4095.
91. Kondo, T., *Stem cell-like cancer cells in cancer cell lines*. Inflammation and Regeneration, 2007. **27**(5): p. 506-511.

92. Goodell, M.A., S. McKinney-Freeman, and F.D. Camargo, *Isolation and characterization of side population cells*, in *Basic Cell Culture Protocols*. 2005, Springer. p. 343-352.
93. Hirschmann-Jax, C., et al., *A distinct "side population" of cells with high drug efflux capacity in human tumor cells*. Proceedings of the National Academy of Sciences of the United States of America, 2004. **101**(39): p. 14228-14233.
94. Kobayashi, Y., et al., *Side population is increased in paclitaxel-resistant ovarian cancer cell lines regardless of resistance to cisplatin*. Gynecol Oncol, 2011. **121**(2): p. 390-4.
95. Hosonuma, S., et al., *Clinical significance of side population in ovarian cancer cells*. Hum Cell, 2011. **24**(1): p. 9-12.
96. Richard, V., et al., *Side population cells as prototype of chemoresistant, tumor-initiating cells*. BioMed research international, 2013. **2013**.
97. Bleau, A.-M., et al., *PTEN/PI3K/Akt pathway regulates the side population phenotype and ABCG2 activity in glioma tumor stem-like cells*. Cell stem cell, 2009. **4**(3): p. 226-235.
98. Zhou, S., et al., *The ABC transporter Bcrp1/ABCG2 is expressed in a wide variety of stem cells and is a molecular determinant of the side-population phenotype*. Nature medicine, 2001. **7**(9): p. 1028-1034.
99. Moreb, J.S., *Aldehyde dehydrogenase as a marker for stem cells*. Current stem cell research & therapy, 2008. **3**(4): p. 237-246.
100. Charafe-Jauffret, E., et al., *Aldehyde dehydrogenase 1-Positive cancer stem cells mediate metastasis and poor clinical outcome in inflammatory breast cancer*. Clinical Cancer Research, 2010. **16**(1): p. 45-55.

101. Chen, Y.-C., et al., *Aldehyde dehydrogenase 1 is a putative marker for cancer stem cells in head and neck squamous cancer*. Biochemical and biophysical research communications, 2009. **385**(3): p. 307-313.
102. Huang, E.H., et al., *Aldehyde dehydrogenase 1 is a marker for normal and malignant human colonic stem cells (SC) and tracks SC overpopulation during colon tumorigenesis*. Cancer Res, 2009. **69**(8): p. 3382-9.
103. Wang, L., et al., *Prospective identification of tumorigenic osteosarcoma cancer stem cells in OS99-1 cells based on high aldehyde dehydrogenase activity*. Int J Cancer, 2011. **128**(2): p. 294-303.
104. Kuroda, T., et al., *ALDH1-high ovarian cancer stem-like cells can be isolated from serous and clear cell adenocarcinoma cells, and ALDH1 high expression is associated with poor prognosis*. PLoS One, 2013. **8**(6): p. e65158.
105. Kato, K., *Endometrial cancer stem cells: a new target for cancer therapy*. Anticancer research, 2012. **32**(6): p. 2283-2293.
106. Yasuda, K., et al., *Ovarian cancer stem cells are enriched in side population and aldehyde dehydrogenase bright overlapping population*. PloS one, 2013. **8**(8): p. e68187.
107. Gao, M.Q., et al., *CD24+ cells from hierarchically organized ovarian cancer are enriched in cancer stem cells*. Oncogene, 2010. **29**(18): p. 2672-80.
108. Massoud, T.F. and S.S. Gambhir, *Molecular imaging in living subjects: seeing fundamental biological processes in a new light*. Genes & development, 2003. **17**(5): p. 545-580.
109. Ray, P., A.M. Wu, and S.S. Gambhir, *Optical bioluminescence and positron emission tomography imaging of a novel fusion reporter gene in tumor xenografts of living mice*. Cancer Research, 2003. **63**(6): p. 1160-1165.

110. Liu, H., et al., *Cancer stem cells from human breast tumors are involved in spontaneous metastases in orthotopic mouse models*. Proc Natl Acad Sci U S A, 2010. **107**(42): p. 18115-20.
111. Baserga, R., *The IGF-I receptor in cancer research*. Exp Cell Res, 1999. **253**(1): p. 1-6.
112. Chapuis, N., et al., *Autocrine IGF-1/IGF-1R signaling is responsible for constitutive PI3K/Akt activation in acute myeloid leukemia: therapeutic value of neutralizing anti-IGF-1R antibody*. Haematologica, 2010. **95**(3): p. 415-23.
113. Chitnis, M.M., et al., *The type I insulin-like growth factor receptor pathway*. Clin Cancer Res, 2008. **14**(20): p. 6364-70.
114. Sarfstein, R. and H. Werner, *Minireview: nuclear insulin and insulin-like growth factor-1 receptors: a novel paradigm in signal transduction*. Endocrinology, 2013. **154**(5): p. 1672-9.
115. Garrett, T.P., et al., *Crystal structure of the first three domains of the type-1 insulin-like growth factor receptor*. Nature, 1998. **394**(6691): p. 395-399.
116. Sachdev, D., et al., *The type I insulin-like growth factor receptor regulates cancer metastasis independently of primary tumor growth by promoting invasion and survival*. Oncogene, 2010. **29**(2): p. 251-262.
117. Werner, H. and D. LeRoith, *The Role of the Insulin-like Growth Factor System in*. Advances in cancer research, 1996. **68**: p. 183.
118. Patel, B.B., et al., *Curcumin enhances the effects of 5-fluorouracil and oxaliplatin in mediating growth inhibition of colon cancer cells by modulating EGFR and IGF-1R*. International Journal of Cancer, 2008. **122**(2): p. 267-273.
119. Yu, Y., et al., *Elimination of colon cancer stem-like cells by the combination of curcumin and FOLFOX*. Translational oncology, 2009. **2**(4): p. 321-328.

120. Conover, C., et al., *Biological characterization of human epithelial ovarian carcinoma cells in primary culture: the insulin-like growth factor system*. Experimental cell research, 1998. **238**(2): p. 439-449.
121. Weroha, S.J. and P. Haluska, *IGF-1 receptor inhibitors in clinical trials--early lessons*. J Mammary Gland Biol Neoplasia, 2008. **13**(4): p. 471-83.
122. Werner, H., et al., *Increased expression of the insulin-like growth factor I receptor gene, IGF1R, in Wilms tumor is correlated with modulation of IGF1R promoter activity by the WT1 Wilms tumor gene product*. Proceedings of the National Academy of Sciences, 1993. **90**(12): p. 5828-5832.
123. Werner, H., *Tumor suppressors govern insulin-like growth factor signaling pathways: implications in metabolism and cancer*. Oncogene, 2012. **31**(22): p. 2703-14.
124. Girnita, L., A. Girnita, and O. Larsson, *Mdm2-dependent ubiquitination and degradation of the insulin-like growth factor I receptor*. Proceedings of the National Academy of Sciences, 2003. **100**(14): p. 8247-8252.
125. Hirano, S., et al., *Clinical implications of insulin-like growth factors through the presence of their binding proteins and receptors expressed in gynecological cancers*. European journal of gynaecological oncology, 2003. **25**(2): p. 187-191.
126. Resnicoff, M., et al., *Growth inhibition of human melanoma cells in nude mice by antisense strategies to the type I insulin-like growth factor receptor*. Cancer Research, 1994. **54**(18): p. 4848-4850.
127. Resnicoff, M., et al., *Rat glioblastoma cells expressing an antisense RNA to the insulin-like growth factor-1 (IGF-1) receptor are nontumorigenic and induce regression of wild-type tumors*. Cancer research, 1994. **54**(8): p. 2218-2222.

128. Sayer, R.A., et al., *High insulin-like growth factor-2 (IGF-2) gene expression is an independent predictor of poor survival for patients with advanced stage serous epithelial ovarian cancer*. *Gynecologic oncology*, 2005. **96**(2): p. 355-361.
129. Zhao, H., et al., *Epithelial–mesenchymal transition predicts sensitivity to the dual IGF-1R/IR inhibitor OSI-906 in hepatocellular carcinoma cell lines*. *Molecular cancer therapeutics*, 2012. **11**(2): p. 503-513.
130. Reya, T., et al., *Stem cells, cancer, and cancer stem cells*. *nature*, 2001. **414**(6859): p. 105-111.
131. Landen, C.N., Jr., et al., *Targeting aldehyde dehydrogenase cancer stem cells in ovarian cancer*. *Mol Cancer Ther*, 2010. **9**(12): p. 3186-99.
132. Tjhay, F., et al., *CD44 variant 6 is correlated with peritoneal dissemination and poor prognosis in patients with advanced epithelial ovarian cancer*. *Cancer Science*, 2015. **106**(10): p. 1421-1428.
133. Shi, M., et al., *Identification of cancer stem cell-like cells from human epithelial ovarian carcinoma cell line*. *Cellular and molecular life sciences*, 2010. **67**(22): p. 3915-3925.
134. Kryczek, I., et al., *Expression of aldehyde dehydrogenase and CD133 defines ovarian cancer stem cells*. *Int J Cancer*, 2012. **130**(1): p. 29-39.
135. Ferrandina, G., et al., *Expression of CD133-1 and CD133-2 in ovarian cancer*. *International Journal of Gynecological Cancer*, 2008. **18**(3): p. 506-514.
136. Luo, L., et al., *Ovarian cancer cells with the CD117 phenotype are highly tumorigenic and are related to chemotherapy outcome*. *Experimental and molecular pathology*, 2011. **91**(2): p. 596-602.

137. Deng, S., et al., *Distinct expression levels and patterns of stem cell marker, aldehyde dehydrogenase isoform 1 (ALDH1), in human epithelial cancers*. PLoS One, 2010. **5**(4): p. e10277.
138. Ma, I. and A.L. Allan, *The role of human aldehyde dehydrogenase in normal and cancer stem cells*. Stem Cell Rev, 2011. **7**(2): p. 292-306.
139. Moserle, L., et al., *The side population of ovarian cancer cells is a primary target of IFN- α antitumor effects*. Cancer Research, 2008. **68**(14): p. 5658-5668.
140. Gao, Q., et al., *Identification of cancer stem-like side population cells in ovarian cancer cell line OVCAR-3*. Ultrastructural pathology, 2009. **33**(4): p. 175-181.
141. Hu, L., C. McArthur, and R. Jaffe, *Ovarian cancer stem-like side-population cells are tumorigenic and chemoresistant*. British journal of cancer, 2010. **102**(8): p. 1276-1283.
142. Dou, J., et al., *Using ABCG2-molecule-expressing side population cells to identify cancer stem-like cells in a human ovarian cell line*. Cell biology international, 2011. **35**(3): p. 227-234.
143. Kolev, V.N., et al., *PI3K/mTOR dual inhibitor VS-5584 preferentially targets cancer stem cells*. Cancer research, 2015. **75**(2): p. 446-455.
144. Gil, M., et al., *CXCL12/CXCR4 blockade by oncolytic virotherapy inhibits ovarian cancer growth by decreasing immunosuppression and targeting cancer-initiating cells*. The Journal of Immunology, 2014. **193**(10): p. 5327-5337.
145. Wang, Y., et al., *Epigenetic targeting of ovarian cancer stem cells*. Cancer research, 2014. **74**(17): p. 4922-4936.
146. McAuliffe, S.M., et al., *Targeting Notch, a key pathway for ovarian cancer stem cells, sensitizes tumors to platinum therapy*. Proceedings of the National Academy of Sciences, 2012. **109**(43): p. E2939-E2948.

147. Yo, Y.-T., et al., *Growth Inhibition of Ovarian Tumor–Initiating Cells by Niclosamide*. *Molecular cancer therapeutics*, 2012. **11**(8): p. 1703-1712.
148. Meng, E., et al., *ALDH1A1 maintains ovarian cancer stem cell-like properties by altered regulation of cell cycle checkpoint and DNA repair network signaling*. 2014.
149. Landen, C.N., et al., *Targeting aldehyde dehydrogenase cancer stem cells in ovarian cancer*. *Molecular cancer therapeutics*, 2010. **9**(12): p. 3186-3199.
150. Shank, J.J., et al., *Metformin targets ovarian cancer stem cells in vitro and in vivo*. *Gynecologic oncology*, 2012. **127**(2): p. 390-397.
151. Samardzija, C., et al., *Attributes of Oct4 in stem cell biology: perspectives on cancer stem cells of the ovary*. *J Ovarian Res*, 2012. **5**(1): p. 37.
152. Wang, X.Q., et al., *Octamer 4 (Oct4) mediates chemotherapeutic drug resistance in liver cancer cells through a potential Oct4-AKT-ATP-binding cassette G2 pathway*. *Hepatology*, 2010. **52**(2): p. 528-39.
153. Wang, Z.X., et al., *Oct4 and Sox2 directly regulate expression of another pluripotency transcription factor, Zfp206, in embryonic stem cells*. *J Biol Chem*, 2007. **282**(17): p. 12822-30.
154. Chew, J.L., et al., *Reciprocal transcriptional regulation of Pou5f1 and Sox2 via the Oct4/Sox2 complex in embryonic stem cells*. *Mol Cell Biol*, 2005. **25**(14): p. 6031-46.
155. Zaehres, H., et al., *High-efficiency RNA interference in human embryonic stem cells*. *Stem Cells*, 2005. **23**(3): p. 299-305.
156. Gaikwad, S.M., et al., *Differential activation of NF-kappaB signaling is associated with platinum and taxane resistance in MyD88 deficient epithelial ovarian cancer cells*. *Int J Biochem Cell Biol*, 2015. **61**: p. 90-102.
157. Zaehres, H., et al., *High-efficiency RNA interference in human embryonic stem cells*. *Stem Cells*, 2005. **23**(3): p. 299-305.

158. Bast, R.C., Jr., B. Hennesy, and G.B. Mills, *The biology of ovarian cancer: new opportunities for translation*. Nat Rev Cancer, 2009. **9**(6): p. 415-28.
159. Rizzo, S., et al., *Ovarian cancer stem cell-like side populations are enriched following chemotherapy and overexpress EZH2*. Molecular cancer therapeutics, 2011. **10**(2): p. 325-335.
160. Baldwin, T.O., *Firefly luciferase: the structure is known, but the mystery remains*. Structure, 1996. **4**(3): p. 223-228.
161. Santaniello, E. and G. Meroni, *Color-tuning of firefly luciferase bioluminescence by modification of enzyme and substrate structure: new opportunities for optical imaging*. Minerva Biotechnologica, 2009. **21**(2): p. 77.
162. Kuo, A., N.V. Blough, and P.V. Dunlap, *Multiple N-acyl-L-homoserine lactone autoinducers of luminescence in the marine symbiotic bacterium Vibrio fischeri*. Journal of bacteriology, 1994. **176**(24): p. 7558-7565.
163. Gaikwad, S.M., et al., *Non-invasive imaging of phosphoinositide-3-kinase-catalytic-subunit-alpha (PIK3CA) promoter modulation in small animal models*. PLoS One, 2013. **8**(2): p. e55971.
164. Pradeep, S., et al., *Hematogenous metastasis of ovarian cancer: rethinking mode of spread*. Cancer cell, 2014. **26**(1): p. 77-91.
165. Charafe-Jauffret, E., et al., *Breast cancer cell lines contain functional cancer stem cells with metastatic capacity and a distinct molecular signature*. Cancer Res, 2009. **69**(4): p. 1302-13.
166. Diebel, M., et al., *ALDH1-positive cancer stem cells mediate metastasis and poor clinical outcome in inflammatory breast cancer*. Clin Cancer Res, 2010. **16**(1): p. 45-55.

167. Sun, S. and Z. Wang, *ALDH high adenoid cystic carcinoma cells display cancer stem cell properties and are responsible for mediating metastasis*. *Biochemical and biophysical research communications*, 2010. **396**(4): p. 843-848.
168. *Human Ovarian Cancer Cells Grown as Multicellular Tumor Abrogation of Taxol-induced G2 -M Arrest and Apoptosis in Spheroids*.
169. Gaikwad, S.M., et al., *Differential activation of NF- κ B signaling is associated with platinum and taxane resistance in MyD88 deficient epithelial ovarian cancer cells*. *The international journal of biochemistry & cell biology*, 2015. **61**: p. 90-102.
170. Iyer, V.R. and S.I. Lee, *MRI, CT, and PET/CT for ovarian cancer detection and adnexal lesion characterization*. *American Journal of Roentgenology*, 2010. **194**(2): p. 311-321.
171. Iagaru, A., et al., *¹⁸F FDG PET/CT Evaluation of Patients with Ovarian Carcinoma*. *Nuclear medicine communications*, 2008. **29**(12): p. 1046.
172. Prakash, P., C.G. Cronin, and M.A. Blake, *Role of PET/CT in ovarian cancer*. *American Journal of Roentgenology*, 2010. **194**(6): p. W464-W470.
173. Blanquart, C., et al., *Monitoring the activation state of the insulin-like growth factor-1 receptor and its interaction with protein tyrosine phosphatase 1B using bioluminescence resonance energy transfer*. *Mol Pharmacol*, 2005. **68**(3): p. 885-94.
174. LeRoith, D. and S. Yakar, *Mechanisms of disease: metabolic effects of growth hormone and insulin-like growth factor 1*. *Nature Clinical Practice Endocrinology & Metabolism*, 2007. **3**(3): p. 302-310.
175. Bertrand, F., et al., *Synergy between an IGF-1R antibody and Raf/MEK/ERK and PI3K/Akt/mTOR pathway inhibitors in suppressing IGF-1R-mediated growth in hematopoietic cells*. *Leukemia*, 2006. **20**(7): p. 1254-1260.
176. Maki, R.G., *Small is beautiful: insulin-like growth factors and their role in growth, development, and cancer*. *Journal of Clinical Oncology*, 2010. **28**(33): p. 4985-4995.

177. Lopez, T. and D. Hanahan, *Elevated levels of IGF-1 receptor convey invasive and metastatic capability in a mouse model of pancreatic islet tumorigenesis*. *Cancer cell*, 2002. **1**(4): p. 339-353.
178. Hellawell, G.O., et al., *Expression of the type 1 insulin-like growth factor receptor is up-regulated in primary prostate cancer and commonly persists in metastatic disease*. *Cancer research*, 2002. **62**(10): p. 2942-2950.
179. Bähr, C. and B. Groner, *The IGF-1 receptor and its contributions to metastatic tumor growth—novel approaches to the inhibition of IGF-1R function*. *Growth Factors*, 2005. **23**(1): p. 1-14.
180. Singh, R.K., et al., *IGF-1R inhibition potentiates cytotoxic effects of chemotherapeutic agents in early stages of chemoresistant ovarian cancer cells*. *Cancer Lett*, 2014. **354**(2): p. 254-62.
181. Heald, A., et al., *Insulin-like growth factor binding protein-2 (IGFBP-2) is a marker for the metabolic syndrome*. *Experimental and clinical endocrinology & diabetes: official journal, German Society of Endocrinology [and] German Diabetes Association*, 2006. **114**(7): p. 371-376.
182. Heald, A., et al., *Polymorphisms in insulin-like growth factor binding protein-1 (IGFBP-1) are associated with increased type-2 diabetes mellitus prevalence*. 2006.
183. Hankinson, S.E., et al., *Circulating concentrations of insulin-like growth factor I and risk of breast cancer*. *The Lancet*, 1998. **351**(9113): p. 1393-1396.
184. Yu, H. and H. Berkel, *Insulin-like growth factors and cancer*. *J La State Med Soc*, 1999. **151**(4): p. 218-23.
185. Yu, H. and T. Rohan, *Role of the insulin-like growth factor family in cancer development and progression*. *J Natl Cancer Inst*, 2000. **92**(18): p. 1472-89.
186. Cohen, P., *Overview of the IGF-1 system*. *Horm Res*, 2006. **65 Suppl 1**: p. 3-8.

187. Yakar, S., et al., *Clinical relevance of systemic and local IGF-I*. *Endocr Dev*, 2005. **9**: p. 11-6.
188. De Meyts, P., et al., *Insulin and IGF-I receptor structure and binding mechanism*, in *Mechanisms of Insulin Action*. 2007, Springer. p. 1-32.
189. Larsson, O., A. Girnita, and L. Girnita, *Role of insulin-like growth factor 1 receptor signalling in cancer*. *British journal of cancer*, 2005. **92**(12): p. 2097-2101.
190. Novosyadlyy, R. and D. LeRoith, *IGF Receptors*.
191. Hartog, H., et al., *The insulin-like growth factor 1 receptor in cancer: old focus, new future*. *European Journal of Cancer*, 2007. **43**(13): p. 1895-1904.
192. Hubbard, S.R. and W.T. Miller, *Receptor tyrosine kinases: mechanisms of activation and signaling*. *Current opinion in cell biology*, 2007. **19**(2): p. 117-123.
193. Macaulay, V., *Insulin-like growth factors and cancer*. *British journal of cancer*, 1992. **65**(3): p. 311.
194. Playford, M.P., et al., *Insulin-like growth factor 1 regulates the location, stability, and transcriptional activity of β -catenin*. *Proceedings of the National Academy of Sciences*, 2000. **97**(22): p. 12103-12108.
195. Sarfstein, R., et al., *Insulin-like growth factor-I receptor (IGF-IR) translocates to nucleus and autoregulates IGF-IR gene expression in breast cancer cells*. *Journal of Biological Chemistry*, 2012. **287**(4): p. 2766-2776.
196. Kurrey, N.K., et al., *Snail and slug mediate radioresistance and chemoresistance by antagonizing p53-mediated apoptosis and acquiring a stem-like phenotype in ovarian cancer cells*. *Stem Cells*, 2009. **27**(9): p. 2059-68.
197. Shelton, J.G., et al., *Synergy between PI3K/Akt and Raf/MEK/ERK pathways in IGF-IR mediated cell cycle progression and prevention of apoptosis in hematopoietic cells*. *Cell Cycle*, 2004. **3**(3): p. 370-377.

198. Peruzzi, F., et al., *Multiple signaling pathways of the insulin-like growth factor 1 receptor in protection from apoptosis*. Molecular and cellular biology, 1999. **19**(10): p. 7203-7215.
199. Macaulay, V., et al., *Downregulation of the type 1 insulin-like growth factor receptor in mouse melanoma cells is associated with enhanced radiosensitivity and impaired activation of Atm kinase*. Oncogene, 2001. **20**(30): p. 4029-4040.
200. Bähr, C. and B. Groner, *The insulin like growth factor-1 receptor (IGF-1R) as a drug target: novel approaches to cancer therapy*. Growth hormone & IGF research, 2004. **14**(4): p. 287-295.
201. Peruzzi, F., et al., *Anti-apoptotic Signaling of the Insulin-like Growth Factor-I Receptor through Mitochondrial Translocation of c-Raf and Nedd4*. Journal of Biological Chemistry, 2001. **276**(28): p. 25990-25996.
202. Heskamp, S., et al., *Upregulation of IGF-1R Expression during Neoadjuvant Therapy Predicts Poor Outcome in Breast Cancer Patients*. PloS one, 2015. **10**(2).
203. Baserga, R., F. Peruzzi, and K. Reiss, *The IGF-1 receptor in cancer biology*. Int J Cancer, 2003. **107**(6): p. 873-7.
204. Medyouf, H., et al., *High-level IGF1R expression is required for leukemia-initiating cell activity in T-ALL and is supported by Notch signaling*. J Exp Med, 2011. **208**(9): p. 1809-22.
205. Wang, L., Y.Y. Shao, and R.T. Ballock, *Thyroid hormone-mediated growth and differentiation of growth plate chondrocytes involves IGF-1 modulation of beta-catenin signaling*. J Bone Miner Res, 2010. **25**(5): p. 1138-46.
206. Hofmann, F. and C. García-Echeverría, *Blocking the insulin-like growth factor-I receptor as a strategy for targeting cancer*. Drug discovery today, 2005. **10**(15): p. 1041-1047.

207. Chang, W.W., et al., *The expression and significance of insulin-like growth factor-1 receptor and its pathway on breast cancer stem/progenitors*. Breast Cancer Res, 2013. **15**(3): p. R39.
208. Hart, L.S., et al., *Human colon cancer stem cells are enriched by insulin-like growth factor-1 and are sensitive to figitumumab*. Cell Cycle, 2011. **10**(14): p. 2331-2338.
209. Hart, L.S. and W.S. El-Deiry, *Invincible, but not invisible: imaging approaches toward in vivo detection of cancer stem cells*. J Clin Oncol, 2008. **26**(17): p. 2901-10.
210. Werner, H. and D. Le Roith, *New concepts in regulation and function of the insulin-like growth factors: implications for understanding normal growth and neoplasia*. Cellular and Molecular Life Sciences CMLS, 2000. **57**(6): p. 932-942.
211. el-Roeiy, A., et al., *Expression of insulin-like growth factor-I (IGF-I) and IGF-II and the IGF-I, IGF-II, and insulin receptor genes and localization of the gene products in the human ovary*. The Journal of Clinical Endocrinology & Metabolism, 1993. **77**(5): p. 1411-1418.
212. Lupu, F., et al., *Roles of growth hormone and insulin-like growth factor 1 in mouse postnatal growth*. Developmental biology, 2001. **229**(1): p. 141-162.
213. Liu, L., et al., *Infertility caused by retardation of follicular development in mice with oocyte-specific expression of Foxo3a*. Development, 2007. **134**(1): p. 199-209.
214. King, E.R., et al., *The insulin-like growth factor 1 pathway is a potential therapeutic target for low-grade serous ovarian carcinoma*. Gynecologic oncology, 2011. **123**(1): p. 13-18.
215. Buck, E., et al., *Compensatory insulin receptor (IR) activation on inhibition of insulin-like growth factor-1 receptor (IGF-1R): rationale for cotargeting IGF-1R and IR in cancer*. Molecular cancer therapeutics, 2010. **9**(10): p. 2652-2664.

216. Shan, J., et al., *Nanog regulates self-renewal of cancer stem cells through the insulin-like growth factor pathway in human hepatocellular carcinoma*. *Hepatology*, 2012. **56**(3): p. 1004-14.
217. Barr, S., et al., *Bypassing cellular EGF receptor dependence through epithelial-to-mesenchymal-like transitions*. *Clinical & experimental metastasis*, 2008. **25**(6): p. 685-693.
218. Lorenzatti, G., et al., *CCN6 (WISP3) decreases ZEB1-mediated EMT and invasion by attenuation of IGF-1 receptor signaling in breast cancer*. *Journal of Cell Science*, 2011. **124**(10): p. 1752-1758.
219. Kajiyama, H., et al., *Chemoresistance to paclitaxel induces epithelial-mesenchymal transition and enhances metastatic potential for epithelial ovarian carcinoma cells*. *International Journal of Oncology*, 2007.
220. Rosano, L., et al., *Acquisition of chemoresistance and EMT phenotype is linked with activation of the endothelin A receptor pathway in ovarian carcinoma cells*. *Clin Cancer Res*, 2011. **17**(8): p. 2350-60.
221. Warsito, D., et al., *Nuclear IGF1R is a transcriptional co-activator of LEF1/TCF*. *EMBO Rep*, 2012. **13**(3): p. 244-50.
222. Lu, X., et al., *Picropodophyllin inhibits epithelial ovarian cancer cells in vitro and in vivo*. *Biochem Biophys Res Commun*, 2013. **435**(3): p. 385-90.
223. Chakrabarty, A., et al., *Feedback upregulation of HER3 (ErbB3) expression and activity attenuates antitumor effect of PI3K inhibitors*. *Proceedings of the National Academy of Sciences*, 2012. **109**(8): p. 2718-2723.
224. Ledermann, J., et al., *Olaparib maintenance therapy in platinum-sensitive relapsed ovarian cancer*. *New England Journal of Medicine*, 2012. **366**(15): p. 1382-1392.

225. Oza, A.M., et al., *Olaparib combined with chemotherapy for recurrent platinum-sensitive ovarian cancer: a randomised phase 2 trial*. *The Lancet Oncology*, 2015. **16**(1): p. 87-97.

Materials and Methods

Cell culture

1. Reagents and chemicals

S. No.	Reagent Name	Source
1	DMEM, MEM, RPMI*	Gibco/Invitrogen, USA
2	Fetal Bovine Serum (FBS)	Hi media, India
3	Penicillin-Streptomycin	Gibco/Invitrogen, USA
4	Trypsin-EDTA	Gibco/Invitrogen, USA
5	G418	Sigma, USA
6	DMSO	Sigma, USA
7	Superfect transfection reagent	Qiagen, Valencia, CA
8	Lipofectomine 2000	Invitrogen
9	Phosphate buffered saline (PBS) pH 7.4**	In-House

*Cell culture media are supplemented with 10% FBS and 1% Penicillin-streptomycin.

**PBS Composition: 137mM NaCl, 2.7mM KCl, 10mM Na₂HPO₄, 2mM KH₂PO₄ (pH 7.4).

2. Cell lines

The different ovarian cancer cell lines used in the present study are mentioned below with their respective culture media.

S. No.	Cell Line Name	Origin	Source	Culture Media
1	A2780	Undifferentiated EOC	ATCC	DMEM
2	SKOV3	Serous adenocarcinoma	ATCC	RPMI
3	OAW42	Serous adenocarcinoma	ATCC	MEM

3. Method

All of these cell lines are adherent and were maintained their respective media supplemented with 10% FBS, 100U/ml penicillin and 100 µg/ml streptomycin solutions as shown in the Table. For every experimental procedure cells with 70 percent confluency were used.

3.1. Procedure for sub culturing

- a) Cell culture media from culture plates were aspirated and gently washed with 1X sterile PBS twice.
- b) 1ml trypsin (for 10cm dish) was added and the cells were incubated at 37⁰C for 5 to 7 min (till all cells started detaching from substratum) as per requirement. Further trypsin were neutralise with 3ml complete medium.
- c) Single cell suspension was made by gently pipetting and cells were centrifuged at 1200 rpm for 5min. Supernatant was discarded and the cells were washed with 1X PBS and centrifuged again at 1200 rpm for 5 minutes.
- d) Cells were either sub cultured with 1:3 split ratio into new culture vessel(s) or required number of viable cells seeded according to the requirement for experimental purpose.
- e) Cell viability was estimated by trypan blue dye exclusion method. In brief, 10µl of cell suspension were diluted with trypan blue dye (1:1 ratio) and viable cells (bright cells due to exclusion of dye) were counted using haemocytometer and number of cells per ml were calculated using following formula:
- f) No of cells/ml = average number of cells per WBC chamber x 10⁴.
- g) Cells were fed with complete medium and incubated at 37⁰C in 5% CO₂ with 95% humidity.

3.2. Procedure for cryopreservation

Cryopreservation media generally consists of a base medium, cryoprotective agent (DMSO) and a protein source (serum). Cryoprotective agents reduce the freezing point of the medium and reduces the risk of ice crystal formation, which can damage cells and cause cell death during freezing.

- a) Cells were trypsinized as described above and single cell suspension was made by gently aspirating the cells. Viable cell count was calculated using Trypan blue dye exclusion method described earlier.
- b) Subsequently freezing medium was prepared by adding 50-70% serum to complete medium along with 5%-8% of DMSO as per requirement.
- c) About 1×10^6 - 2×10^6 cells were gently resuspended in 1ml of chilled freezing medium with gentle pipetting and immediately transferred to a cryopreservation vial (cryo vials).
- d) Further cryo vials were slowly cooled approximately at a rate of 1-2^o/hr till it reaches first at -20^oC for 2 hours and overnight at -80^oC and then transferred to liquid nitrogen for cryopreservation.

3.3. Revival of cryopreserved cells

- a) Cryo vial from the liquid nitrogen was thawed using water bath at 37^oC.
- b) Since DMSO is toxic to cells, after thawing the cryovial 5 ml media was added to it. Cells were then centrifuged at 800 rpm for 5 minutes at 4^oC and the cell pellet was resuspended in complete media with gentle pipetting.
- c) Then the cell suspension was transferred to a new culture vessel or plate.
- d) Cells were then incubated at 37^oC in 5% CO₂.

3.4. Procedure for transient/stable transfection of cell lines:

Transfection is the process of introduction of foreign DNA into eukaryotic cells by non-viral methods. Transfection was performed using Superfect or Lipofectamine transfection reagent as per manufacturer's instructions.

- a) Prior to the day of transfection, a required amount of viable cell were seeded in culture vessel, primarily in 24 well plate.
- b) DNA-Superfect reagent complex were prepared by adding required amount of plasmid/s and transfection reagent as per instructed in definite volume of incomplete medium with gentle mixing. This mixture was then incubated for 10 minutes at room temperature.
- c) In the meantime the medium was aspirated from the culture vessel and washed twice with 1X PBS twice.
- d) Definite amount of complete media was added to the transfection mixture and this was administered in the culture vessel. The plate was swirled gently to uniformly distribute the complex and incubated at 37°C, 5% CO₂.
- e) After 3 hours, the transfection media was aspirated, washed with 1X PBS and complete media was added to the cells.
- f) For stable transfection, after 24-48 h of transfection, the cells are trypsinized and are sub cultured in the selection media containing antibiotics like G418.

MTT Assay

MTT assay is a colorimetric assay in order to monitor cellular viability and proliferation rate. Cellular enzymes like NAD(P)H-oxidoreductase enzyme reflects the number of viable cells present. These enzymes are capable of reducing the tetrazolium dye MTT 3-(4, 5-dimethylthiazol-2-yl)-2, 5-

diphenyltetrazolium bromide) into its insoluble formazan crystals. The absorbance of the coloured solution can be quantified by the spectrophotometer at wavelength 560- 670nm.

1. Reagents and chemicals

S. No.	Reagent Name	Source
1	DMSO	Sigma, USA
2	MTT	Sigma, USA

2. Method

- a) The cells were seeded in 96 well plate at density of 2000 cells per well. The experiment was performed in quadruplet.
- b) According to the need of experiment either cytotoxicity of drugs or cell proliferation the cells were proceeded for the experiment and incubated for required duration at 37°C, 5% CO₂. All the cytotoxicity test were performed after drug treatment and the cells were incubated for 72 hours.
- c) For cell proliferation assay, the cell were seeded in required amount and incubated for different time points like (0, 24, 48 h, etc.)
- d) At end point, cells were treated with 20µl of 5mg/ml MTT and incubated for 3 hours.
- e) Post MTT incubation, the spent media from each well were removed completely and formazan crystals were dissolved by adding 100µl DMSO per well.
- f) The absorbance of solubilise dye were estimated at wavelength 560nm and 670nm.
- g) Note- The absorbance at560nm is subtracted from the absorbance at 670nm to remove the background caused by the presence of DMSO.

Real-Time Quantitative PCR

1. Reagents and chemicals

S. No.	Reagent Name	Source
1	2X Syber green master mix	Invitrogen

2. Primers Used

The table shows the primer sequences used in the qPCR in present study.

S. No.	Gene Name	Sequence
1	Oct4 Forward	GTGGAGAGCAACTCCGATG
2	Oct4 Reserve	TGCAGAGCTTTGATGTCCTG
3	Sox2 Forward	AACCCCAAGATGCACAACCTC
4	Sox2 Reverse	GCTTAGCCTCGTCGATGAAC
5	Nanog Forward	AAAGCTTGCCTTGCTTTGAA
6	Nanog Reserve	AAGTGGGTTGTTTGCCTTTG
7	IGF-1R Forward	CTGGACTCAGTACGCCGTTT
8	IGF-1R Reserve	GGAACTGAAGCATTGGTGCG
9	SP1 Forward	TCATACTGTGGGAAACGCTT
10	SP1 Reverse	GACACTCAGGGCAGGCAAA
11	FOXO 3 Forward	TCTACGAGTGGATGGTGCGTT
12	FOXO 3 Reverse	CGACTATGCAGTGACAGGTTGTG
13	GAPDH Forward	TGCACCACCAACTGCTTAGC
14	GAPDH Reverse	GGCATGGACTGTGGTCATGAG

3. Method

- a) All the PCRs were carried out in a final volume of 10 µl containing 10 ng of cDNA, 10 Picomole of each primer and 1X Power SYBR Green PCR Master Mix (Applied Biosystems, Foster City, CA).
- b) The qPCR reactions for each sample and each gene were performed in triplicates.
- c) The PCR conditions were as follows:

S. No.	Step	Temperature °C	Time (sec)
1	Initial Denaturation	95	600
2	Denaturation	95	15
3	Annealing	60	60
4	Repeat steps 2 and 3	40 cycles	
5	Sybr Green dissociation step 1	95	15
6	Sybr Green dissociation step 2	60	15
7	Sybr Green dissociation step 3	95	15

- d) Specificity of each amplified reaction product were confirmed by melting curve analysis.

4. Data analysis and representation in terms of relative and fold change i.e. $2^{-\Delta C_t}$ and $2^{-\Delta\Delta C_t}$ respectively:

Relative expression of each target gene were estimated by ΔC_t method as follows with GAPDH as a normalisation control.

$$\Delta C_t = C_t \text{ Gene} - C_t \text{ GAPDH}$$

$$\Delta\Delta C_t = \Delta C_t \text{ control} - \Delta C_t \text{ Test}$$

Bacterial Cell Culture

1. Reagents and chemicals

S. No.	Reagent Name	Source
1	LB broth	Hi media, India
2	LB agar	Hi media, India
3	Yeast extract	Hi media, India
4	Bactotryptone	Hi media, India
5	Kanamycin	Sigma, USA;
6	Ampicillin	Sigma, USA;
7	DMSO	Sigma, USA;

2. Method

2.1. Preparation of Luria-Bertani (LB) medium and agar

- a) Powdered Luria Broth (20g) was dissolved in 800 ml deionized 'MilliQ' processed water (D/W) and the volume was adjusted to 1 litre (L) with D/W and sterilized by autoclaving.
- b) For making LB-agar plates, 35g Luria agar powder was dissolved/ L sterilized by autoclaving and poured in 90 mm sterile plates.
- c) Specific antibiotic either ampicillin or kanamycin was added in the medium according to the plasmid antibiotic marker.

2.2. Preparation of ultra-competent cells

- a) Composition of Transformation Buffer (TB)

The following components were added to 100 ml of distilled water; 10mM PIPES, 15 mM CaCl₂, 250 mM KCl, adjusted pH to 6.7 with 5N KOH, 55 mM MnCl₂, filter sterilized through 0.2 μ membrane filter.

- b) Composition of Super Optimal Broth (SOB)

Following components were mixed in the required volume of D/W; 2% Bactotryptone, 0.5% Yeast extract, 10 mM NaCl, 2.5 mM KCl, 10 mM MgCl₂, 10 mM MgSO₄;

2.3. Procedure

- c) E.coli strain DH5 α strain was streaked on a LB agar plate without antibiotics and incubated overnight at 37°C.
- d) Single colony was suspended into 1ml SOB and inoculated in 250 ml SOB broth and incubated at 18°C/250 rpm till O.D. reach to ~0.4 at 600nm (Approximately 3-4 days of incubation are required).
- e) The cells were harvested by pelleting down at 4°C and resuspended in 80 ml of TB followed by incubation on ice for 10 min and centrifuged at 4°C for 10 minutes at 3000 rpm.
- f) The cell pellet was resuspended in 18.6 ml TB. 1.4 ml (7%) DMSO was added to the cells and mixed completely.
- g) 100 μ l aliquots of the cells were made in sterile microfuge tubes and snap frozen in liquid nitrogen followed by storage at -80°C.

2.4. Procedure for bacterial transformation

- a) Competent cells (100 μ l) were thawed on ice and mixed with 1-5ng of plasmid DNA or 20 μ l of ligation mixture and incubated on ice for 30 min.
- b) Heat shock is given to the mixture at 42°C for 60 sec and the sample was snap chilled on ice.
- c) LB medium was added to the cells and incubated at 37°C for 60 minutes at 170 rpm.
- d) The cells are then plated on an LB agar plate with the appropriate antibiotic.

2.5. Plasmid DNA isolation from bacterial cells by mini-preparation

The plasmid isolation was performed following the procedure described in the Qiagen mini prep kit. Briefly following steps were performed.

- a) Overnight grown, 1-5 ml of bacterial cultures transformed with plasmids were centrifuged at 3500 rpm for 15-20 minutes at 4°C.
- b) Bacterial pellet was resuspended in 250µl of Buffer P1 (Re-suspension buffer containing RNase (10mg/ml)).
- c) The cells were incubated at room temperature (RT) for 5 min and 250µl Buffer P2(lysis solution) was added followed by invert mixing.
- d) The cells were incubated at RT for 5 min and 350µl of Buffer N3 (neutralizing solution) was added and incubated at RT for 5 min. after complete invert mixing.
- e) The above mixture was then centrifuged at 12,000Xg for 10 min.
- f) The supernatants from step 5 was applied to the QIAprep spin column by decanting or pipetting.
- g) The column was centrifuged for 30–60 s and the flow-through was discarded.
- h) QIAprep spin column was washed by adding 0.75 ml Buffer PE and centrifuging for 30–60 s.
- i) The flow-through was discarded and centrifuged at full speed for an additional 1 min to remove residual wash buffer.
- j) The QIAprep column was placed in a clean 1.5 ml micro centrifuge tube. DNA was eluted by addition of 50 µl Buffer EB (10 mM Tris Cl, pH 8.5) or water to the centre of each QIAprep spin column for 1 min and centrifuged for 1 min

Cloning

1. Reagents and chemicals

S. No.	Reagent Name	Source
1	Tris Borate–EDTA buffer (TBE)*	In-house
2	Agarose powder	Hi media, India
3	6X gel loading dye	Fermentas
4	Ethidium bromide (EtBr)	Fermentas
5	DNA marker: 100 bp	Fermentas
6	DNA marker: 1 Kb or Mass ruler	Fermentas

*Composition of the TBE: 0.9 M Tris base, 0.9 M Boric acid, 0.02 M EDTA
(10X buffer stock was made and diluted to 1X for use)

2. Method

2.1. Protocol for agarose gel electrophoresis

- a) The agarose gel percentage varying from 0.7% – 2% (according to the size of the DNA to be resolved) was prepared along with EtBr as an intercalating agent.
- b) Solidified gel was transferred to the electrophoresis tank that has electrode fitted to it at the two ends.
- c) The required 1X TBE buffer is then poured into the tank. Before loading the PCR product into the wells, the PCR product is mixed with the 6X loading dye containing glycerol for viscosity and bromophenol blue as a tracking dye.
- d) An appropriate reference DNA ladder were run in parallel. The gel was run at 80V for 1hour.
- e) EtBr stained DNA bands were visualized and documented with Gel documentation system.

2.2. Protocol for Gel extraction

The PCR amplified product/restriction digested DNA was gel extracted and purified by using QIAGEN gel extraction kit. Briefly, the following procedure was followed:

- a) The DNA fragment from the agarose gel was excised with a clean, sharp scalpel.
- b) The gel slice was weighed in a micro centrifuge tube. Buffer QG was added three time to 1 volume gel (100 mg ~ 100 μ l).
- c) Reaction was incubated at 50°C for 10 min (or until the gel slice has completely dissolved). Vortex the tube every 2–3 min to help dissolve gel.
- d) 1 gel volume of isopropanol was added to the sample and mixed. Thereafter, a QIAquick spin column were placed on a 2 ml collection tube and the above reaction mix was added in the column.
- e) The tube was incubated for 1-2 minutes and centrifuged for 1 min at 13000 rpm.
- f) The flow-through was discarded and further washed with 0.5ml of buffer QG by centrifugation for 1min at 13000rpm.
- g) Buffer PE (0.75 ml) was added to QIAquick column and was incubated for 5 minutes before centrifuging for 1 min at 13000 rpm. The flow-through was discarded and was given another wash with buffer PE.
- h) An additional dry spin was given to the column and the column was placed in a clean 1.5 ml micro centrifuge tube.
- i) To elute DNA, 50 μ l Buffer EB (10 mM Tris·Cl, pH 8.5) or water was added to the centre of the QIAquick membrane and centrifuged at 13000 rpm for 1 min.

2.3. Protocol for restriction digestion

One unit of restriction endonuclease (RE) activity is defined as the amount of enzyme required to completely digest 1µg of substrate DNA in a total reaction volume of 50µL in one hour using the buffer provided. Restriction digestion is a tool for many molecular applications like ligation, gene isolation, etc.

- a) Source of RE enzymes: HpaI, NotI, NheI, Bam HI, and EcoRI was used from NEB, UK.
- b) Both insert and vector were digested with two RE enzymes simultaneously. NEB buffer that results in maximum activity of both the enzymes was chosen using the enzyme activity chart.
- c) Before beginning with digestion the recommended buffer was allowed to thaw completely on ice also the water bath was set at 37°C.
- d) A typical restriction digestion mix consists of following components:

Reaction Mixture
10 X NEB buffer
DNA (insert/ vector)
Enzyme/(s)
Distilled water

- e) The reaction mixture was incubated at 37°C water bath, overnight.

2.4. Protocol for Ligation

Ligation is performed by using DNA ligase is a special type of enzyme that catalyses the formation of phosphodiester bond between juxtaposed 5'phosphate and 3'hydroxyl terminal in duplex DNA or RNA. This enzyme joins blunt and sticky ended termini as well as repair single stranded nicks in duplex DNA, RNA or DNA/RNA hybrids. The ligation reaction was set

depending upon the concentration of the insert. Ideally the vector to insert ratio is (1:3) which is essential for carrying out successful ligation reaction.

- a) Source of reagents: Quick ligase enzyme and its 10 X buffer was obtained from NEB, UK.
- b) The ligation reaction was carried out at room temperature and incubated for 10-15 minutes before performing bacterial transformation.
- c) After transformation the LB agar plates were placed in the incubator for overnight. After 16-18 hrs of incubation, the plates were checked for colonies.
- d) Colonies were cultured in LB broth and plasmid were isolated. Screening for the positive clone was performed by restriction digestion.
- e) Positive clone obtained by cloning was further verified by DNA sequencing.
- f) Sequencing was performed using the ABI automated DNA sequencer available with Genomics facility of ACTREC.

Total RNA Isolation, Visualisation and Quantification

Total RNA was isolated from different cell lines using Qiagen total RNA isolation kit. Isolated RNA was further visualized on gel and quantified using Nano drop. Isolated RNA is further used to synthesize cDNA by reverse transcription PCR and used to estimate transcript levels of different genes.

1. Reagents and chemicals

S. No.	Reagent Name	Source
1	DEPEC	Sigma, USA
2	Total RNA isolation kit	BIOLINE
3	Formaldehyde	Sigma, USA
4	Formamide	Sigma, USA

5	Ethidium bromide	Sigma, USA
6	6X RNA loading dye	Sigma, USA
7	Agarose	Hi media, India
8	MOPS	Sigma, USA

10X MOPS buffer: 0.2M MOPS, 50mM sodium acetate, 10mM.

Preparation of Tank buffer: 30 ml 10X MOPS buffer+ 30ml formaldehyde and Volume was made up to 300ml.

Preparation of RNase Free MQ: 1ml of Diethyl Pyrocarbonate (DEPEC) was added to 1000ml of fresh MilliQ water and incubated overnight at 37°C followed by autoclaving.

2. Method

2.1. Procedure for total RNA isolation

- a) Four million of cells were harvested and washed with 1X PBS for 5mins at 1200rpm 4°C. The supernatant was discarded.
- b) The pellet was resuspended in Lysis buffer R (400µl) by pipetting and incubated for 3mins.
- c) The lysed solution was transferred to spin column R1 placed in a collection tube and it was spun at 10,000Xg for 2 minutes.
- d) The filtrate was saved and the Spin column R1 was discarded.
- e) Equal volume of 70% ethanol (400µl) was added in the filtrate, mixed well and transferred to spin column R2 placed in a fresh collection tube.
- f) The column was spun at 10,000Xg for 2 minutes. The filtrate was discarded.
- g) The spin column R2 was placed in the fresh collection tube. 500µl of wash buffer AR was added in the column and spun at 10000Xg for 1min. The filtrate was discarded.

- h) Wash buffer BR (700µl) was added in the column and spun at 10000Xg for 1minute.
- i) The filtrate is again discarded and the column is placed in the collection tube. A dry spin of 10000 X g for 3 minutes was given to the Spin column R2.
- j) The Spin column R2 was placed in the 1.5cm³ elution tube and 30-80µl (50µl) of RNase free water to spin column R2.
- k) The column was incubated for 5-10 mins and spun at 6000Xg for 1 minute to elute the RNA. The
- l) RNA was stored at -80°C. The RNA was quantified by using nanodrop.

2.2. Preparation of denaturing gel for visualisation of RNA (90ml):

- a) Agarose (1.08g) + RNase free water: 76.5 ml was boiled to melt agarose completely.
- b) 10X MOPS buffer (9ml) and formaldehyde (4.5ml) and EtBr was added.
- c) The gel is poured in the gel casting tray with a comb and allowed to solidify.

2.3. Preparation of RNA sample for gel loading

Reagent	Quantity (µl)
Formaldehyde	1
Formamide	3
10X MOPS buffer	2
RNA sample	1-2

- a) The following components are added to form a reaction mix:
- b) The reaction mix is incubated for 5-10min a 65°C for denaturation. 6X RNA loading dye (1-2 µl) was added to load on a gel. The gel was visualised on UV trans-illuminator.

cDNA Synthesis From Total RNA

A good quality total RNA isolate has an O.D 260/280 ratio of 1.8-2 and O.D 260/230 ratio of 1.8 or more. The cDNA was synthesized from total RNA using a cDNA synthesis kit from NEB,UK, according to the manufacturer's protocol.

1. Reagents and chemicals

- a) Superscript™ First-Strand Synthesis System for RT-PCR from Invitrogen

2. Method for First-Strand Synthesis Using Random Primers

- Starting material: 1 ng–5 µg total RNA or 50–500 ng poly(A)+ RNA
- Control reactions: Use 1 µl of Control RNA (50 ng/µl)

- a) For each reaction, combine the following in a sterile 0.5-ml tube:

S. No.	Component	Amount
1	RNA (1-2 µg)	X µl
2	10mM dNTP mix	1 µl
3	Random hexamer (50ng/µl)	1 µl
4	DEPC treated water to make volume	10 µl

- b) Incubate the RNA/primer mixture at 65°C for 5 minutes, then place on ice for at least 1 minute.

- c) In a separate tube, prepare the following 2X reaction mix, adding each component in the indicated order.

S. No.	Component	Amount
1	10X RT Buffer	2 µl
2	25 mM MgCl ₂	4 µl
3	0.1 M DTT	2 µl
4	RNaseOUT (40U/ µl)	1 µl

- d) Add 9 µl of the 2X reaction mix to each RNA/primer mixture from step 3, mix gently, and collect by brief centrifugation.

- e) Incubate at room temperature (~25°C) for 2 minutes.
- f) Add 1 µl of SuperScript™ II RT to each tube.
- g) Minus RT Control: Add 1 µl DEPC-treated water instead of the RT.
- h) Incubate at room temperature for 10 minutes.
- i) Incubate at 42°C for 50 minutes.
- j) Terminate the reaction at 70°C for 15 minutes. Chill on ice.
- k) Collect the reaction by brief centrifugation. Add 1 µl of RNase H to each tube and incubate for 20 minutes at 37°C. The reaction can be stored at -20°C.

Protein isolation from cells and estimation procedure

1. Reagents and chemicals

S. No.	Reagent Name	Source
1	Passive Lysis buffer (5X)	Promega
2	Protease inhibitor cocktail (10X)	Sigma,USA
3	Bradford reagent	Sigma,USA

2. Method

2.1. Preparation of lysates

- a) Cells were trypsinized and harvested by centrifugation at 1200 rpm for 5 minutes at 4°C.
- b) The cell pellet were resuspended in 1X PBS by centrifugation at 1200 rpm for 5 minutes.
- c) Supernatant was discarded and approximately 50µl of 1X passive lysis buffer per one million cells was added.

- d) Thereafter, 1µl of 10X protease inhibitor per 100µl of 1X passive lysis buffer was added in the cell lysate.
- e) The reaction was thoroughly mixed by vortexing and incubated at RT for 10-15 minutes.
- f) After incubation the reaction mixture was centrifuged at 13,000 rpm for 25 minutes at 4°C.
- g) The supernatant was collected and protein estimation was performed using Bradford reagent.

2.2. Bradford assay

Bradford is a colorimetric protein assay based on the absorbance shift of the dye Coomassie Brilliant Blue G-250 in which under acidic conditions the red/brown form of the dye is converted into its bluer form to bind to the protein being assayed. This colour change is estimated by using the formula obtained by plotting the absorbance of standards (1-5 µg/ml) in a linear regression analysis.

The procedure for the Bradford assay is as follows.

- a) BSA standards were made by serially diluting 1mg/ml BSA stock.

S. No.	Concentration (µg)	BSA stock (µl)	1X PBS (µl)
1	1	5	20
2	2	10	15
3	3	15	10
4	4	20	5
5	5	25	0
6	Blank	0	25

- b) Standards and sample were taken in triplicates.
- c) 250µl of Bradford reagent was taken per well in a 96 well plate.

- d) Lysates were diluted 1:5 using 1X PBS.
- e) 5 µl of each standards and 1:5 diluted samples were added to 250µl of Bradford reagent.
- a) Absorbance was measured at 595nm, values were subtracted against the blank and a standard curve was plotted by using the linear regression analysis.
- f) Protein concentration for lysate samples were calculated using equation derived from the standard curve.
- g) Lysates were diluted 1:5 using 1X PBS.

Western Blotting/ Immunoblotting

Immunoblotting is a technique used for analysis of individual proteins in a protein mixture (e.g. a cell lysate). The protein mixture is applied to a gel electrophoresis in a carrier matrix (SDS-PAGE, native PAGE, isoelectric focusing, 2D gel electrophoresis, etc.) to sort the proteins by size and charge in individual protein bands. The separated protein bands are then transferred to a carrier membrane (e.g. nitrocellulose membrane (NCM), nylon or PVDF). This process is called blotting. The proteins adhere to the membrane in the same pattern as they have been separated due to interactions of charges. The proteins on this immunoblot are then accessible for antibody binding for detection.

1. Reagents and chemicals

S. No.	Reagent Name	Source
1	Acrylamide and Bisacrylamide	Sigma,USA
2	SDS	Sigma,USA
3	Ammonium Per sulphate (APS)	SRL Chemicals, India
4	N,N,N',N'-tetramethylethylenediamine (TEMED)	Sigma,USA
5	Glycine	Sigma,USA

6	Butanol	Qualigens
7	Pre-stained protein marker	Fermentas
8	Tris base	Sigma,USA
9	Nitrocellulose Membrane (NCM)	Mdi, India
10	Beta mercaptoethanol	Sigma,USA
11	Tween20	Sigma,USA
12	Sodium chloride	SRL Chemicals, India
13	Gel cast, run unit with power pack	BioRad

- a) Composition of 30% Acrylamide: (29.2% acrylamide / 0.8% bisacrylamide) weight/volume in distilled water
- b) Composition of Resolving Buffer: 1.5mM Tris base, adjust the pH to 8.8 using 1N-HCl
- c) Composition of Stacking Buffer: 0.5mM Tris base, adjust the pH to 6.8 using 1N-HCl
- d) Composition of Running Buffer: 25mM Tris-Cl- 3.208g; 200mM Glycine- 15.012g;0.1% w/v SDS-1g
- e) Composition of Gel loading Dye: 50mM Tris HCl, pH 6.8, 2% SDS, 20% Glycerol, 12.5mM EDTA, 0.02% Bromophenol blue.
- f) Composition of Transfer buffer: 25mM Tris base, 190mM Glycine, 0.04% SDS, 20% methanol
- g) Composition of Tris Buffered Saline: (TBS) Tris base, 150mM NaCl, adjust the pH to 7.6 using 1N-HCL.
- h) Composition of blocking buffer: 1X TBS with 5% BSA
- i) Composition of Wash buffer (TBSt): 1X TBS with 0.05% Tween 20
- j) Composition of stripping buffer: 20%SDS, 100 μ M β -mercaptoethanol and 50 μ M Tris, pH6.8

2. Method

2.1. Gel casting

a) Contents of resolving gel

S. No.	Gel percentage	Milli Q (ml)	30% acrylamide (ml)	1.5M Tris-Cl pH-8.8 (ml)	10% (w/v) SDS (μ l)
1	8	4.7	2.7	2.5	100
2	10	4.1	3.3	2.5	100
3	12	3.4	4	2.5	100
4	15	2.4	5	2.5	100

b) This mixture were degassed and 50 μ L of APS and 5 μ L TEMED was added followed by gentle mixing.

c) Contents of stacking gel.

S. No.	Gel percentage	Milli Q (ml)	30% acrylamide (ml)	0.5 M Tris-Cl pH-6.8 (ml)	10% (w/v) SDS (μ l)
1	4	1.26 ml	260 μ L	500 μ L	10 μ L

d) This mixture were degassed and 5 μ L of APS and 2 μ L TEMED was added followed by gentle mixing.

2.2. Preparation of sample

a) Appropriate volume of protein lysate for the desired concentration was taken and mixed with protein gel loading dye.

b) The reaction mix was heated at 100°C on dry bath for 3 minutes and a short spin was given. The samples were kept on ice until they were loaded on the gel.

2.3. Procedure of Western blotting

a) Glass plates were cleaned thoroughly and were set up carefully in the casting stand.

- b) As per the requirement suitable percentage of resolving gel was prepared.
- c) Immediately the resolving gel solution was loaded between the glass plates using the pipette and the gel was overlaid with 200 μ L of water saturated butanol.
- d) The gel was allowed to polymerize for 35-40 minutes.
- e) After the resolving gel was solidified completely the butanol layer was washed thoroughly and the stacking gel was prepared.
- f) The wells for loading the samples were formed by placing the 10-well comb. The gel was allowed to polymerize for 15-25 minutes.
- g) The solidified gel was placed in the cassette and fitted with electrodes in the tank.
- h) The tank was filled with 1X running buffer till (1/4)th of its volume. The comb was then gently removed and the wells were washed with the buffer to remove the traces of any acryl/bisacrylamide deposits.
- i) The sample prepared was then loaded into respective wells and 4 μ L of pre-stained ladder was also loaded in one of the wells.
- j) The gel was then allowed to run at 60V, 400mA. After the sample entered the resolving gel the voltage was gradually increased to 80V. The run was stopped as soon as the dye reached the bottom of the gel.
- k) The gel, blotting paper and NCM were then soaked in 1X transfer buffer and incubated for 10 minutes.
- l) Onto the base of the Trans blot system the two soaked blotting papers were placed one after another, the transfer buffer was poured on top of the membrane and the air bubbles were removed carefully. Then, the NCM was placed and the gel was placed over it properly.

- m) The remaining two blotting papers were placed on the top of the gel and same as before the transfer buffer was poured, ensuring that the bubbles were removed. Then, the system was started and the transfer was set to 13V, 400mA for 1 hr.
- n) After complete transfer the membrane was removed carefully and then incubated in 40 ml of 5% blocking buffer for 1 hr on a shaker.
- o) After blocking, the membrane was probed with primary antibody(s) and incubated overnight at 4°C with gentle shaking.
- p) Next day, the membrane was washed thrice with the wash buffer (1X TBSt) and then incubated with the secondary antibody for 2 h.
- q) After the secondary Ab incubation the membrane was again washed thrice with the wash buffer.
- r) The proteins present on the membrane could be visualized by using the Enhanced Chemiluminescence (ECL) detection system.

2.4. Stripping and reprobing the membrane:

- a) In order to reprobe the membrane with another primary antibody stripping protocol is used.
- b) For stripping the membrane was incubated with the stripping buffer for 10 minutes at RT.
- c) The membrane was then washed thrice with 1X TBSt, blocked with the blocking buffer for 1 hour, then incubated with primary antibody overnight at 4°C with gentle shaking.
- d) The next day, the membrane was again washed with 1X TBSt, incubated with secondary antibody for 1-2 h at RT with continuous shaking and then washed with wash buffer and developed in dark with the ECL detection system.

A. Immunofluorescence

Immunofluorescence is an antigen-antibody reaction where the antibodies are tagged (labelled) with a fluorescent dye and the antigen-antibody complex is visualized using ultra-violet (fluorescent) microscope. Immunofluorescence can be used to determine the localization, abundance and co-localization with another proteins.

1. Reagents and chemicals

S. No.	Reagent Name	Source
1	Paraformaldehyde	Sigma,USA
2	Bovine Serum Albumin	Sigma, USA
3	DAPI	Sigma, USA
4	Vectashield (Mounting media)	Vector Labs, USA
5	Triton X 100	Sigma, USA
6	Anti-Mouse FITC	Sigma, USA
7	Anti-Rabbit FITC	Sigma, USA
8	Anti- Rabbit Dy Light 633	Sigma, USA
9	Anti-Mouse Dy Light 633	Sigma, USA

2. Method

2.1. Preparation of 4% paraformaldehyde

- a) Paraformaldehyde was weighed equal to 4% volume of the final solution (for 100 ml final volume, weigh 4 g of paraformaldehyde) and added in 1X PBS (volume equal to slightly less than 2/3 of the final desired volume).
- b) The mixture stirred at 60⁰C using a magnetic stirrer and after complete dilution of PFA the final volume was made up.
- c) The solution was filtered by Watman filter paper and was chilled on ice before use. Freshly prepared paraformaldehyde solution was usually preferred for the experiment.

2.2. Staining procedure

Different staining and fixation procedures were followed to stain the cells with different antibodies. The general procedure for immuno-fluorescence was as follows:

- a) 80% confluent plate was trypsinized and 30,000 - 40,000 cells were seeded per cover slip in a 6 well plate. Two cover slips per sample: One for secondary antibody control (without primary antibody) and the other as a test sample for staining were seeded.
- b) Cells were then incubated in 5% CO₂ at 37°C for 24h.
- c) After 24h, the spent medium was aspirated and cells were washed twice with 1X PBS.
- d) Cells were fixed on coverslip with 2ml of 4% PFA and incubated at room temperature for 10min. PFA was then removed and cells were washed thrice with PBS.
- e) Permeabilization is often required for nuclear staining. Coverslips containing cells were then incubated in Triton X 100 (0.025 to 0.3%) in 4% PFA. The permeabilization solution was removed and cells were washed thrice with PBS.
- f) The cells were now incubated with 5% BSA for 60 min at room temperature (blocking).
- g) Each cover slip (containing cells) was then incubated with 50µl of primary antibody (1:100 dilution in 1X PBS) on a clean glass slide. Cover slip was placed with cell surface facing downward.
- h) Cells were incubated with the primary antibody overnight in a moist chamber at 4°C.

- i) On the next day, cover slips were washed thrice with PBS. Each cover slip (containing cells) was then incubated with 50µl of secondary antibody (1:200 dilution in 1X PBS) on a clean glass slide. Cover slip was placed with cell surface facing downward.
- j) Incubation was carried out for 2 hours at room temperature in dark after which cells were washed thrice with PBS.
- k) Cells were counter stained with 50µl of DAPI (0.05%) for 30 seconds and after washing for three times with PBS, coverslips were mounted on clean glass slide (cell surface facing downward) using Vectashield mounting medium.
- l) Cells were observed under confocal laser scanning microscope within 1hour. Argon, Helium/Neon and diode lasers were used to capture images on a Carl Zeiss LSM 510 Meta confocal microscope and the images were analysed using LSM Image Browser.

In Vivo Bioluminescence Imaging in NOD/SCID mice

In vivo bioluminescence imaging (BLI) is sensitive tool that is based on detection of light emission from cells or tissues. BLI allows a non-invasive, and real-time analysis of biological processes at the molecular level in living organisms. *In vivo* imaging allows longitudinal monitoring of disease like tumor formation in the same animal and offers desirable alternative to analyse number of animals at many time points during the progression of tumor formation. The *in vivo* BLI in mice uses the following procedure.

1. Reagents and chemicals

- a) D luciferin
- b) Isoflurane

2. Method

2.1. Cell preparation

- a) Luciferase (firefly luciferase) expressing ovarian cancer cell lines (Pac^{ER}, Pac^{LR}, Cis^{LR}) were established in the laboratory.
- b) These cells are highly tumorigenic and can be used in pre-clinical mouse models.
- c) The cells were sorted through FACS (SP and NSP)/grown as spheroid under non adherent culture condition followed by implantation in NOD/SCID mice.

2.2. Animal Injection

- a) A 70-80% confluent flask cells were harvested by trypsinisation and counted using trypan blue.
- b) 10,000-50,000 cells per mouse were used for implantation.
- c) Accordingly total number of cells required for all the mice were counted and collected in a microfuge tube.
- d) The final count of the cell number was dissolved in 50µl of 1X PBS and the cells were kept in ice.
- e) Care should be taken that the mice should be kept ready for implantation to avoid loss of viable cells and cells should be immediately implanted in mice.
- f) Usually, in order to facilitate optimal formation of tumor NOD/SCID immunocompromised mice were preferred for implantation.
- g) Animal care and euthanasia were performed with the approval from Institutional Animal Ethics Committee of ACTREC.
- h) If SCID (Severe Combined Immuno-deficiency) mice were used, then the fur of the mice were removed by razor, to facilitate proper implantation and optical imaging. For nude mice no such pre-treatment is required.

- i) Prior to implantation, animals were anesthetized by Isoflurane in the incubation chamber.
- j) Required amount of cells were loaded in a syringe with 26 guage needle.
- k) The skin of the mice was lifted to make a tent and the cells were injected at the base to get a subcutaneous injection.
- l) The newly injected mice can be imaged immediately.

2.3. Animal imaging

- a) For each imaging session, D-luciferin (100 µl of 30mg/ml per mouse) was given through intraperitoneal.
- b) After substrate injection the animals were imaged with optical imaging system or IVIS-Spectrum optical imager.
- c) In both the system, the bioluminescence signals from the animal were captured by a back-thinned charge coupled device camera cooled to -90°C.
- d) Imaging was performed through IVIS-SPECTRUM, ROIs were drawn over the tumors and quantified by using the LIVING IMAGE 4.4 software.
- e) Bioluminescence signals were recorded as maximum (photons/s/cm²/sr). Photon flux (bioluminescence signal) from the tumor is proportional to the number of live cells expressing luciferase so bioluminescence correlates directly with tumor size.
- f) In LIVING IMAGE 4.4 software, exposure time, aperture size (f-stop) and pixel binning can be optimized based on the expression level of the cell line.

DCV Staining: FACS instrument provided by the institute is not equipped with UV laser, rather it has violet laser. Hence the choice of DCV was made over Hoechst dye during side population assay

1. Reagents and chemicals

- a) DCV
- b) Verapamil 50uM

2. Method

- a) Use cells at 75% confluency for DCV staining.
- b) Trypsinize the cells and take cell count using trypan blue dye.
- c) Make three aliquots cells as described below:
 - Tube 1 = 0.5 million cells unstained
 - Tube 2 = 1 million cells Verapamil+ DCV (Cover with foil)
 - Tube 3 = 1 million cells for DCV staining (Cover with foil)
- d) Centrifuge these 3 tubes at 1200 rpm for 5 min at 4°C to get rid of trypsin.
- e) Discard the supernatant and re-suspend cells in PBS.
- f) Centrifuge these 3 tubes at 1200 rpm for 5 min at 4°C.
- g) Discard the supernatant and re-suspend cells in 1 ml of media
- h) Add 1ul of 50µM stock verapamil to tube 2 for 15 minutes.
- i) After 15 minutes add 1µl of DCV dye to tube 2 and 3, keep them at 37⁰C for 90 min (every 15 minutes mix the cells by tapping).
- j) After 90 minutes centrifuge these 3 tubes at 1200 rpm for 5 min at 4°C.
- k) Discard the supernatant and re-suspend cells in PBS.
- l) Re-suspend tube 1, 2 and 3 in 500ul PBS in FACS tube and acquire within 3 hours.

Clonogenic Assay

1. Method

- a) Use cells at 75% confluency for starting the experiment.
- b) Trypsinize the cells and take cell count using trypan blue dye.

- c) Seed equal number of cells in 6 well dish or 60mm dish
- d) After 12 hours add drug in appropriate dilution for stipulated time.
- e) Change the media and allow the cells to grow for 1-3 weeks.
- f) Monitor the plates for colony formation.
- g) Give 1 PBS wash followed by fixation of colonies with chilled methanol for 10 minutes.
- h) Give two more PBS wash and then stain with 0.5% w/v crystal violet stain for 10 minutes.
- i) Wash out the extra stain with tap water.
- j) Count the colonies and calculate surviving fraction according to following formula;

The plating efficiency (PE) is the ratio of colonies to cells.

$$PE = \frac{\text{Number of colonies}}{\text{Number of cells}} \times 100\%$$

The number of colonies that arise after treatment of cells is called surviving fraction (SF).

$$SF = \frac{\text{PE of treated sample}}{\text{PE of control}} \times 100$$

Soft Agar Assay

- 1. Reagents and chemicals**
 - a) 2X DMEM with 20% FBS
 - b) 1X DMEM with 10% FBS
 - c) 2% Low Melting Agarose (autoclaved)
 - d) 35mm plate

2. Method

2.1. Preparation of basal layer (1% Agarose)

- a) Mix 0.5ml 2% low melting agarose and 0.5ml 2X DMEM. With 20% FBS.
- b) For 3 plates make 4 ml basal layer solution and pour 1ml media in 35mm plate without getting any air bubble.
- c) Let it solidify properly in the culture hood for 60 min, once it gets solidified it can be stored at 40C.

2.2. Preparation of upper layer (1% Agarose)

- a) Mix 0.2ml 2% low melting agarose and 0.5ml 2X DMEM with 10% FBS.
- b) Mix them properly and make 1ml aliquots of this mix
- c) Add required number of cells to be seeded to each aliquot.
- d) Pour drop wise on the basal layer.
- e) Let it solidify in the culture hood for 40 minutes.
- f) Put the plates in the CO₂ incubator.
- g) After every two days add 2-3 drops of 1X DMEM
- h) Monitor it on daily basis, count the no. of clones

B. Spheroid formation assay

a) Spheroid media composition:

- Serum free medium
- EGF: 10ng/ml
- Rh-FGF: 10ng/ml
- Insulin: 10ng/ml
- Pen-Strept- 1%
- LIF- 10ng/ml
- **Spheroid Plates:** Low adherent plates are used or 1% agarose coated plates

1. Method

- a) Number **of cells seeded:** 2000cells/ml.
- b) Spheroid Plates: Low adherent plates are used or 1% agarose coated plates.
- c) Trypsinize the cells and give one PBS wash at 1200 rpm for 5 minutes at 4°C.
- d) Take the cell count using trypan blue staining and seed at a density of 2000 cells/ml in spheroid media.
- e) Replenish the spheroid media every three days and then monitor for spheroids to form.
- f) To test the self-renewal ability of spheroids it has to be serially passaged.
- g) For serial passaging collect the spheroids and centrifuge at 1200 rpm for 5 minutes at 4°C.
- h) Add 10 ul of trypsin to the pellet and incubate for 1-2 minutes.
- i) Add complete media to neutralize the trypsin and again centrifuge and give one PBS wash.
- j) Take the cell count using trypan blue staining and seed at a density of 2000 cells/ml in spheroid media.
- k) Repeat the assay at multiple passages.